A study of different structures of central nervous system implicated in Parkinson's disease neuropathic pain

Mennatallah Elshennawy

ÉCOLE DOCTORALE Sciences, Santé, Agronomie et Environnement

Université Clermont Auvergne

THESE

Présentée pour obtenir le grade de :

DOCTEUR DE L'UNIVERSITE DE CLERMONT AUVERGNE
DOCTEUR DE L'UNIVERSITE D'AIN SHAMS

Faculté de médecine

Spécialité : Neuroscience

soutenue le 15 Décembre 2021

par

Mennatallah ELSHENNAWY

A study of different structures of central nervous system implicated in Parkinson's disease neuropathic pain

Dirigée par : Dr. Aziz HAFIDI

TGI-IGCNC, Institut Pascal, UCA

Membres du jury :

Pr. Jean-Louis GUILLOU (Université de Bordeaux, Professeur, Rapporteur, Président du Jury)

Pr. Monique MAJCHRZAK (Université de Strasbourg, Professeur, Rapporteur)

Dr. Aziz HAFIDI (Université Clermont Auvergne, Directeur de Thèse)

Pr. Shahira YOUSSEF (Université d' Ain Shams, Co-directrice de Thèse)

Pr. Adel KAMEL (Université d' Assiut, Examinateur)

Pr. Kawthar HAFEZ (Université d' Ain Shams, Examinatrice)

Acknowledgement

I wish to express my deep appreciation and sincere gratitude to ***Associate Professor Aziz Hafidi***, for providing me with this scientific opportunity to complete my work in his laboratory and for his kind support, supervision, and valuable instructions. He has generously devoted much of his time and effort for the thesis accomplishment and has provided a collaborative work atmosphere.

Also, I'd like to thank ***Professor Franck Durif*** for accepting me in his team and many thanks to all the members of the **team EA7280** for their support. Many thanks to ***Omar Ouachikh*** for teaching me how to produce our model and perform the different tests and for his help throughout the experiments. Thanks to ***Madame Laurence Douhairie*** for always being there for the administrative tasks.

I am grateful to ***Youssef Aissouni*** for teaching me western blot techniques and for his valuable tips and support. Thanks to all the members of **NEURODOL team, *Mireille Montbel, Eric Chapuy and Julie Barbier*** for their collaboration and lovely spirit.

Thanks to the members of the thesis committee, ***Professor Philippe Michaud, Professor Christine Courteix and Professor Paul Avan*** for their kind support and valuable time and comments.

Special thanks to ***Doctor Karim Alloui, Didier Meunier, Franck Audigier and Alexandra Rezard;*** who are in charge of the animal house for their collaboration, help and valuable tips for the wellbeing of the rats.

I'd like to thank ***Professor Monique Majchrzak*** and ***Professor Jean-Louis Guillou*** for offering us their valuable time to read and comment on the manuscript and being members of the Jury. Also, I'd like to thank ***Dr. Kawthar Hafez*** and ***Dr. Adel Kamel*** for participating in the Jury committee and for their valuable comments.

Many thanks to ***Professor Monique Alric*** and all ***the doctoral school committee members*** for accepting my registration in the doctoral school and for their encouragement and support. Many thanks to ***Mesdames Rita Bouzaboune and Mélanie Moulin*** for their sincere help in the administrative aspects.

I'm grateful to my supervisors ***Professor Shahira Youssef, Professor Shahira Samir, Associate Professor Shereen Adel***, ***Doctor Yasmin Ramadan***, and all my colleagues in the department of Anatomy and Embryology, Faculty of Medicine, Ain Shams University, for their kind help and sincere support. My sincere thanks to the head of Anatomy and

Acknowledgement

Embryology department, ***Professor Hemmat Abd ElKader***, for her kindness and sincere support.

Many thanks to the ***Egyptian Embassy in Paris, the Ministry of Higher Education, Ain Shams University members and Pharco pharmaceuticals*** for their continuous support.

Finally, I'd like to thank my family who supported me all through my life and career. My deep appreciation to ***My Father, My Mother***, ***My Brother*** and ***My Husband's*** encouragement and love. And to ***My lovely Son*** to whom I dedicate it all ….

…

List of Contents

List of Contents

List of Contents

List of Figures & Tables

List of Figures

List of Tables

Communications and Publications

Communications

Elshennawy, M., Ouachikh, O.,Youssef, S., Zaki, S.S., Hafidi, A (Clermont-Ferrand, June 2020). A study of different structures of central nervous system implicated in Parkinson's disease neuropathic pain. Journées de l'école doctorale Science de la vie et de la Santé.

Publications

Elshennawy, M., *Ouachikh, O., Shereen Adel Saad, Ramadan, Y., Durif, F., & Hafidi, A. (**2021**). Nigrostriatal dopamine depletion promoted an increase in inhibitory markers (parvalbumin, GAD67, VGAT) and cold allodynia.* ***Neuroscience letters****, 762, 136135.* ***https://doi.org/10.1016/j.neulet.2021.136135*** ***(Published)***

Elshennawy, M., *Ouachikh, O., AISSOUNI, Y., YOUSSEF, S., Zaki, S.S., Durif, F., & Hafidi, A. (2021). Behavioral, cellular and molecular responses to cold and mechanical stimuli in the rat with bilateral dopamine depletion in the mesencephalic dopaminergic neurons.* ***Neuroscience****, 479, 107-124. https://doi.org/10.1016/j.neuroscience.2021.10.026* ***(Published)***

Abbreviations

6-OHDA	6-hydroxydopamine
AC	Adenyl cyclase
ACC	Anterior cingulate cortex
AMPA	α-amino-3-hydroxy-5-methyl-4-ioxazolepropionic acid
Amyg	Amygdala
ATP	Adenosine Triphosphate
BSA	Bovine serum albumin
Ca+++	Calcium
CB 1	Cannabinoid receptor
CCI	Chronic constriction injury
CFOS	Pain marker CFOS
CGRP	Calcitonin gene related protein
CMA	Chaperone-mediated autophagy
COX-2	Cyclooxygenase-2
CL	Central lateral nucleus
CNS	Central nervous system
COMT	Catechol-O-methyl transferase in the extracellular compartment
CREB	cAMP-response element binding protein
DF	Descending facilitatory
DI	Descending inhibitory
DA	Dopamine
DATs	Dopamine active transporters
DLPAG	Dorsolateral periaqueductal grey
DMPAG	Dorsomedial periaqueductal grey
D1R	Dopamine 1 receptor
D2R	Dopamine 2 receptor
EDS	Excessive Daytime Sleepiness

Abbreviations

EOPS	Free from organisms specific pathogens Exempt d'organismes pathogènes spécifiques
Fe++	Iron
FG	Fluorogold
FR	Fluororuby
GABA	Gamma aminobutyric acid
GAD67	Gluatamate decarboxylase 67
GFAP	Glial fibrillary acidic protein
GIRK	G-protein-gated inwardly rectifying potassium
GFR α-3	Glial cell line- derived neurotrophic factor family of receptors – alpha 3
GlyT1	Glycine transporter
GSH	Glutathione
HIV	Human immunodeficiency virus
HLA	Human leucocyte antigen
HTR	Hydroxytryptamine (serotonin) receptor
IASP	International association for the study of pain
IHC	Immunohistochemistry
K+	Potassium
KCC2	Potassium chloride cotransporter isoform 2
LatC	Lateral cervical nucleus
LSp	Lateral spinal nucleus
LPAG	Lateral periaqueductal grey
LTMRs	Low threshold mechanoreceptors
MAPK	Mitogen-activated protein kinase
MCI	Mild Cognitive Impairement
MDH	Medullary dorsal horn
MDS	Movement Disorder Society
MDvc	Ventral caudal part of the medial dorsal nucleus

Abbreviations

MEK	Mitogen-activated protein kinase kinase
MFB	Medial forebrain bundle
mGluRs	Metabotropic glutamate receptors
miRNAs	Micro ribonucleic acids
Mn++	Manganese
MPTP	1-methyl-4-phenyl-1,2,3,6-tetrahydropyridine
MS	Multiple sclerosis
Na+	Sodium
NA	Noradrenaline
NMDA	N-methyl D-aspartate receptor
nNOS	Neuronal nitric oxide synthase
NP	Neuropathic Pain
NR2B	N-methyl D-aspartate receptor subtype 2B
Opioid R	Opioids receptor
PAFs	Primary afferent fibers
PAG	Periaqueductal grey
PBS	Phosphate buffered saline
PD	Parkinson's Disease
pERK	Phosphorylated extracellular signal-regulated kinase
PFC	Prefrontal cortex
PIGD	Postural Instability and Gait Disorders
piRNAs	Piwi interacting RNAs
PKC-γ	Protein kinase C - gamma
PN	Projection neurons
PNS	Peripheral nervous system
PPC	Posterior parietal cortex
PV	Parvalbumin
PVN	Hypothalamic paraventricular nucleus

Abbreviations

RAF	RAF kinase
RAS	RAS GTPase
RBD	Rapid Eye Movement Sleep Behavior Disorder
RNA	Ribonucleic acid
ROS	Reactive oxygen species
RVM	Rostral ventral medulla
S1	Primary sensory cortex
SDH	Spinal dorsal horn
SEM	Standard error of the mean
siRNAs	Small interfering RNAs
SMA	Supplementary motor area
SN	Substantia Nigra
SNpc/ SNc	Substantia Nigra pars compacta
SNpr	Substantia Nigra pars reticulata
SOD	Superoxide Dismutase
TBS	Tris-buffered saline
Th	Thalamus
TH	Tyrosine Hydroxylase
TPP	Thermal place preference
TRP	Transient potential channels
TRPM8	Transient receptor potential melastatin 8
TrpV1	Transient receptor potential cation channel subfamily V member 1 (TrpV1)
UK	United kingdom
UPDRS	Unified Parkinson's Disease Rating Scale
UPS	Ubiquitin-proteasome system
VFT	Von Frey Test
VGAT	Vesicular GABA transporter

Abbreviations

VGLUT 3/ 1	Vesicular glutamate transporter
VL	Ventral lateral nucleus
VLPAG	Ventrolateral periaqueductal grey
VM	Ventral medial nucleus
VPI	Ventral posterior inferior nucleus
VPL	Ventral posterior lateral nucleus
VTA	Ventral tegmental area

Abstract

Pain is the major non-motor symptom in Parkinson's disease (PD). Its mechanism is still poorly understood although an increase in excitation or a decrease in inhibition have been reported in preclinical studies. These studies have mostly investigated mechanical pain by considering the decrease in a nociceptive threshold. Only a few studies have focused on thermal pain in animal models of PD. Besides, fluorescence tracers have been widely used to label projecting neurons, but the linkage between the susbtantia nigra and the spinal pain process hasn't yet been demonstrated thoroughly. Therefore, the goal of this study was to assess the thermal nociceptive behavior of rats subjected to 6- hydroxydopamine (6-OHDA) administration, which constitutes an animal model of PD. Also, to investigate gamma aminobutyric acid (GABA) inhibition in the 6-hydroxydopamine (6-OHDA) PD rat model. Therefore, the expression of three inhibitory markers parvalbumin, glutamate decarboxylase 67 (GAD67) and vesicular GABA transporter (VGAT) was evaluated in bilateral 6-OHDA lesioned rat. Also, Fluororuby (FR) has been injected in the substantia nigra pars compacta to assess its anterograde projections to discover whether it has dopaminergic projections to the spinal cord or not. Our results demonstrated significant thermal sensitivity to cold temperatures of 10 °C and 15 °C, and not to higher temperatures, in 6-OHDA-lesioned rats when compared with sham. 6-OHDA-lesioned rats also showed cold allodynia as demonstrated by a significant difference in the number of flinches, latency and reaction time when subjected to acetone stimulus. Ropinirole administration, a dopamine receptor 2 (D2R) agonist, blocked the acetone-induced cold allodynia in 6-OHDA-lesioned rats. In addition, mechanical hypersensitivity and static allodynia, as demonstrated by a significant difference in the vocalization threshold and pain score respectively, were noticed in 6-OHDA-lesioned rats. Acetone stimulus induced a significant increase in extracellular signal-regulated protein kinases 1 and 2 (ERK1/2)phosphorylation, a pain process molecular marker, in the spinal dorsal horn (SDH), the insular and cingulate cortices, besides the increase of CFOS excitatory pain marker in the SDH, in 6-OHDA-lesioned rats when compared to sham. There was a significant increase in the expression of the three inhibitory markers parvalbumin, GAD67 and VGAT within the SDH of 6-OHDA lesioned rats. In parallel, there was also an increase of the excitatory marker protein kinase C gamma (PKCγ). PKCγ cells have a crucial role in pain chronicity and are regulated by GABAergic influences. This highlighted an increase in excitation and a decrease in inhibition in the SDH. After tracing the FR (Fluororuby) coupled with dopaminergic Tyrosine hydroxylase marker, some brain stem structures received the tracer having dopaminergic origin, nevertheless, the spinal cord lacked dopaminergic projections from the SNpc. In conclusion, the present study demonstrated a clear cold thermal hypersensitivity, in addition to a mechanical

Abstract

one. Moreover, there was an increased expression in inhibitory markers, which may reflect a disinhibition or a decreased inhibition in 6-OHDA lesioned rats. The spinal pain process involves dopaminergic imbalances that most probably aren't of direct SNpc origin.

Keywords: Parkinson's disease, allodynia, hyperalgesia, cold, mechanical, fluorouby

Aim of the work

The main question of the study was to see if inhibition within different structures of central nervous system was decreased after dopamine depletion, Ropinirole (D2R agonist) was given to see the effect of treatment on these markers and on painful behavior:

1- The production of Parkinsonian rat model and the verification of the model by testing Substantia Nigra against Tyrosine Hydroxylase.

2- The assessment of cold allodynia using the Acetone Drop test (non- painful stimuli).

3- The assessment of mechanical hypersensitivity (vocalization threshold)

4- The assessment of static allodynia (pain score)

5- The quantification of pERK in the SDH, the insular and cingulate cortices and CFOS (pain markers) in the SDH.

6- The quantification of PKCγ (the sensitization and chronicity of pain) in the SDH.

7- The quantification and semi- quantification of the inhibitory system mediators (GAD67, VGAT and Parvalbumin).

8- Semi-quantification of the D2R protein.

9- The injection of Fluororuby in the SNpc and its tracing in various structures co-labeled with Tyrosine Hydroxylase

Introduction – Bibliography

Literature Review – Parkinson's Disease

1. Parkinson's Disease

Parkinson's disease (PD) is the second most prevalent neurodegenerative disease worldwide. The percentage of parkinsonian patients is 0.5-1 % at age 65-69 and 1-3 % at age 80 and above, affecting around 10 million patients. Its prevalence increases with age; and as the mean age of population increases; the incidence and prevalence of the disease is expected to increase 30% when reaching 2030 (De Miranda & Greenamyre, 2017; Kouli al., 2018).

1.1. Etiology:

PD is multifactorial. The risk of disease increases with aging, especially in males. It has been proved that pesticides (as MPTP and Rotenone) and herbicides (as Paraquat) are risk factors as they lead to nigrostriatal degeneration. Other compounds as Manganese, Carbon monoxide and ß2 adrenoreceptor antagonists increase the risk for Parkinsonian disease. On the other hand, the risk to develop the disease decreases with drinking caffeine, tea, smoking cigarettes, calcium channel blockers and statins (De Miranda & Greenamyre, 2017; Kouli et al.,2018; Balestrino & Schapira, 2020).

Genetics also play a role in this disease, although it is not involved except in small percentage as familial (10-15%) and only 5 % Mendelian inheritance. 1st degree relatives of Parkinsonian patients have increased relative risk of 2-3 folds than normal population. Genetic mutations lead to mitochondrial dysfunction, protein degradation or oxidative stress (De Miranda & Greenamyre, 2017; Kouli et al., 2018).

In addition, environmental factors play a role in causing epigenetic variations of gene expression such as DNA methylation, histone modifications or changed microRNA (miRNAs) and other non-coding RNAs (small interfering RNAs (siRNAs) or piwi interacting RNAs (piRNAs)) which have been probably implicated in pain inflammatory processes as they participate in regulating genes and RNA silencing. Epigenetic modulation is crucial for variations in gene expression mandatory for maintaining the different cellular mechanisms such as growth, cellular fate commitment and adjustment to the environment. Disruption of these functions may be a risk factor for neurodegenerative diseases including PD (Delgado-Morales, 2017; Sommer et al., 2018).

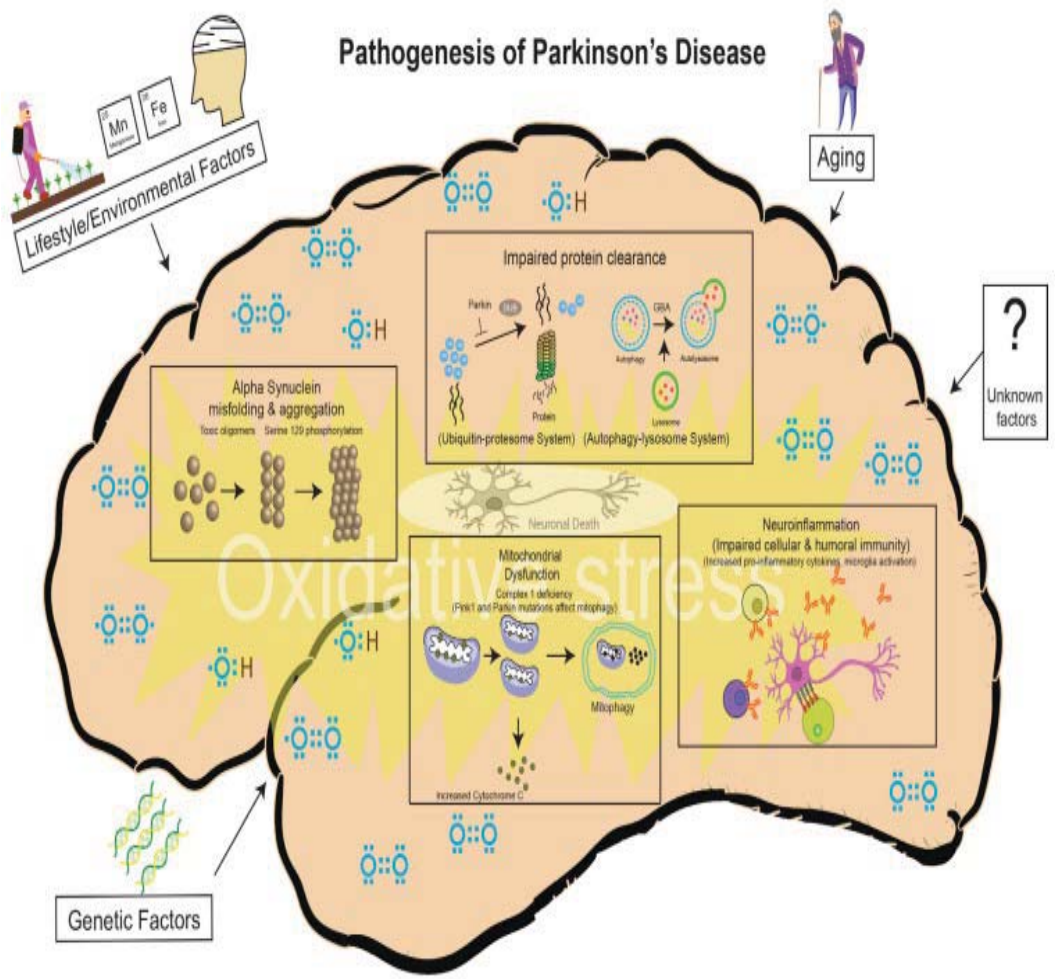

Fig. (1): a diagram showing the pathogenesis of PD.

Note. Reprinted with permission from "Parkinson's disease: Etiopathogenesis and treatment," by J. Jankovic and E. K. Tan, 2020, Journal of Neurology, Neurosurgery & Psychiatry, 91(8), p.799 (http://dx.doi.org/10.1136/jnnp-2019-322338). Copyright 2020 by J. Jankovic and E. K. Tan. Published by BMJ.

1.2.Pathogenesis:

PD is a complex disease developing through multiple stages, processes, cell types and tissues. Gross morphology in the brain of Parkinson's disease is distinctive. Generally, there may be mild atrophy of frontal cortices and dilatation of the ventricles. The most distinguishing feature is the loss of neuromelanin dopaminergic neurons in substantia nigra pars compacta (SNpc) & loss of noradrenergic neurons in locus coeruleus leading to loss of their dark pigmented areas. The specific pattern of dopaminergic neuron loss in the substantia nigra (SN) is that it is not even, in contrary to dopaminergic cells loss during aging which is affecting evenly the dorsal tier of substantia nigra (De Miranda & Greenamyre, 2017; Kouli et al., 2018;Hölscher, 2020).

There is a preclinical stage before the appearance of known signs and symptoms occurring since axons terminals projecting to striatum are degenerated before nerve injury in SNpc. There is literature showing that multiple non- dopaminergic systems' modulation is causative of some non-motor PD symptoms, such as the serotonergic, glutamatergic, GABAergic, nor-adrenergic, histaminergic, cholinergic and adenosinergic (Kouli et al., 2018).

The SN dopaminergic cells are more vulnerable to neurotoxicity more than ventral tegmental area (VTA). Distal terminals are more subjected to degeneration; may be due to the theory that mitochondria away from cell body have less ATP (adenosine triphisphate), produce more reactive oxygen species (ROS) and thus more vulnerable to neurotoxicity. Dopamine is a catecholamine formed from tyrosine due to enzymatic reactions between tyrosine hydroxylase and decarboxylase amino acids. Dopamine itself helps in the pathogenesis of PD; mitochondrial dysfunction and α-synuclein aggregation leads to its leakage from synaptic vesicles to cytosol resulting in its oxidation or non-enzymatic oxidation. If these products cannot be detoxified by glutathione (GSH) and catalase, Fenton cycling of electrons could occur by intermingling with the transient brain metals (Fe2+, Mn2+, Cu2+) causing hydroxyl radicals production and neurotoxicity. Microarray studies have shown less glutathione associated genes with the augmentation of proinflammatory cytokines marker (De Miranda & Greenamyre, 2017).

1.3. Histopathology:

The pathological distinctive feature is the microscopical presence of Lewy bodies which are neuronal cytoplasmic eosinophilic deposits immunoreactive for α-synuclein and mostly associated with Lewy axonal neurites. Their diameter ranges from 5 to 30 μm. One neuron may have multiple bodies. They consist of granular and fibrillar hyaline centers surrounded by pale peripheral halos. Cortical Lewy bodies have fewer sharp outlines and there are no halos and smaller compared to brainstem ones. In the SN, similar structures are considered precursors of Lewy bodies and are named 'pale bodies'. α-synuclein is normally present in our bodies; in Parkinson's disease, its filamentous structures become amyloid like, phosphorylated and grouped (Kouli et al., 2018; Balestrino & Schapira, 2020).

The halo of Lewy Body is mainly made up of α-synuclein too. α-synuclein is generally unfolded in the brain with no specific outlined tertiary structure except in aqueous environment; it becomes tertiary without aggregation. It folds into α – helical structure when intermingles with negatively charged phospholipids of cell membranes through N-terminal while in PD, it takes the shape of β-sheet-rich amyloid-like structure through serine 129 phosphorylation, ubiquitination and C-terminal truncation leading to its aggregation forming different structures:

unfolded monomers, soluble oligomers, protofibrils and high molecular weight insoluble fibrils; the most toxic to neurons of them is the early oligomers which have a high capability of aggregation and spreading in the brain leading to dysfunction of mitochondria, lysosomes, proteosomes, disruption of cytoskeleton and biological membranes, besides changing synaptic function causing neurodegeneration (Kouli et al., 2018; Balestrino & Schapira, 2020).

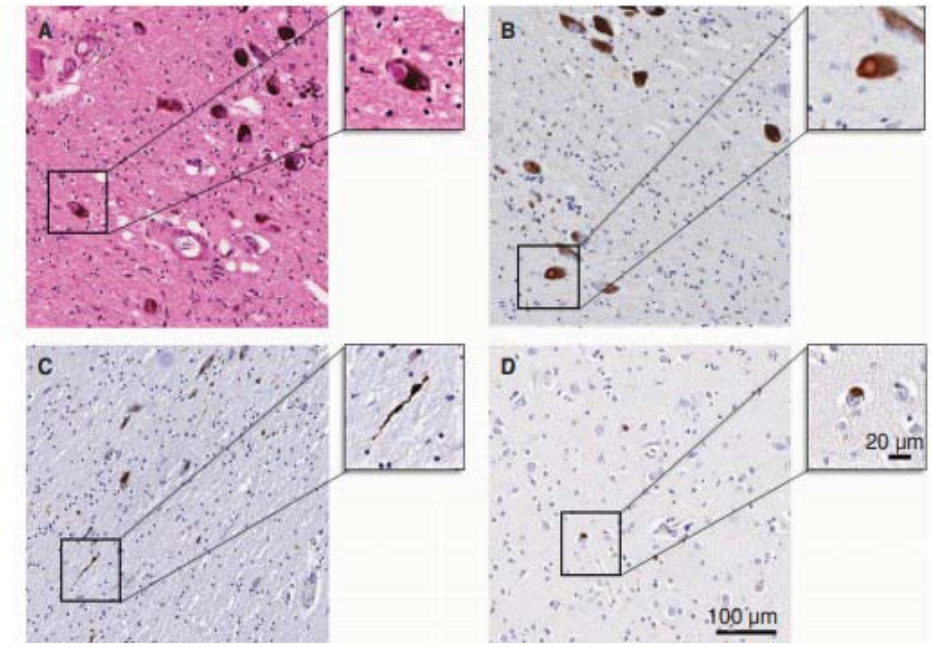

Fig. (2): shows Lewy bodies in Substantia Nigra pars compacta in images A to C while D is in prefrontal cortex. A) Lewy body stained with Hematoxylin and Eosin, B) Lewy body detected by alpha synuclein immunohistochemical stain (notice the halo), D) Lewy body in the cortex not well defined and no halo.

Note. From Parkinson's Disease: Pathogenesis and Clinical Aspects (p.11), by A. Kouli et al., 2018, Codon Publications. Copyright 2018 by Codon Publications (CC BY-NC 4.0).

1.4. Pathophysiology:

The main causative factor is α-synuclein aggregation, in addition, there are other mechanisms suggested to be involved in the pathogenesis as mitochondrial dysfunction, neuroinflammation and non-standard protein clearance (Kouli et al., 2018).

Mitochondrial dysfunction plays a role in PD due to deficiency of mitochondrial complex-I, that plays a big role in the electron transport chain. When Dopamine (DA) neurons take up oxidized neurotoxins, this leads to dysfunction of complex-I leading to energy diminution, the production of cytochrome C and initiation of caspase cascade, eventually causing dopaminergic cell death. Also, PD hereditary genes have function in mitochondrial homeostasis such as parkin (PARK2 and PARK6) which are involved in getting rid of dysfunctional

mitochondria (i.e. mitophagy). α-synuclein itself can interact with the mitochondrial membrane precipitating within its matrix harming mitochondrial complex-I activity increasing oxidative stress (Kouli et al., 2018; Jankovic & Tan, 2020).

Dysfunctional proteins are removed either by ubiquitin-proteasome system (UPS) or by autophagy lysosome pathway. UPS breaks abnormal proteins by adding ubiquitin tag and transfers them for proteosome for breaking down. On the other hand, autophagy lysosome pathway is represented by macro-autophagy, which engulfs cytosolic proteins using autophagosome and lysosome or micro-autophagy which destroys cytoplasmic components using only lysosomes, or chaperone-mediated autophagy (CMA) that selects more proteins that are specific and destroys them through lysosomes. The dysfunction in these clearance systems leads to the accumulation of abnormal proteins, like soluble misfolded α-synuclein, which contributes to PD (Kouli et al., 2018).

Substantia nigra and striatum of PD patients have increased microglial and complement activation, T-lymphocyte infiltration, and augmented level of pro-inflammatory cytokines. Astrocytes, the most spread brain glial cells play import role in PD pathogenesis and neuropathic pain. Reactive glial cells contribute to inflammatory processes by producing many toxic products including reactive oxygen species causing neurodegeneration (De Miranda & Greenamyre, 2017; Sommer et al., 2018).

Both innate and adaptive immunity systems are believed to be related to PD. Now, it is believed that microglial cells play crucial role in causing neurodegeneration and not being only a reaction as was thought in the past.

Other studies have shown that α-synuclein activates microglia and increases inflammation. Besides, as human leucocyte antigen (HLA) class II is associated with PD, this gives more insight that immune system is involved in PD pathogenesis. This is confirmed by the fact that the use of non- steroidal anti-inflammatory medication Ibuprofen decreases PD risk. High serum immune markers are associated with worsen motor and cognitive functions. Thus, recently, immunity modifying treatments may be a hope for treating PD (Kouli et al., 2018).

These molecular mechanisms are accompanied with disturbance in the molecular transport, microtubular structure disruption, neuronal toxicity, disruption of iron metabolic pathway, endoplasmic reticulum damage... etc., leading eventually to apoptosis and necrosis. There are nowadays clinical trials to prevent the formation of oligomeric α-synuclein and its propagation (Jankovic & Tan, 2020).

2. Clinical Features

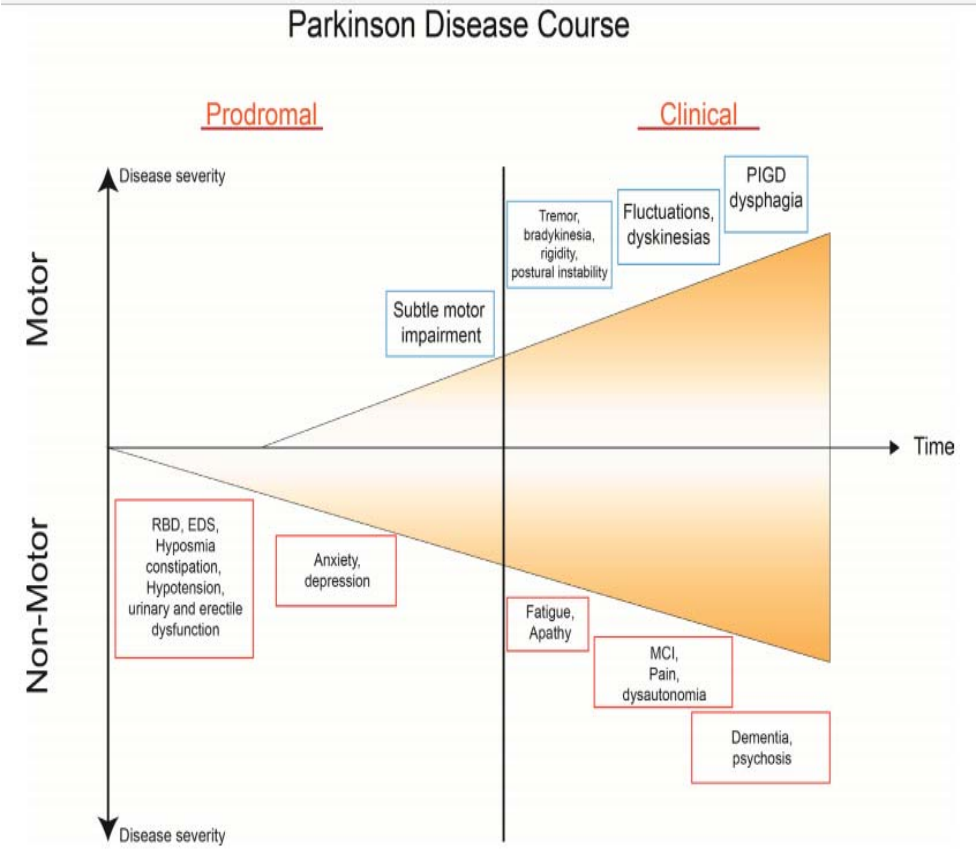

Fig. (3): shows PD's symptoms in prodromal and clinical phases. RBD Rapid Eye Movement Sleep Behavior Disorder, EDS Excessive Daytime Sleepiness, MCI Mild Cognitive Impairment, PIGD Postural Instability and Gait Disorders.

Note. Reprinted with permission from "Parkinson's disease: Etiopathogenesis and treatment," by J. Jankovic and E. K. Tan, 2020, Journal of Neurology, Neurosurgery & Psychiatry, 91(8), p.796 (http://dx.doi.org/10.1136/jnnp-2019-322338). Copyright 2020 by J. Jankovic and E. K. Tan. Published by BMJ.

There are various clinical criteria scaling systems for the trial of reaching early diagnosis for PD. Such as: UK Parkinson's Disease Society Brain Bank criteria which include the existence of bradykinesia, in addition to rigidity, 4–6 Hz rest tremor or postural unsteadiness, besides three more symptoms. While the criteria of International Parkinson's and Movement Disorder Society (MDS) include bradykinesia, in addition to either rest tremor or rigidity with no exclusion criteria (such as cerebellar gait, parkinsonian symptoms related to lower limbs only

for 3 years, no adequate response to high dose Levodopa in moderately diseased patients, standard functional neuroimaging of presynaptic dopaminergic system ..) and no red flags (such as bilateral symmetric parkinsonism, repeated falls more than once a year in case of the disease starting in less than 3 years, respiratory dysfunction during respiration, fast progression of gait impairment ..), with the presence of supportive criteria (such as good response to dopaminergic treatment, olfactory impairment, levodopa treatment related dyskinesia..). There are also scales made for assessing disease severity and development as Unified Parkinson's Disease Rating Scale (UPDRS). Progression of non-motor symptoms is the result of dysfunction of non-dopaminergic systems. Prodromal phase is the phase preceding motor symptoms in PD patients where neurodegeneration begins without being manifested in patients. It may take up to 15-20 years. This phase may include some symptoms as depression, olfactory impairment, autonomic system impairment, rapid eye movement sleep behavior disorder and diabetes mellitus (Balestrino & Schapira, 2020; Jankovic & Tan, 2020).

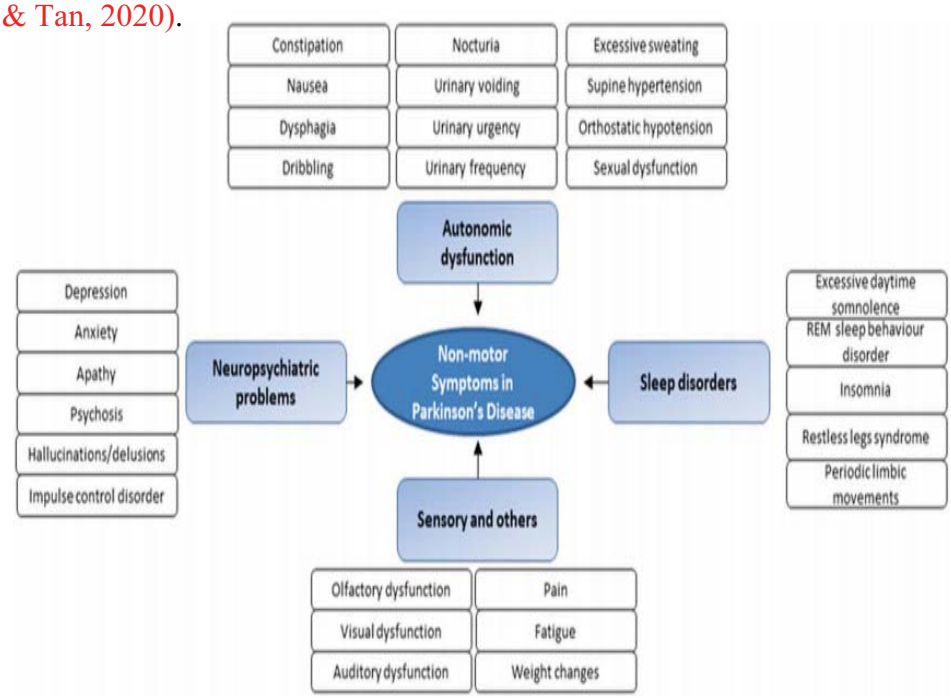

Fig. (4): showing non- motor PD symptoms.

Note. From "Presynaptic dopaminergic terminal imaging and non-motor symptoms assessment of Parkinson's disease: Evidence for dopaminergic basis?," by M. Qamar et al., 2017, Npj Parkinson's Disease, 3(1), 5, p.2 (https://doi.org/10.1038/s41531-016-0006-9). Copyright 2017 by M. Qamar et al. Published by Nature publishing group.

Literature Review – Clinical Features

When patients are diagnosed, it is almost 60% of dopaminergic neurons are being affected. Motor symptoms occur in a late phase of the disease where almost 80% of the neurons are degenerated. Non-motor symptoms occur earlier, but they are not reliable for diagnosis. This makes it difficult to save the neurons with any neuroprotective treatment before detrimental neuronal loss. Levodopa (L-dopa which is the dopamine precursor) is the effective treatment for multiple PD symptoms as bradykinesia, tremors, and rigidity, but unfortunately, it has severe side effects including dyskinesia, hallucinations, worsening of impulse control disorder and wearing off consequences (De Miranda & Greenamyre, 2017).

There is a known classification of PD: 1) Tremor Dominant subtype: responds well to dopamine agonists and has less other motor symptoms 2) Non-tremor dominant subtype has rigidity and postural imbalances with increasing probability of developing non- motor symptoms. Both subtypes are mostly caused by different factors and pathogenesis, and lead to different disease progression and prognosis. 83% of PD patients develop dementia after being diagnosed. All symptoms, either motor or non – motor can become irresponsive to treatment on the long run (Kouli et al., 2018).

Non-motor symptoms can be classified into autonomic, neuropsychiatric, or sensory. Autonomic such as thermoregulatory changes, urinary dysfunction, hyperhidrosis, and CVS; neuropsychiatric disturbances as depression, anxiety and dementia; sensory as restless leg syndrome, numbness, visual troubles and pain.

3. Pain in PD

Ford (2010) and Goetz et al. (1986) categorized non-motor PD pain symptoms into musculoskeletal, radicular-neuropathic, dystonia, akathisia and central neuropathic pain. Pain may prevail in about 68- 95% of PD patients. Pain appears at any phase of the disease even before diagnosis. The International Association for the Study of Pain (IASP) has defined pain as follows: "A sensory and emotional experience associated with real or potential injuries or described in terms of such injuries - pain arising as a direct consequence of a lesion or disease affecting the somatosensory system". Central Neuropathic pain is persistent pain not localized to certain nerve or territory where there are sensory symptoms as paresthesia and shooting affecting different body areas, for example the abdomen, chest and mouth. PD pain may occur due to local changes in primary afferent nociceptors or decrease of the inhibitory effect of descending dopaminergic pathways, which may lead to increase sensitivity to noxious sensation. Around 50 % of PD patients take treatment for pain (Fil et al., 2013; Smith et al. 2013; Buhmann et al., 2020).

Pain makes patients suffer in all stages of PD. In the early phase of the disease, pain is the most annoying symptom for these patients (Skogar and Lökk, 2016).

Dorsal spinal horn receives pain signals from different body areas through primary afferent fibers (PAFs). These signals undergo different mechanisms, which enhance or suppress their transfer through projection neurons (PN) upwards to higher structures and receives either positive or negative descending modulatory nerve fibers signals from cerebral structures. Thus, there is a gate like mechanism that processes signals at the dorsal spinal horn level before its

transmission to higher structures (Melzack and Wall, 1965). There is no fixed rule for control of nociception, certain supraspinal areas may either send descending facilitatory (DF) signals or descending inhibitory (DI) ones according to the mechanism processed. The same concept for neurotransmitters, which may play excitatory or inhibitory roles according to the target receptor receiving this neurotransmitter

3.1. Anatomy and Pathophysiology of pain:

According to Rexed (1952) spinal cord laminae classification, nociceptors relay these painful stimuli to lamina I, II (substantia gelatinosa) of dorsal spinal horn then sensation is transmitted to T-cells of lamina V and then to the brain (Cordero-Erausquin et al., 2016). Normally nociceptive fibers stimulation leads to inhibition of substantia gelatinosa, thus the inhibition of substantia gelatinosa on t-cells decrease leading to t-cells activation reducing the ability of t-cells to receive more stimuli and thus having less reactivity (i.e. gate – theory). The pain is transmitted to higher brain structures through two pathways, either medial or lateral systems. The medial system is responsible for the emotional, cognitive and memory aspects of pain and autonomic reactions, while the lateral system is responsible for the discriminative function; location and duration of pain (Fil et al., 2013).

These spinal cord laminae receive Aδ- and C-peptidergic primary afferents fibers and encloses interneurons and projection neurons.

Table (1): Types of nerve fibers:

Types	Size	Myelination	Function
Aβ	Large	Highly	Fast conduction of low threshold tactile stimuli
Aδ	Smaller	Thinly	Slower conduction for higher threshold, thermal and mechanical painful stimuli (1st stimulated)
C	Smallest	Unmyelinated	Slowest conduction with highest threshold of activation for painful stimuli either painful mechanical, thermal or chemical. (2nd stimulated)

(D'Mello & Dickenson, 2008; Fil et al., 2013; Garcia – Larrea & Peyron, 2013)

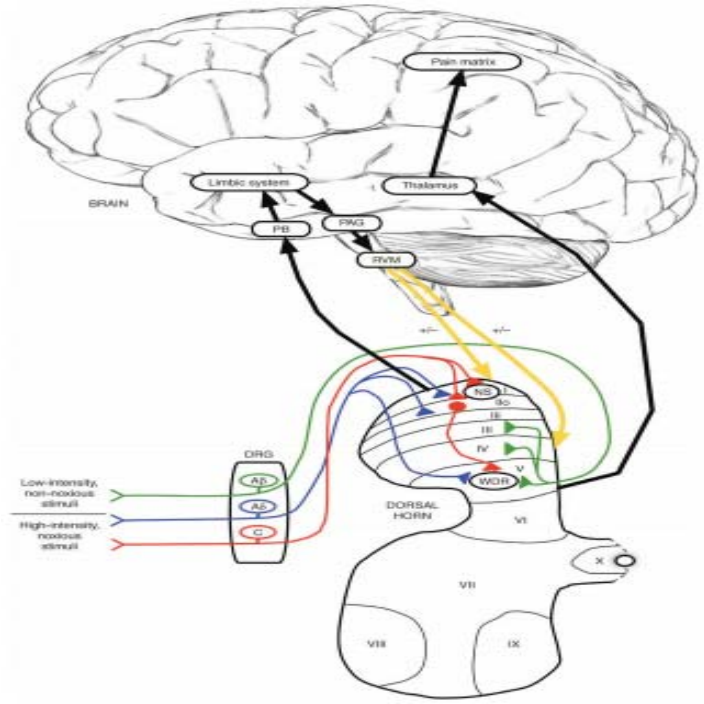

Fig. (5): Peripheral afferent fibers convey painful impulses from periphery to spinal cord dorsal horn, which ascend to be processed in higher structures. Also, higher structures modulate these painful sensations through descending pathways.

Note. Reprinted with permission from "Spinal cord mechanisms of pain.," by R. D'Mello and A. H. Dickenson, 2008, British journal of anaesthesia, 101(1), p.9 (https://doi.org/10.1093/bja/aen088). Copyright 2008 by British Journal of Anaesthesia. Published by Elsevier.

Lamina I contains interneurons, which modulate pain, and projection neurons, which convey pain to higher structures while lamina II has interneurons and excitatory vertical cells projecting to lamina I.

The substantia gelatinosa (Lamina II) has 3 subdivisions:

1) Outer subdivision: Lamina IIo; has glutamatergic fibers coming from lamina I modulating pain, in addition to polysynaptic fibers from deeper laminae. It encloses vertical cells and glutamatergic stalked ones, which feeds back lamina I and their dendrites extend to other subdivisions of laminae II and lamina III. It has also excitatory central cell neurons with short caudal projections. Other inhibitory islet interneurons have short caudal projections releasing GABA and glycine. In addition, there are excitatory A β fibers conducting touch.

2) Lamina IIid (inner dorsal): has C non peptidergic fibers afferents

3) Lamina IIiv (inner ventral): encloses PKCγ and calretinin excitatory interneurons (Alles & Smith, 2018).

Pain pathways:

- **1st order processing: concerned with nociception.**

Neurons from laminae I, V and VII project to posterior nuclei of thalamus forming the spinothalamic projections which projects to different primate structures in the cortex as follows: [Posterior insula 40 %, middle part of cingulate cortex 24 %, in addition to medial part of parietal operculum 30 %], which are involved in neuropathic pain in humans while in acute pain, posterior insula and operculum are the structures involved.

- **2nd order matrix: concerned with cognition and consciousness of pain.**

Other structures do not receive direct spinothalamic tract projections such as anterior cingulate cortex, middle and anterior part of insular cortex, posterior part of parietal and prefrontal cortices, striatum, hippocampus and cerebellum: all are involved in pain processing depending on the situation and themselves, they do not produce pain if stimulated. These areas projects top- down to first order pathway modulating their activities.

- **3rd order networks: concerned with self-control over the painful stimulus to convert it from severely unpleasant to modestly less painful sensation.**

These structures are orbitofrontal, perigenual, cingulate cortex and anterolateral prefrontal cortex (PFC). They can modulate ascending signals to higher cortical structures (Garcia – Larrea & Peyron, 2013).

3.2 ***Pain Matrix:***

Higher cerebral components also modulate pain through descending fibers leading to the secretion of serotonin, noradrenaline and dopamine, which modulates pain in the spinal cord dorsal horn. PD can affect pain pathways at different levels and structures, starting from peripheral components to higher structures. Both free and encapsulated nerve endings may be affected in PD regardless the duration and severity of the disease. In the early phases of PD, spinal cord may be affected; neurons of Lamina I of the dorsal horn have been found to be affected. The last regions of the descending pathway are the nucleus raphe magnus and gigantocellular reticular nucleus, these areas are impacted early in PD (Fil et al., 2013).

Pain matrix components as spinal cord dorsal horn, cortex and hippocampus have NMDA subtype 2B (NR2B) subunit which has (N-methyl D-aspartate receptor) NMDA receptors (Zhuo et al., 2011).

There is no exclusive pain center in the brain but there are multiple regions that integrate

together forming the pain matrix including (Insular, anterior cingulate, prefrontal and 1ry and 2ry somatosensory cortices, PAG (periaqueductal grey), locus coeruleus, RVM (rostral ventral medulla), amygdala, medial PFC, nucleus accumbens and hippocampus). Brainstem RVM is facilitatory and it helps in the sustainability but not the initiation of the painful sensation. This pathway is involved in mechanical allodynia. Studies now focus on the trials for understanding the complexity of pain matrix connections and structures in order to get more insight into chronic neuropathic pain (D'Mello & Dickenson, 2008; Alles and Smith, 2018; Puopolo, 2019; Thompson and Neurgebauer, 2019).

The pain matrix means that certain brain structures are activated all together when subjected to a painful stimulus. This theory entails different aspects of pain which are all involved in the etiology of pain including emotional and cognitive aspects. The majority of pain matrix structures aren't exclusive for pain (Garcia – Larrea & Peyron, 2013).

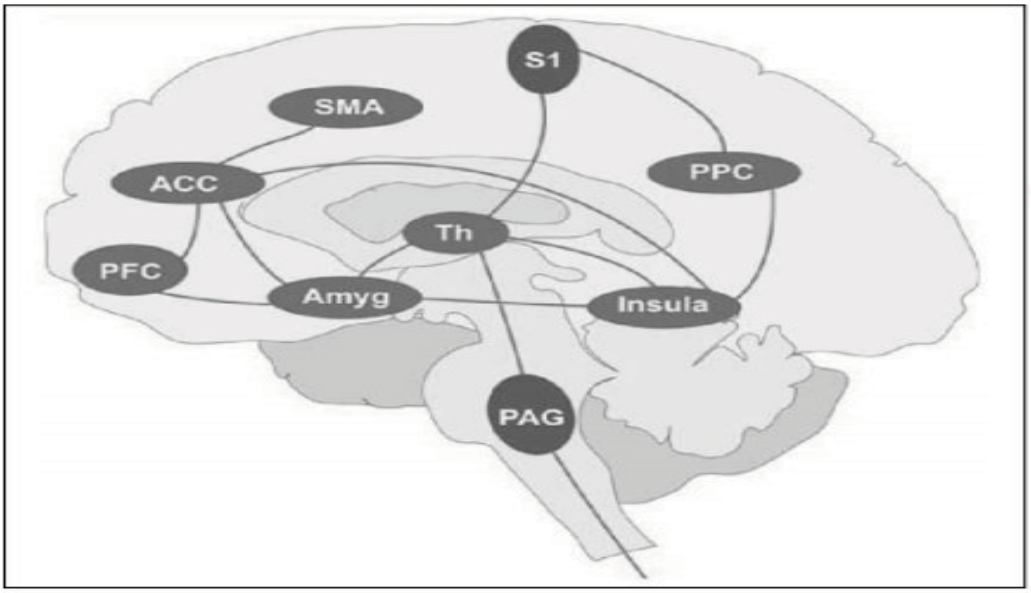

Fig. (6): Shows constituents of pain matrix:
PAG: periaqueductal grey, Insula, PPC: posterior parietal cortex, Amyg: amygdala, Th: thalamus, S1: primary sensory cortex, PFC: prefrontal cortex, ACC: anterior cingulate cortex, SMA: supplementary motor area.

Note. From "A review of diagnostic and functional imaging in headache," by A. May, 2006, The Journal of Headache and Pain, 7(4), 175. (https://doi.org/10.1007/s10194-006-0307-1). Copyright 2006 by Springer-Verlag Italia.

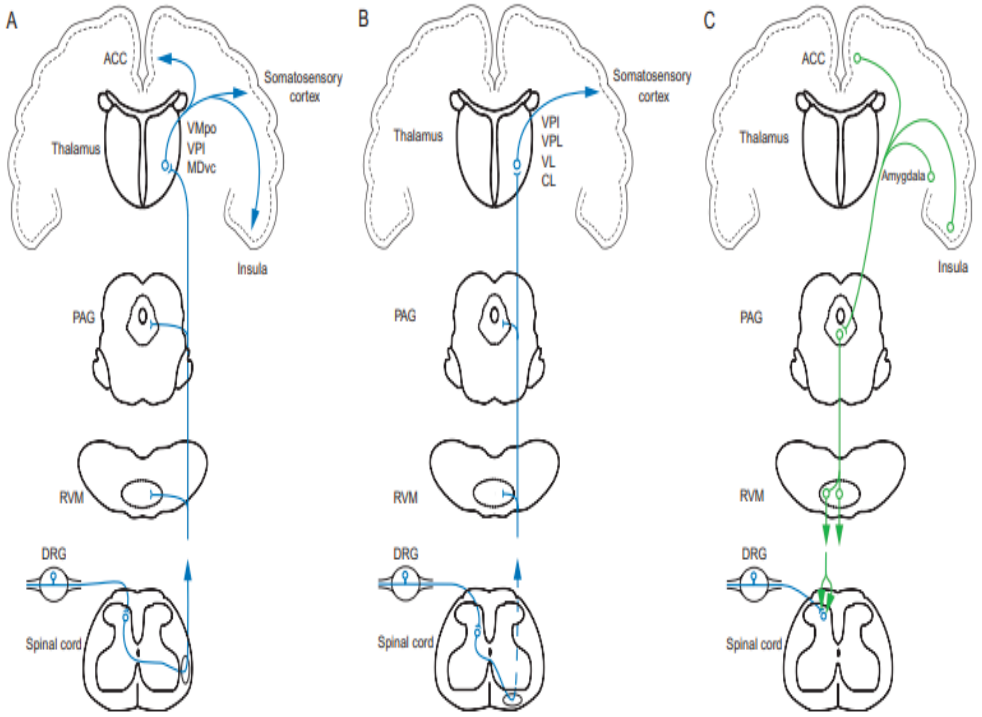

Fig. (7): Shows pathways carrying pain in the CNS. A) The lateral spinothalamic tract (main central pain pathway) carries painful signals from lamina I neurons to RVM, PAG and Thalamus then to ACC, Somatosensory Cortex and Insula B) The anterior spinothalamic tract carries signals from laminae IV and V to RVM, PAG and Thalamus then to Somatosensory Cortex.
C) There are descending facilitatory and inhibitory pathways. There are modulations descending to PAG from ACC, Insula, hypothalamus and amygdala. Then spinal cord receives mainly descending fibers from RVM.
ACC: anterior cingulate cortex, RVM: rostral ventromedial medulla, PAG: periaqueductal grey CL: central lateral nucleus, MDvc: ventral caudal part of the medial dorsal nucleus, VL: ventral lateral nucleus, VMpo: ventral medial nucleus, VPI: ventral posterior inferior nucleus, VPL: ventral posterior lateral.

Note. From Basic Neurochemistry (Eighth Edition, p.932), by P. Inquimbert and J. Scholz., 2012, Academic Press. Copyright 2012 by Elsevier.

3.3. ***Neuropathic Pain:***

Pain is unpleasant sensation and the suffering from pain for long duration leads to anxiety and depression (Thompson and Neugebauer, 2019).

Neuropathic pain (NP) according to the (IASP) is stated as: "pain initiated or caused by a primary lesion or dysfunction of the nervous system". There are multiple diseases associated with neuropathic pain as: dorsal horn lesions and syringomyelia where nociceptive pathways are affected with impaired thermal pain threshold (Garcia-Larrea and Magnin, 2008).

NP percentage worldwide varies between 1.5% and 8%. It represents 10-12 % in PD patients. To diagnose neuropathic pain, the pain should be in the nervous system having illness history with confirmatory tests of the disease and distribution (Fil et al., 2013; Alles & Smith, 2018).

The difference between nociception and neuropathic pain that nociception is physiological and responds to usual analgesics while NP is due to lesion within the nervous system where normal non – painful stimuli as brushing or air puffing become painful resulting in tactile allodynia. Different types of NP: 1) Mechanical: as in carpal tunnel syndrome 2) Metabolic: as in diabetic neuropathy 3) Neurotoxicity: as in chemotherapy 4) Viral: as in HIV
5) Inflammatory: as in MS (Raina et al., 2012).

NP does not respond to traditional treatment and does not subside from itself. There is malfunction of physiological processes of both peripheral and central nervous systems, sometimes, it is even not correlated to tissue injury or inflammatory processes. The main differences between nociceptive physiological pain and neuropathic pain are: physiological pain is protective against the injury that happens due to the exposure to acute thermal, chemical, inflammatory or mechanical stimulus, and this pain stops gradually when painful stimulus stops while neuropathic pain is aimless and happens due to injury of either or both central nervous system (CNS) and peripheral nervous system (PNS). It is usually chronic and remains for long time where sensory signals are abnormal. Parkinson's disease may cause NP. This pain is due to cellular modifications and neuroplasticity where neurons may have alterations in their function & structure due to the exposure of painful stimulus in either the CNS or the PNS (Pasero, 2004).

CNS injury leads sometimes to maladaptation of bodily functions making the normal balance between excitatory and inhibitory signals disruptive. Thus, more excitation and less inhibition exist within the nervous system leading to central sensitization to signals within the spinal cord (Alles & Smith, 2018).

There are multiple factors affecting conveying nociception in the spinal cord by enhancing or lessening it. Such as:

Interneurons which may be excitatory or inhibitory, stimulation of NMDA receptors, descending brainstem pathways either inhibitory or facilitatory (which may interchange in case of pathologies) (D'Mello & Dickenson, 2008).

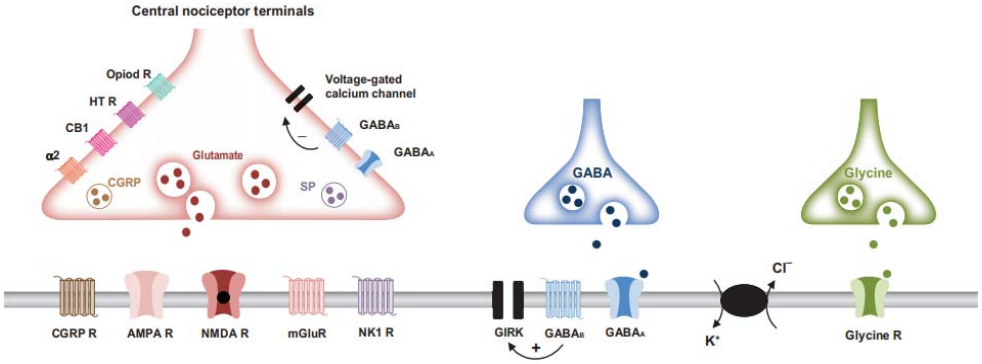

Fig. (8): Dorsal horn signals involved in nociception. During painful stimuli, glutamate and neuropeptides are released. Receptors on which glutamate has action are: postsynaptic (AMPA) α-amino-3-hydroxy-5-methyl-4-ioxazolepropionic acid and (mGluRs) metabotropic glutamate receptors. (NMDA) N-methyl-D-aspartate is a type of glutamate receptor implicated in pain. (GABA) γ-aminobutyric acid and glycine are inhibitory neurotransmitters.
α2 and α2-adrenergic receptors ; CB1 cannabinoid receptor ; CGRP calcitonin gene related protein ; GIRK G-protein–gated inwardly rectifying potassium ; HTR hydroxytryptamine (serotonin) receptor ; KCC2 potassium chloride cotransporter isoform 2; NK1 R neurokinin 1 receptor; opioid R opioids receptors; SP substance P (Inquimbert & Scholz, 2012).

Note. From Basic Neurochemistry (Eighth Edition, p.931), by P. Inquimbert and J. Scholz., 2012, Academic Press. Copyright 2012 by Elsevier.

Evoked pains where an ordinary physical stimulus produces an unusual or exaggerated sensation of pain include allodynia and hyperalgesia. Allodynia is a kind of pain due to a stimulus, which does not normally provoke pain. Temperature or physical stimuli can provoke allodynia, and it often occurs after injury to a site (Roy & Ghosh, 2013).

Mechanical allodynia is the occurrence of pain when touch carrying A fibers are stimulated and have change in their structure and release excitatory neurotransmitters as substance P leading to painful sensation in absence of painful stimulus (Millan, 2002; Sandkühler, 2009).

NP has different forms either continuous or episodic, as a response to a stimulus or spontaneous or a mix of all of these. It is usually moderate to severe. Pathology in the Spinothalamic tract plays a role in pain sensation especially of cold thermal origin (Garcia et

al., 2016).

NP is still not a clear disease. It causes much stress and suffering for patients (Liu et al., 2019).

During wearing off, pain represents 50 % and chronic pain (which duration is more than three months) represents 70 %. This pain responds to Levodopa. One point that differentiates between central pain and other types, is that central pain appears only in the off state while other types of pain [including also central] are exaggerated during the off state (Young Blood et al., 2016).

4. Dopamine role

When the level of dopamine falls, painful symptoms appear in high percentage of Parkinsonian patients. Dopamine is a catecholamine neurotransmitter that is familiar for its action on movement function and cognition and involved in reward system. Spinal cord receives dopaminergic projections. Dopamine is synthetized from L-Tyrosine amino acid, using Tyrosine Hydroxylase to be converted to L-Dopa. After that, L-Dopa is decarboxylated by Dopa decarboxylase. In a part of neurons, dopamine may be converted into norepinephrine. There are some brain structures as PAF have less dopamine active transporters (DATs). In these structures, dopamine is reuptaken by noradrenergic terminals. Postsynaptic neurons and glial cells produce catechol-O-methyl transferase in the extracellular compartment (COMT). Presynaptic neurons do not have COMT. Dopamine receptors are metabotropic G protein – coupled ones. D1 and D5 receptors are excitatory via coupling to stimulating Gs proteins while D2, D3 and D4 receptors are inhibitory via coupling to inhibitory Gi proteins (Wood, 2008).

4.1. Dopaminergic receptors and projections:

Descending pathways modulate pain either by enhancing or impeding pain transmission within either the spinal cord or the medullary dorsal horn. These effects take place due to the release of monoamines (Serotonin, Norepinephrine and Dopamine). Dopamine has 5 receptors: D1, D5, D2, D3 and D4 (Liu et al., 2019).

There are two families of dopamine receptors, D2 like ones (D2, D3 and D4) and D1 like ones (D1 and D5). D2 family stimulation leads to the inhibition of adenyl cyclase (AC) through Gi/O while D1 family stimulation leads to augmentation of AC production via Gq. Thus, stimulation of D2Rs (dopamine 2 receptors) decreases neuronal activity while stimulation of

D1Rs increases it (Millan, 2002).

Major dopaminergic projections are from substantia nigra pars compacta, ventral tegmental area, and hypothalamus towards nigrostriatal, meso-cortical, mesolimbic and tuberoinfundibular regions mediating various non- motor symptoms as sleep and pain. VTA also projects to: amygdala, hippocampus, olfactory bulb, and cingulate cortex. Dopamine plays a big role in pain modulation at various levels such as spinal cord, periaqueductal grey, basal ganglia, thalamus, and cingulate gyrus. It was found that when D2 receptors are blocked, serotonin is not secreted. Studies found that serotonin plays a role in pain processing in different brain areas as insular, prefrontal, and cingulate cortices (Fil et al., 2013; Skogar and Lökk, 2016; Li et al., 2019).

The spinal cord receives dopaminergic neurotransmitter from cerebral areas and (SNpc and paraventricular nucleus of hypothalamus (PVN) for minor projections), however, A11 hypothalamic area is the main origin of descending dopaminergic pathways (Millan et al., 2002).

Descending modulatory fibers from higher structures to spinal cord include noradrenergic, GABAergic, serotonergic, and dopaminergic ones. NA (Noradrenaline), serotonin and GABA roles are included in many studies. Dopaminergic neurons from Hypothalamic A11 area are the main source of spinal cord dopamine and give projections to all spinal cord levels. Both primary nociceptors and spinal neurons across various laminae have dopaminergic receptors i.e., dopamine interacts pre and post synaptically to modify nociceptive processes. D2 like receptors have anti-nociceptive effects while D3-like receptors have pro-nociceptive ones (Puopolo, 2019).

4.2. ***Treatment:***

It is suggested that neuropathic pain is caused due to the interaction between different mechanisms, thus a need for multimodal treatment is more effective (Sandkühler, 2009).

There are alleges that even dopamine receptor agonist treatments lead to cellular toxicity aggravating neurodegeneration. New therapies now are being tried such as anti-inflammatory medications to protect from the effect of oxidative stress. Up to this moment, there is no definitive PD treatment proved effective in Phase III clinical trials (De Miranda & Greenamyre, 2017).

For treatment of neuropathic pain, there are many trials. Up till now we lack an effective medication due to various etiologies, ethnicities, pathologies of the disease, genetic discrepancies, epigenetic adjustments, and differences between the efficacy of medications between rodents and humans. First line ones are Tricyclic antidepressants, Serotonin – noradrenaline uptake inhibitors as pregabalin. Second line medications as opioids, for example tramadol. Third line treatments as cannabinoids. Fourth line medications as methadone and botulinum toxins (Alles & Smith, 2018).

NP can be treated with dopaminergic agonists as it is most probably due to medial spinoreticulothalamic pathway dysfunction; if patients aren't responsive to this treatment; analgesics, opiates and tricyclics may be tried (Fil et al., 2013; Skogar and Lökk, 2016).

Microglia and astrocytes have pro-inflammatory role. Thus anti-inflammatory medications play a role in neuropathic pain treatment (Sommer et al., 2018).

The new advances in medications in treatment of NP pain makes the resort to surgical procedures less likely except in cases which are resistant to medications or suffering from severe drugs side effects. Surgery depends on the ablation of certain areas of structures of pain matrix to interfere with pain pathways. Also, deep brain stimulation, spinal infusion of analgesics or trying implants releasing analgesics such as opioids might be used (Garcia et al., 2016).

Around 50% of PD patients take medications for pain. There is no consistency over the efficiency of Levodopa as dopamine replacement therapy in PD patients. Levodopa is used to check if the patient responds to dopamine treatment or not, but further assessment of the long-term effect of the medication should take place. Cannabinoid receptors in basal ganglion structures involved in pain render them anti-nociceptive impact, but no conclusive results are confirmatory of its effect until now (Buhmann et al., 2020).

Anticonvuslants Gabapentine and Pregabaline lead to the decrease of glutamate production, they may be used to treat central pain. Also, the anti-depressant Duloxetine has a role in PD central pain treatment, but it has been used with caution as it may cause psychosis and sedation. Lidocaine patches, Rotigotine and Accupuncture can be tried (Buhmann et al., 2020).

Dopamine Reuptake Inhibitor as Bupropion lessens mechanical allodynia. On the other side, drugs having serotonergic action as Fluoxetine and drugs with Norepinephrine activity as Reboxetine or with both NA/Serotonin one as Venlafaxine are not effective in treating allodynia (Wood, 2008).

Bromocriptine increases pain threshold. Ropinirole and Pramipexole are D3/D2 receptor agonists with very few affinities for D4 and no affinity for D1/D5, serotonin, histamine acetylcholine, muscarinic, opioids or adrenergic receptors. A study in 2008 failed to show the effect of Ropinirole significantly due to small sample size but there was a therapeutic effect achieved that showed that it may influence pain (Wood, 2008).

L-Dopa in high dosage was found to aggravate oxidative stress worsening PD. On the other side, Ergot dopamine agonists, are known to scavenge free radicals protecting neurons. Ropinirole, which is non- ergot dopamine agonist- also scavenges free radicals. The main mechanism of Ropinirole neuroprotection is through glutathione , catalase and superoxide dismutase activation mediated through D2Rs (Iida et al., 1999).

Ropinirole is (4-[2-(dipropylamino) ethyl] – 2- indolinone monohydrochloride). Some studies have shown that bromocriptine was more potent than ropinirole in rodents' PD models while ropinirole was more potent in non- human primates' PD model. Ropinirole binds to D2 like receptors with avoiding ergot – like side effects. Ropinirole activates D2 receptors in CNS and PNS. The efficiency of ropinirole was better than bromocriptine after 3 years treatment. In different animal models, ropinirole had antiparkinsonian effect (Fukuzaki et al., 2000).

Ropinirole treats PD symptoms in laboratory studies and clinical trials. Ropinirole antiparkinsonian effect depends on both D2R and D3R. Side effects are: peripheral edema, less neuropsychiatric effect (hallucinations) and decreased somnolence (Matsukawa et al., 2007).

Eventually, Ropinirole -as dopamine agonist- is effective as a therapy for early and progressing PD symptoms including pain in PD models. Unilateral injury led to bilateral dorsal horn spinal cord neurons hyperexcitability and augmented D2R function bilaterally (Shill & Stacy, 2009; Tang et al., 2021).

5. Markers involved in the mechanism of Neuropathic pain

Injuries or diseases in the CNS may cause imbalance between excitatory and inhibitory neurotransmitters, leading to more excitatory state and less inhibitory one leading to neuropathic pain (Alles & Smith, 2018).

5.1. Excitatory markers:

5.1.1 pERK (phosphorylated ERK):

MAPK (Mitogen activated protein Kinase) signaling pathway has a small G protein (RAS) and three protein kinases (RAF, MEK, ERK). Kinases are enzymes, which catalyze the transferal of phosphate groups from donor molecules to acceptors. When a ligand binds to a transmembrane protein, signaling pathway is initiated and ERK is translocated to the nucleus (McCain, 2013).

MAPK converts stimulus that is extracellular to different reactions inside the cell through inducing pre and post-transcriptional alterations of intended proteins. MAPK is a kind of serine/ threonine protein kinases that entails ERK (extracellular signal-regulated protein kinase) (ERK= p44/42 MAPK). ERK is implicated in cell proliferation, differentiation, and neuronal plasticity during adulthood. Painful skin stimuli lead to the production of pERK in dorsal root ganglion neurons and superficial dorsal spinal cord horn which is involved in hyperalgesia. Thus, under painful stimuli, pERK is produced during the process of neuropathic pain (Kim et al, 2005; Suzuki et al., 2013).

When there is a painful stimulus, pERK is stimulated within only one minute and is expressed in many neuronal structures as cytoplasm, nucleus, axons, and dendrites (Ji et al., 1999; Dieb et al., 2014-2015). pERK plays a crucial role in acute and chronic inflammatory neuropathic processes (Zhuang et al., 2005; Gao and Ji, 2009).

pERK also augments dorsal horn neurons NMDA and AMDA excitatory glutamate receptors' actions and decreases K+ channels inhibitory ones. pERK is transmitted into the dorsal horn nuclei for stimulating CREB (cAMP response element-binding protein) phosphorylation (transcription factor involved in long term plasticity). CREB regulates CFOS, cox-2, neurokinin 1, prodynorphin and nNOS which are decreased by MEK inhibitor (Gao and Ji, 2009).

5.1.2. CFOS:

The protooncogene protein, CFOS, is a molecular signature that is expressed in superficial and deep horn neurons under painful peripheral stimuli. CFOS is stimulated within more time, around 30-60 minutes. CFOS expression is only limited to neuronal nucleus. CFOS converts also extracellular signals to intracellular modifications. Normally, CFOS has low level of expression, which increases tremendously in the dorsal horn of spinal cord under stimulus with high threshold distributed in the layers receiving 1ry afferents from the hind paw. CFOS is a good marker for detecting painful stimuli as it is easily performed using immunohistochemistry and easily counted. Being confined only in nuclei makes it feasible to study concomitantly with other neuronal markers and tract tracers and thus C-Fos is a suitable marker being specific, fast, and durable (Gao and Ji, 2009).

Table (2): Laminae distribution of CFOS & pERK after acute stimulus (Gao and Ji, 2009)

Percentage	CFOS	pERK
Mostly	I - II	I - II
Few	III - IV	III - VI
Some	V - VI	
None		Ventral horn and contralateral side

5.1.3. PKCγ (protein kinase C- gamma):

PKCγ cells are translocated from cytoplasm to cell membrane on excitation. The role of PKCγ is achieved by production of excitatory neurotransmitters, changing conductivity of channels by phosphorylation and augmenting the trafficking of receptors to cell membranes (Sluka & Audette, 2006).

- There are 3 subgroups of PKC which belong to (serine/threonine) kinases:

(c) conventional isoenzymes: α, βI, βII, and γ isoforms: Ca++ and diacylglycerol dependent.

(n) novel isoenzymes: δ, ε, η, and θ: Ca++ dependent and diacylglycerol independent

(a) atypical isoenzymes: ξ and λ/ι: Ca++ and diacylglycerol independent

- PKC contribute to the processes of cell differentiation, proliferation, migration, and apoptosis. TRPV1 which plays a role in hyperalgesia is activated by different inflammatory products as prostaglandins and bradykinin via PKC. GABA neurotransmitters are decreased by substance P through PKC receptor phosphorylation resulting in less inhibition. Thus PKC has

multiple roles in promoting excitatory pathways or inhibiting inhibitory ones (Velazquez et al., 2007). PKCγ cells have multiple forms: central, vertical, islet, radial and unclassified (Wang et al., 2020).

NMDA receptors excitability leads to temporary hypersensitivity in spinal cord while chronic hypersensitivity is suggested to be due to modifications in 2nd messenger downstream systems. When the gene encoding PKCγ is deleted, the immediate processes responding to pain are normal but the allodynic reactions that occur after multiple days are abnormal. In the spinal cord dorsal horn, PKCγ is present in lamina II interneurons away from nociceptive projection neurons to CNS. PKCγ is crucial for long-term hypersensitivity and needed for the sensation of maximum allodynia. It is important for the sensitization of neurons existing in lamina V besides the interactions with various spinal cord circuits to activate NMDA receptors leading to persistent nociception. PKCγ have excitatory function as they lack inhibitory markers (Martin et al., 2001; Miraucourt et al., 2007). PKCγ and pERK ½ are crucial in the pathogenesis of neuropathic pain (Dieb et al., 2015).

Chronic mechanical allodynia pathogenesis involves PKCγ cells, which are present in excitatory interneurons in laminae IIi and III. PKCγ cells receive synapses from VGLUT1 axons including A – LTMRS (low threshold mechanoreceptors) and from inhibitory interneurons containing glycine in lamina III where parvalbumin (PV) cells are present. PKCγ cells and Lamina III inhibitory interneurons receive Aß afferents thus making feed-forward inhibitory circuit that inhibit low threshold mechanical input reaching PKCγ cells. Excitatory PKCγ cells make synapses with transient central cells located in Lamina II. These transient central cells synapse with vertical cells, which synapse with projection neurons in Lamina I. Thus, these connections form polysynaptic circuit in which tactile inputs from A-LTMRs may reach projection neurons in lamina I (Miraucourt et al., 2007; Todd, 2017).

PKCγ affect group of NMDA circuits in dorsal spinal horn leading to chronic persistent pain. Allodynia occurs when the inactive circuit in normal circumstances becomes activated. PKCγ cells are augmented in peripheral neuropathy diseases. PKCγ cells receive direct Aß fibers connecting them to superficial laminae neurons facilitating neuropathic pain through polysynaptic circuits and interneurons when inhibitory markers are blocked (Miraucourt et al., 2007). Tonic inhibition, because of cell inhibitory coupling keeps this connection non-noxious. In case of disease, nociception is perceived. This polysynaptic pathway is composed of PKCγ, glutamate decarboxylase 67 (GAD67) and PV cells (Ouachikh et al., 2018).

PKCγ cells are in lamina II mostly forming 1/3 of all neurons in medullary dorsal horn. PKCγ is present mostly on plasma membranes and near post synaptic densities normally (Peirs et al., 2014).

Gate theory of pain:

Lamina II inhibitory interneurons in the spinal cord dorsal horn prevents the communication between painful and non-painful signals. Effect of glycine as an inhibitor on Aβ excitatory fibers on PKCγ neurons renders a feed forward circuit that hinders signals from Aβ fibers to stimulate pain-modulating pathway. When a problem happens to this inhibitory circuit, Aβ fibers activate nociceptive pathway. Lamina II and III also have Parvalbumin expressing neurons inhibiting myelinated afferents having role in tactile allodynia (Lu et al., 2013; Wang et al., 2020).

5.2. Inhibitory neurotransmitters:

Pain occurs when inhibitory system is compromised:

1) If tonic inhibition decreases → spontaneous pain in dorsal horn neurons
2) Inadequate feed forward inhibition
3) Inhibitory interneurons: they normally stop excitatory deep touch signals from conveying to superficial painful fibers. Malfunctioning of this mechanism leads to allodynia.
4) Inhibition normally augments neuroplasticity threshold in response to pain preventing acute to chronic conversion of pain. Malfunctioning of this mechanism leads to allodynia.

Major inhibitory markers are: GABA (gamma amino buteric acid), Glycine, Opioids (Enkephalins and Dynorphin), besides, monoamines 5-hydroxytryptamine from RVM and NA from locus coeruleus. The synthesis, storage and production of these neurotransmitters or cell death; change inhibitory markers level (Sandkühler, 2017).

Astrocytes, microglia, and vascular cells and may be mast cells have GABA receptors. Inflammation within the nervous system modulates inhibitory system in spinal cord dorsal horn (Sandkühler, 2017).

Inhibition could be transformed into excitation by:

1. Modifications in driving forces of ions through postsynaptic plasma membrane; modulating the ion flux via neurotransmitter receptor channels.

2. Removal of the inhibition (i.e. disinhibition) of polysynaptic excitatory circuits between deep tactile lamina and superficial nociceptive lamina in spinal dorsal horn leading to conveyance of touch sensation in the form of pain (Sandkühler, 2017).

5.2.1. GABA and Glycine:

GABA receptors are of two types: GABAA and GABAB. GABAA has pentameric ionotropic ion channels formed of 18 various subunits having inhibitory effect through chloride permeability. GABAB receptors are metabotropic heterodimers that increase K+ availability and decreases Ca++ leading to inhibition of neuronal activities. GABA receptors are present in superficial laminae of dorsal horn of spinal cord in the endings of PAFs and PNS. They are related to the pathogenesis of multiple neuropsychiatric diseases. GABA has excitatory function during development while it has inhibitory function after maturation (Millan, 2002; Li et al., 2019).

Therefore, there is direct inhibition of painful stimuli by inhibitory GABAergic signals acting on projection neurons, in addition to the descending inhibitory serotonergic pathways, which stimulate GABAergic inhibitory interneurons in the dorsal spinal cord horn. Descending noradrenergic pathways have GABA colocalized with NA in their neurons; besides the colocalization of GABA with histamine in histaminergic neurons of tuberomammillary nucleus giving various sources of GABA from higher structures to suppress pain in dorsal horn. Glycine receptors mimic GABAA receptors in structure; they have pentameric form, chloride permeable and decreases neuronal pain. Inhibitory interneurons also have glycine; in addition, RVM descending inhibitory pathways have glycine leading to an inhibitory effect in dorsal spinal horn. Dorsal horn has neurons containing GABA colocalized with Glycine, in addition to descending inhibitory pathways entailing both GABA and Glycine in their neurons, besides their colocalization in inhibitory interneurons as well. Glycinergic neurons are found within projection neurons within deep SDH laminae and might also be present in superficial laminae within PAF. Thus, Glycine and GABA neurotransmitters and receptors collaborate to inhibit nociceptive inputs in the dorsal spinal horn. GABAergic neurons inhibit brainstem cells. Theoretically all monoaminergic cells are inhibited by GABA and Glycine (Millan, 2002).

GAD67 (67KDa) is a cytoplasmic protein that synthesizes 90% of GABA. GABA is synthesized by both neurons and glial cells. It is synthesized by GAD65 and GAD67. GAD65 is a protein associated with cell membrane releasing vesicular GABA from axon terminals. Neuronal and glial cells mobilize GABA to inside cells from the extracellular space. This is due to GABA transporters having elevated affinity to GABA. Inside the cells,

GABA is transformed into glutamate via GABA transaminase followed by the transformation into glutamine by glutamine synthase. Glutamine enters neurons as a substrate for GABA or Glutamate.

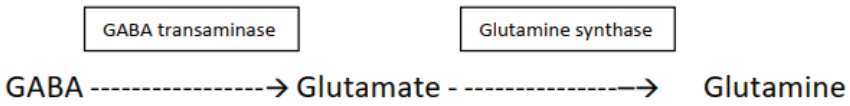

Thus forming (GABA- Glutamate -Glutamine) cycle based on concentration feedback mechanisms (Gwak & Hulsebosch, 2011; Li et al., 2019).

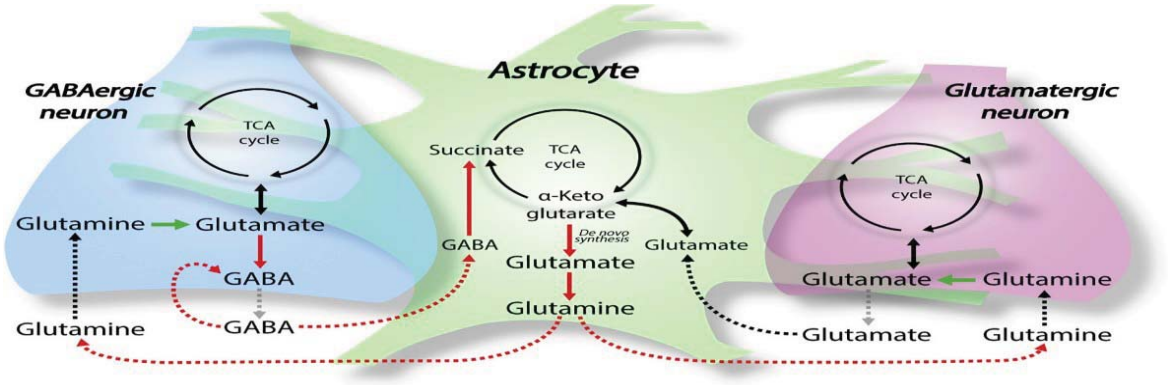

Fig. (9): Showing (GABA- Glutamate -Glutamine) cycle.

Note. From "Deficient astrocyte metabolism impairs glutamine synthesis and neurotransmitter homeostasis in a mouse model of Alzheimer's disease," by J.V. Andersen, 2021, Neurobiology of disease, 148, 105198, p.10 (https://doi.org/10.1016/j.nbd.2020.105198). Copyright 2021 by Elsevier.

Catalysis of GABA-by-GABA transporters (GAT-1,2,3 and 4) is responsible for its metabolism. Catalysis removes extra GABA. GABA plays inhibitory role in CNS, as in cerebral cortex, hippocampus, and spinal cord. GAD65 is present mostly in lamina I and lamina II while GAD67 is mainly present in deeper laminae (Li et al., 2019).

5.2.2. VGAT and GAD:

Vesicular GABA transporter (VGAT) transports GABA which is newly synthesized from cytosol to synaptic vesicles. Unilateral 6-hydroxydopamine (6-OHDA) led to increased VGAT mRNA in striatopallidal and decreased VGAT mRNA in striatonigral neurons while L-Dopa in subchronic doses led to augmentation of VGAT mRNA levels bilaterally, also VGAT was increased in striatonigral neurons. VGAT is transported from cytosol and synaptic vesicle cavity. VGAT was explicitly expressed in rodents' GABA neurons' synaptic vesicles inside the brain. VGAT was expressed too much in L-Dopa treated rats. Chronic dopaminergic neurons degeneration led to increased vesicular GABA release (Wang et al., 2007).

5.2.3. Parvalbumin:

Parvalbumin cells represent a marker for neurons that release both GABA and Glycine. This cell subtype has been shown to be electrically connected (Ouachikh et al., 2018), and forms a gate pathway for non-noxious stimuli to reach the nociceptive pathway. PV neurons synapse onto PKCγ excitatory neurons of the SDH (Petitjean et al., 2015).

D2R changes led to changes in Parvalbumin interneurons expression playing a role in multiple neuropsychiatric disorders (Graham et al., 2015).

6. Thermal and mechanical allodynia

Nociceptors are the nerve endings of specialized peripheral sensory neurons having various ion channels. They become stimulated by thermal, mechanical, and chemical stimuli. In neuropathic pain, there is augmented sensitivity to different stimuli. Besides peripheral sensitization, the central nervous system neurons are malfunctioning. While pain is protective, chronic pain is aimless and sometimes non-painful stimuli become painful (allodynia). This pain may persist for long time, i.e., chronic. When nociceptors are stimulated, successive action potentials occur conveyed to CNS, then encoded into information about the onset, for how long, territory, strength and type of stimulus leading to reflex action or certain sensation (Viana, 2018).

There are two types of nociception either non- stimulus or stimulus evoked. Non-stimulus as: grimace scales, burrowing assays, gait analysis, weight bearing and automated behavioral analysis, while stimulus evoked as: mechanical stimuli (e.g.: Manual and electric Von Frey Test (VFT), Randall Selitto test), thermal stimuli (e.g., acetone), chemical or electrical. Non-stimulus evoked nociception (pain without stimulus) may be more relevant to human conditions than stimulus evoked measures (Barrot, 2012; Deuis et al., 2017).

6.1. Cold allodynia:

Acetone application leads to skin cooling to 15-21 degree Celsius. Although rats may have olfactory response to acetone not only pain, acetone test is validated in many neuropathic and inflammatory pain models. Acetone test can be unilateral and in bilateral cases it is more ethical to be used, and certain behavior is scored. Acetone evaporation leaves cold sensation which is painful in case of pathology (Barrot, 2012; Deuis et al., 2017).

Painful cold stimulus activates various brain structures mainly contralateral and ipsilateral posterior insular cortex and ACC. Modulation in voltage gated Na+ channels leads to acute pain while chronic pain involves pain matrix functional and structural plasticity (Viana, 2018).

Cold allodynia is found in multiple neuropathic and inflammatory pain pathologies. Specific artemin receptor, glial cell line- derived neurotrophic factor family of receptors- alpha 3 (GFR α- 3), is involved in cold allodynia. Also, it may occur due to decrease of lkD in high – threshold cold thermoreceptors and also in TRPM8 nociceptors (Lippoldt et al., 2016; Gonzalez et al., 2017).

6.2. Mechanical Allodynia:

There are three categories of mechanical allodynia:

- Dynamic: brushing trigger e.g., Towels
- Punctate: Touch trigger e.g., VFT
- Static: (superficial, deep) pressure trigger e.g., finger or pressure algometer

Manual VFT is still a gold standard for mechanical allodynia, designed by Maximilian Von Frey (physiologist). In manual VFT, animals are not restrained leading to less stress in which there is a certain threshold which initiates an avoidance behavior. So either the stimulus has increasing value or fixed stimulus successively (Barrot, 2012; Deuis et al., 2017).

VF filaments are made of plastic, with length 5 cm and different diameters, in addition, being attached to an applicator. The hairs have blunt terminals. On a grid, they are applied until bending where fixed pressure is applied. When a certain filament cause paw withdrawal in disease model without withdrawal in control; this shows mechanical allodynia (Barrot, 2012).

7. Animal Models

There are two mechanisms for Animal Models either genetic where specific mechanisms known to induce PD are used but there is no apparent neurodegeneration and traditional phenotypes or neurotoxic such as 6-OHDA (Dawson et al., 2010; Welchko et al., 2012).

P.O.C. / Neuro-toxic Model	Motor Symptoms	Nigrostriatal Lesion	Lewy Body Formation	Functions	Negative aspects of the model
6-OHDA Neurotoxin	Unilateral lesion: rotational behavior	Dopaminergic Cells are degenerated at lesion site	No inclusions, few synuclein present	Search PD mechanisms and treatments	Needs expertise for intracerebral Injections, high mortality in bilateral model
MPTP Neurotoxin	Motor deficits	Dopaminergic Cells are degenerated at lesion site	Few inclusions and synuclein immunopositive	Search PD mechanisms and treatments, can be used in bilateral PD models. Crosses BBB	Non progressive model, functional recovery occurs and rats are resistant
Rotenone Pesticide	Less motor activity	Loss of dopaminergic neurons	Synuclein immunopositive in dopaminergic	Search treatments and side effects of pesticides	High mortality rates and human toxicity
Paraquat And Maneb Herbicide and fungicide	Some motor impairment	Loss of dopaminergic neurons	No inclusions with Synuclein immunopositive in dopaminergic neurons	Search treatments and side effects of pesticides' exposure	Affecting other neurotransmitters, human toxicity Isn't well established and parquat causes pulmpnary fibrosis in big doses
Alpha-synuclein	There are motor impairments	Not much dopaminergic degeneration	Synuclein immunopositive in dopaminergic neurons	Get more insight about synuclein accumulation	Not much dopaminergic degeneration
LRRK2	Less motor impairments	Not much dopaminergic degeneration	None	For testing the role of LRRK2 mutations	Not much dopaminergic degeneration

Table (3): showing different neurotoxic PD animal models (Duty and Jenner, 2011; Blesa et al., 2012; Konnova and Swanberg, 2018).

Our model, which is 6-OHDA; was 1st used in the 1950s. 6-OHDA degenerates dopaminergic and nor- adrenergic neurons. Noradrenaline reuptake inhibitor (e.g., Desipramine) is used to protect noradrenergic neurons from the toxic insult. 6-OHDA structure is similar to dopamine except that it has extra hydroxyl group rendering its toxic characteristics. The effect of lesion depends on multiple factors: 6-OHDA concentration injected, location of injection and animal species tested. This model leads to depletion of dopamine, death of nigrostriatal fibers and changes in neurobehaviors. 6-OHDA does not produce Lewy bodies although there is information that 6-OHDA has interaction with α-synuclein. Bilateral 6-OHDA injections leads to aphagia, adipsia and death (Tieu et al., 2011; Blesa et al., 2012). 6-OHDA model gives insight into various non-motor symptoms, emotional and cognitive functions (Campos et al., 2013).

6-OHDA is hydroxylated dopamine analog that makes chemical denervation "i.e., neurotoxic molecule which targets certain cell group". It is used to induce nigrostriatal dopaminergic system lesion. Plasma membrane transporters, dopamine transporter and noradrenergic transporter have high affinity for 6-OHDA. 6-OHDA accumulates into neurons leading to its oxidation producing ROS (reactive oxygen species) leading to cytotoxicity. For by passing BBB, 6-OHDA is injected into certain brain structures via stereotaxic surgery. Rats are most commonly used than mice for easier access to structures. The percentage of neurodegeneration depends mainly on the site of injection. 6-OHDA can be injected into: substantia nigra, MFB (medial forebrain bundle): region where dopaminergic nigro-striatal tract ascends, or striatum. Nerve terminals are more sensitive than other nerve structures (axon and neuron body) in response to degeneration caused by 6-OHDA. In models where SN or MFB are lesioned, total, and fast neurodegeneration of the nigrostriatal pathway occurs. 6-OHDA injection in SN leads to dopaminergic neurons loss after 12 hours while in striatum, the loss occurs after 2-3 days. In MFB model, striatal terminals are lost before dopaminergic ones. 6-OHDA doesn't show age progression in PD nor Lewy bodies (Duty & Jenner, 2011; Tieu et al., 2011). 6-OHDA is transported inside the cells via DAT (Nass and Chen, 2008).

The percent of lesion can be known from counting Tyrosine hydroxylase (TH) – positive cells in SNpC and performing behavioral tests. High 6-OHDA dose leads to complete (> 90%) lesion. The complete lesion model is mostly done using SNpC or MFB lesions. The SNpc (A9) dopaminergic cells are lost in this model more than VTA (A10) dopaminergic ones (Duty & Jenner, 2011).

Motor dysfunction occurs in contralateral limb. 6-OHDA is the most commonly used model in rats due to their suitable size and feasibility of noticing their behavioral changes. In experiments, mechanical, thermal, chemical, and cold hypersensitivities were observed

confirming having a valid model. These alterations in nociception appear after 1 week from the lesion and remain for about 12 weeks indicating stable changes and plasticity for long time. The behavioral alterations are seen bilaterally due to bilateral supraspinal processes at the brainstem under modifications of the upper dopaminergic systems (Buhidma et al., 2020).

8. Fluorescence Tracers

Dextrans as tetramethylrhodamine label parts of neurons (cell body, axons and dendrites) and is transported in anterograde manner. Also, macrophages and blood vessels pericytes are labelled. Some studies have shown retrograde and anterograde functions of fluorescent – conjugated dextrans.

Tetramethylrhodamine conjugated dextrans, can be uptaken and transported by both intact and injured axons in the area of the injection site (Nance & Burns, 1990).

Schmued and Heimer (1989) study showed that 10,000 molecular weight dextran was transported axonally in anterograde manner (e.g., was transported from the hypothalamus to the spinal cord).

When dextrans were injected, retrogradely, few cell bodies were labelled, and more fibers of passage were labelled as well. Range of concentration (2-20%) for 3-14 days was injected, which was adjusted depending on the region of the target structure, the presence of main fibers bundles and the needed transport distance. The anterograde marker was efficient but there was a potential for transport by axons and fibers of passage and damaged axons (Nance & Burns,1990).

FluoroRuby is found to be stable for months in the nervous system, without toxicity and kept within target structures and being used for anterograde labelling in axons and terminal efferents (Bowyer & Schmued, 2006).

In rat CNS, FluoroRuby (FR) can be used mainly for anterograde, and for retrograde labelling. The injection can be manipulated using pressure or iontophoretically. Tissues can be examined under microscope directly and other techniques can be used concomitantly at the same time. The tracers are taken by neurons and transported by axons to examine connections between certain brain areas. Fluorescent techniques are easy, highly sensitive and can be compatible with some other techniques. Anterograde tracers are less commonly used due to some limitations. Famous Fluorochromes as dextrans labelled with fluorescent dyes as Fluorescein, Rhodamine B, Tetramethyl Rhodamine or Texas Red are used. Dextrans can be conjugated to lysine molecules and can be fixed in formalin (Schmued et al.,1990).

Cells of SNpC are dopaminergic while the majority of substantia nigra pars reticulata (SNpr) are non-dopaminergic. Due to SNpc being thin, there is little staining in pars reticulata or dorsal tegmental part (Beckstead et al., 1979).

Literature Review – Fluorescence Tracers

Dopaminergic innervation is present in the spinal dorsal horn and intermediolateral cell column from A11 diencephalic region. The fibers between diencephalon and spinal cord are uncrossed. Also, dopaminergic fibers may be descending within lateral funiculus. SDH receives dopaminergic innervation from hypothalamic A11 region which acts as D2 receptors (Skagerberg et al., 1982; Domenici et al., 2019).

Dopaminergic neurons are marked using tyrosine hydroxylase. A11 group from diencephalon projects to multiple segments of the spinal cord. FG (Fluorogold) present posterior to substantia nigra and within VTA and red nucleus (Qu et al., 2006).

PAG receives inputs mainly from nucleus cuneiformis and susbstantia nigra. The 4 subdivisions of it receive inputs from brainstem and higher CNS. PAG is involved with analgesia in rats. Also, spinal dopaminergic pathway might be implicated in nociception that could be reversed with dopamine. In addition, the reticular hindbrain nuclei (reticular formation) are implicated in pain (Chudler and Dong, 1995; Liang et al., 2011).

Besides, PAG (ventrolateral region) was involved in pain where dopaminergic and GABAergic neurons are interconnected. Dopamine, Noradrenaline and Serotonin are all involved in pain modulation by decreasing their amount. Increase GABA in vlPAG might be due to compensatory mechanism. Chronic pain in Parkinson's disease is due to disequilibrium between descending inhibitory and excitatory (facilitatory) pathways. GABA dysregulation in vlPAG might lead to excitation of descending facilitatory system, decreasing spinal opioids causing painful sensation (Domenici et al., 2019).

Material and Methods

Material and Methods – PD model lesion

1. Animals

81 male Sprague- Dawley rats (Charles River, France) initially weighing 280 – 350g were bred in the Animal House at Clermont Auvergne University, Clermont-Ferrand, France to be used in the present experiments. The animals were dealt with according to ethical guidelines of the animal ethics committee of Clermont Auvergne University (APAFIS#19965-20190325052285) and according to guidelines of the CARE (Committee of Animal Research Ethics) of faculty of medicine, Ain-Shams University. The concept of 3R (Reduction, Replacement and Refinement) was addressed throughout all the experiments. The animals were housed in suitable environment; at EOPS (Free from Organisms Specific Pathogens) facility, 3 rats/cage, they had free access to food pellets and water. All animals were exposed to 12 hours light-dark cycle, good ventilation and suitable temperature 22°-25° C and humidity 55 ± 10%. Animals were habituated for one week before experiments. At the end of experiments, animals were anaesthetized and euthanasia was done by decapitation. After that, dissection of the required tissues took place and disposal of animal remnants was done following French local rules.

2. Experimental Design

2.1. Study Groups:

81 Rats were used in the present study. The rats were divided into 3 groups. Each group consisted of 27 Rats.

Group I (Sham): Sham operated (rats undergoing the same operation for inducing Parkinson's disease model except being injected with saline instead of 6 – OHDA neurotoxin in Medial Forebrain Bundle - MFB), subjected to non-painful cold stimulus (acetone).

Group II (6-OHDA-lesioned): Parkinson's Disease rat model, injected with 6 – OHDA neurotoxin, subjected to non-painful cold stimulus (acetone).

Group III (6-OHDA-treated): Parkinson's Disease rat model treated with Ropinirole (5 mg/ kg/ml) (Tremblay et al., 2017) {intraperitoneal injection; 30 minutes before behavioral tests and before the sacrifice of rats} and subjected to non-painful cold stimulus (acetone).

In each group, the following structures were examined:
A: Insular Cortex
B: Cingulate Cortex
C: Spinal Cord dorsal horn

2.2. Statistical Analysis:

The results were expressed as median ± interquartile range and some as mean ± SEM. Statistical analysis was performed using Student's t-test for parametric data and Mann-Whitney test for non-parametric data when c omparing two groups together. Also, one-way ANOVA was used to compare the three group, followed by Tukey's posthoc multiple comparisons test for parametric data and the Kruskal -Wallis test, followed by Dunn's posthoc multiple comparisons test for non-parametric data .Two-way ANOVA, followed by Sidak's posthoc multiple comparisons test and Friedman's test were used when convenient. The level of significance was determined at P value ≤ 0.05 except if stated otherwise. Data were analyzed using GraphPad Prism Software (v.8.0.2) and SPSS (v. 1.0.0.1447). Fixed-effect model ANOVA was used as variables were fixed factors in the experiment. Also, in the two-way ANOVA analysis, variables were fixed factors in both rows and columns factors.

3. Surgical procedures

3.1. Table (4): Pharmaceutical Substances used:

Substance	*Dose*	*Route of administration*	*Manufacturing company*
Ketamine KETAMINE 1000	60 mg/kg/ml	intraperitoneal	VIRBAC, FRANCE
Xylazine Rompan 2%	10 mg/kg/ml	intraperitoneal	Bayer, France
6-OHDA	3 µg/µL	intracerebral	Sigma-Aldrich, France
Desipramine	25 mg/kg/ml	subcutaneous	Sigma-Aldrich, France
Ropinirole	5 mg/kg/ml	intraperitoneal	Sigma-Aldrich, France
Fluororuby	10 %	intracerebral	Fisher Scientific, USA
Ascorbate Saline	0.02 %	Vehicle for 6-OHDA	Sigma-Aldrich, France

Material and Methods – PD model lesion

3.2.Parkinson's disease model lesion surgery:

3.2.1. Anesthesia

Rats were weighed at the day of surgery and handled gently, xylazine (10 mg/kg) was injected intraperitoneally. After 5 minutes, Ketamine (60 mg/kg) was injected intraperitoneally for deep anesthesia. To preserve adrenergic neurons from 6-OHDA toxicity, animals received desipramine (25 mg/kg, i.p., Sigma-Aldrich, France) 30 minutes prior to the toxin injection to keep the level of Noradrenaline the same (Charron et al., 2014).

3.2.2. Stereotaxic Surgery:

- The workflow platform was prepared as follows:

  The stereotaxic frame (David Kopf Instrument, CA, USA) was cleaned, clean tissues were put on the platform, the injecting syringes were cleaned with saline and the syringe used for 6-OHDA injection was covered with aluminum foil as it is photosensitive.

- The rats' hair on the head was removed using a razor and then disinfected with betadine.
- A vertical line was drawn on the scalp skin and an incision was done with a clean razor, bleeding was stopped using cotton buds soaked in oxygenated water.
- Rats were fixed on the fixing bars (2 lateral for the ears and one in the front for the teeth).
- A clamp was being put to retract rats' head incised skin.
- The apparatus coordinates from Bregma was adjusted to target the median forebrain bundle bilaterally as follows:

At tooth bar + 3.4

Anterior (A) −4.0

Lateral (L) ± 0.8

Ventral (V) -8.0

At tooth bar −2.4

Anterior (A) −4.4

Lateral (L) ± 1.2

Ventral (V) −7.8

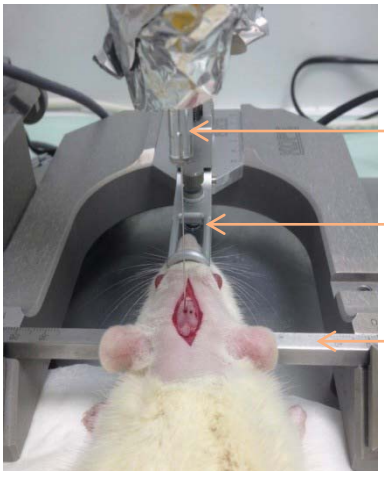

- A drill was used to make holes bilaterally corresponding to the above coordinates.

Material and Methods – PD model lesion

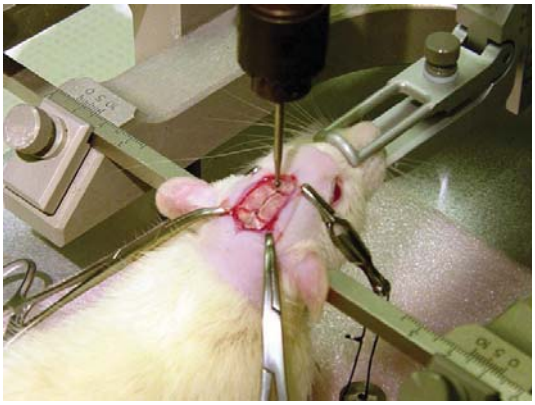

- 6-OHDA was injected (using Hamilton Syringe, Thermo Fisher) at rate (0.25 µL/min), dissolved in a vehicle solution (0.02 % ascorbate saline) at a concentration of 3 µg/µL (Sigma-Aldrich, France) in two deposits (final volume= 2.25 and 2.85 µl), at tooth bars +3.4 and −2.4 respectively for 6-OHDA lesioned rats. Sham-lesioned rats received only the vehicle at the same coordinates (Desipramine was given 30 minutes subcutaneously prior to the surgery).
- The injection syringe was retracted (1 mm/ minute slowly).
- After that, the head wound was closed with surgical knots and the rat was kept on heating pad until it recovered from anesthesia, then it was kept in a separate cage until it was fully recovered.
- Bilateral lesions of the MFB caused aphagia and/or adipsia and animals' weight was checked daily after surgery. 6-OHDA lesioned rats were weak and not capable of feeding themselves. They were fed (wet food pellets + water) using syringe feeding two times per day, for 8–10 days.

Material and Methods – Fluorescent Tracing Technique

3.3. Fluorescent tracing technique:

Substantia nigra was injected bilaterally in various medial to lateral divisions of the pars compacta (during 15 minutes each side) with 10% Tetramethylrhodamine Dextran - 10,000 Molecular Weight- Lysine Fixable (Fluororuby) in different volumes. Areas receiving these injections were traced. At first 2 microliter was tried, then 1 microliter was injected. Due to wide spread of fluorescence, a more precise volume was eventually used which was 0.5 microliter.

Different Substantia Nigra coordinates:

1) Toothbar: 3.3
   A: 5.4, L: 2.2, V: 7.5

2) Toothbar: 3.3
   A: 5.4, L: 2, V: 8

3) Toothbar: 3.3
   A: 5.4, L: 2.4, V: 7.6

4) Toothbar: 3.3
   A: 6.12, L: 1.6, V: 8.4

Different cut sections were taken at the level of Substantia nigra, PAG and Spinal cord cervical segments. Some sections were stained immunohistochemically with primary monoclonal antibody solution (1:5000 mouse anti-TH, Sigma-Aldrich, France) Tyrosine Hydroxylase and then secondary antibody (1:500 goat anti-mouse 488) is added to check dopaminergic fibers in double staining with Fluororuby. These sections were photographed with motorized Zeiss Axioplan 2 microscope equipped with a Hamamatsu C4742-95 digital camera (Hamamatsu Photonics France SARL, Massy, France) (switching between FITC and Texas Red filter sets) driven by MetaMorph 5.4 software.

N.B. Substantia nigra lies posterior to cerebral peduncle and formed of median size uniform cells compacted dorsally in pars compacta more than in larger adjacent pars reticulata. There is a clear distinct even plane between pars compacta and reticulata. The only part with less distinction is the pars lateralis which lies in nigral lateral quarter (Beckstead et al., 1979). Artifacts: injections spread to nearby regions or dye taken by injured fibers passing through injected area (But practically the most affected area is the one near the injecting tip) (Chudler & Dong, 1995).

4. Immunohistochemistry

1. At the end of behavioral studies; 6-OHDA-lesioned, 6-OHDA-treated and sham groups were deeply anesthetized with ketamine (60 mg/kg) and Xylazine (10 mg/kg) i.p. and were transcardiacally perfused with saline followed by 4% paraformaldehyde in phosphate buffered saline (PBS).

2. Brains and spinal cords were then removed and placed in 30% sucrose and 0.05% sodium azide solution overnight at 4°C.

3. Coronal sections (40 μm) were obtained using a freezing microtome and collected in 0.05 M Tris-buffered saline (TBS).

4- Free-floating sections were placed in 1% normal goat serum at room temperature for 1 hour before overnight incubation in primary antibodies, **Table (5)**:

Primary Antibody	Source	Mono/poly-clonal	Concentration	Company
anti-TH	mouse	monoclonal	1:5000	Sigma-Aldrich, France
anti–pERK	rabbit	monoclonal	1:200	Cell Signaling Technology
anti-GAD1	rabbit	monoclonal	1:1000	Cell Signaling Technology
anti- PKC γ	mouse	monoclonal	1: 500	Santa- Cruz Biotechnology
anti-CFOS	rabbit	monoclonal	1:2000	Cell Signaling Technology
anti-VGAT	rabbit	polyclonal	1:100	Sigma-Aldrich
anti-Parvalbumin	mouse	monoclonal	1:200	Sigma-Aldrich

5. After several rinses, sections were incubated with a secondary antibody **(Table 6)** for 2 hours at room temperature.

Secondary Antibody	Source	Concentration	Company
anti-mouse 488	goat	1:500	Cell Signaling Technology
anti-rabbit 555	goat	1:500	
anti-mouse 555	goat	1:500	
anti-rabbit 488	goat	1:500	

6. All antibodies were diluted in TBS containing 0.25% bovine serum albumin and 0.3% TritonX-100.

7. The sections were finally rinsed in TBS, mounted onto Thermo Scientific SuperFrost plus slides, slipped with Dako Fluorescence Mounting Medium.

8. The specificity of immunostaining was assessed by omitting primary antibodies which resulted in the absence of signals.

9. Photomicrographs of immunostained sections were captured using a motorized Zeiss Axioplan 2 microscope equipped with a Hamamatsu C4742-95 digital camera (Hamamatsu Photonics France SARL, Massy, France) -switching between FITC and Texas Red filter sets- driven by MetaMorph 5.4 software.

10. In each rat, image acquisition and fluorescent signal quantification were done using multiple sections depending on the structure taken. To lessen the degree of variability in staining between different sections, the same area of the target structure was taken into consideration for quantification of the fluorescent signal. The final data are presented as a mean value of the total sections of every group.

11. Spinal cord sections were taken from Lumbar (L3 -L6) spinal cord region and for the insular and cingulate cortices, a square area of equal dimensions is applied for all counted sections. Number of TH immunopositive cells was counted alone in SNpc, also in VTA alone and then added together.

12. The cells were quantified using multipoint cursor in ImageJ Software (ImageJ v1.6, National Institutes of Health, Bethesda, MD) where number of cells was displayed in results window.

13. The fluorescence intensity was measured using a method modified from Christine Labno (Integrated Light Microscopy Core, University of Chicago) using Image J software (ImageJ v1.6, National Institutes of Health, Bethesda, MD). The RGB image was converted to 16 bit image to have grayscale one, then the image was duplicated, after that threshold was assigned to create binary image where sliders were adjusted to highlight the antibody expression, the pixels used range was used to compare between all slices of all groups. Then the grayscale image was analyzed, and the measured mean pixels intensities were in the results section. The mean of all results of each group was calculated and compared to other groups (N.B. Pixels of immunoreactive objects were quantified based on a constant threshold of optical density) (Yoshizumi, 2012; Berrocal et al., 2014).

Material and Methods – Immunohistochemistry

Sham = S, 6-OHDA-treated = T , 6-OHDA-lesioned =L

For Cell Counting Measurement			
Antibody	***Structure***	***Area counted***	***Number of Slices***
pERK Phosphorylated extracellular signal-regulated kinase	Spinal cord	Dorsal Horn Laminae	S = 28, T = 38, L = 32
	Insular Cortex	Rostrocaudal slices from 2.04 mm to – 0.48mm in relation to Bregma	S =9, T =18, L =10
	Cingulate Cortex		S =10, T = 24, L= 16
PKC γ Protein Kinase C gamma	Spinal cord	Dorsal Horn Lamina IIi	S =10, T = 24, L = 16
Parvalbumin	Spinal cord	Dorsal Horn Laminae	S =8, T = 8, L = 8
CFOS	Spinal cord	Dorsal Horn Laminae	S =14, T = 10, L = 8
TH Tyrosine Hydroxylase	Substantia nigra and Ventral Tegmental area (VTA)	Rostro-caudal slices from -5.16mm to -6.12mm in midbrain were analyzed	S = 27, L =13
For Fluorescence Intensity Measurement			
Antibody	***Structure***	***Area counted***	***Number of Slices***
PKC γ	Spinal cord	Dorsal Horn Laminae	S =6, T = 6, L = 6
GAD67	Spinal cord	Dorsal Horn Laminae	S =9, T = 9, L = 9
Parvalbumin	Spinal cord	Dorsal Horn Laminae	S =8, T = 8, L = 8
VGAT	Spinal cord	Dorsal Horn Laminae	S =8, T = 8, L = 8

Table (7) and (8): Number of sections used for cell counting measurement and fluorescence intensity measurement.

5. Western Blot

1. At the end of behavioral experiments, 6-OHDA lesioned, treated and sham groups were anesthetized with ketamine (60 mg/kg) and Xylazine (10 mg/kg) and sacrificed by decapitation.

2. Fresh tissues {spinal cord from L3 to the end of the spinal cord, pieces from insular and cingulate cortices bilaterally (2mm)} were punched and snap frozen in liquid nitrogen then kept at -80 °C till used.

3. Proteins were extracted using extraction buffer {(Stopping buffer Qsp Vtotal: Hepes 50mM, NaCl 150 mM, EDTA 10mM, Tetra-sodium pyrophosphate decahydrate 10 mM, Vanadate ph 7.5 2 mM, NaF 100 mM, distilled H2O, pH 7.5), PMSF 0.5 mM, complete protease inhibitor cocktail pills, Triton 10% -1%}.

4. 200 µl of the extraction buffer was added to each sample, then homogenized with a glass homogenizer.

5. Then in the sonicator for 3 minutes, then left 20 minutes in ice, after that 100 µl extraction buffer was added and then centrifugation 14,000× g for 15 minutes at 4 °C. Then the supernatant (140 µl then 140 µl) was taken, separating 10 µl aside for protein dosage and samples are left at -80 °C till used.

6. The 10 µl samples taken for dosage were taken and the cell lysates were titrated with Pierce BCA Protein Assay Kit (Thermofisher Scientific, USA).

7. 7 dilutions of BSA were made, **Table (9):**

Scale	0	1	2	3	4	5	6	7
BSA	0	2.5	5	12.5	25	37.5	50	75
Lysis Buffer	100	97.5	95	87.5	75	62.5	50	25

8. 45 µl of lysis buffer + 5 µl of each sample were prepared

(N.B. bubbles present were centrifuged for 2 minutes and not mixed by pipetting)

- Samples were vortexed
- Samples were centrifuged for 30 seconds and 2 minutes if bubbles were present.

9. BCA reaction buffer was prepared (50 part of A to 1 part of B) and was kept out form light.
10. 200 µl reaction buffer was added to 25 µl of sample or standard.

11. Samples' plates were kept covered at 37 degree for 30 minutes.

12. Optical density meter was used to check samples' optical densities (spectrophotometer at 562 nm).

13. After the optical density was read, the amount of protein concentration for each sample was determined to be used in the following steps.

14. Samples then were prepared for gel electrophoresis by adding each sample (x µl) to (1+2):

1) recovery buffer 5x 13 µl (Tris 200 mM, SDS 12 %, glycerol 40 %, distilled water at pH 7.6)

2) β -mercaptoethanol 2x / 13 µl

Then the product was kept at – 20 °C after vortexing, heating at 100 °C for 5 minutes and centrifugation for 30 seconds.

15. Buffers' preparation **(Table 10)**

Migration Buffer	Transfer Buffer
BioRad 10x Tris/Glycine/ SDS buffer 2 Litres: 200 ml buffer + 1800 distilled H2O	BioRad 10x Tris/Glycine 2 Litres: 200 ml buffer + 1800 distilled H2O

16. Samples were heated to 100 °C for 5 minutes, then centrifuged for 30 seconds before being loaded for western immunoblotting. After the combs were removed from gels using thumb, the wells were rinsed with buffer and sides of the wells were straightened if needed.

17. The gel cassettes were placed in the tetra cell (if only one or three cassettes, the buffer dam was being added).

18. The two cassettes were placed together at angle 30 at first, where the short dam was placed internally and was fitting under the green gasket notch.

19. Then the cassettes were locked using the green side arms.

20. The electrophoresis module was then put into the tank with 200 ml buffer filling the inner chamber and 800 ml filling the outer chamber if 4 gels or 550 ml if 2 gels.

21. Precision Plus Protein Molecular Weight Standard (BioRad, USA) was used (7 µl). Volumes of samples having equal total proteins weight (40 µg) were loaded into wells of 4- 20 % Mini-PROTEAN TGX polyacrylamide gels (BioRad, USA) using Mini-PROTEAN Tetra Cell (BioRad, USA) for vertical gel electrophoresis {for 4 gels, voltage used was 300 and 240 mAmp}.

22. The migration was stopped when the dye reached the reference line at the bottom of the cassettes.

23. The electric power was turned off, the cassetttes were opened using the specific levers and gels were equilibrated in transfer buffer for 10 minutes.

24. Then the separated proteins (according to their molecular weight gradient) were transferred to nitrocellulose membranes through Wet/ Tank blotting systems (BioRad, USA).

25. The gel was placed near the black plate and the nitrocellulose membrane was placed towards the red plate of the cassette between foam and filter paper sheets (a roller was used to remove any air bubbles between blot assembly layers).

26. Cassettes were placed into transfer modules into tanks.

27. A cool unit and a stirring bar were added.

28. The tank then was filled with transfer buffer.

29. The tank was placed on a stirring plate to assure even dissipation of temperature and ions concentration during the transfer (The power supply was set to 45 volt and 250 mAmp for two hours).

30. Washing buffers constituted of TBS-T (20mm Tris-HCl and 140 mM NaCl containing 0.1% Tween 20, distilled water at pH 7.6), washing was done 3 times each for 15 minutes and membranes were incubated on rotating plates.

31. Membranes were incubated in 5 % (Bovine serum albumin) BSA in TBS-T to block unspecific binding sites for 1 hour at room temperature.

32. After that, membranes were incubated in 1ry antibodies diluted in 5 % BSA in TBS-T at 4 °C overnight.

Primary antibodies used were, **Table (11):**

Primary Antibody	Source	Mono/poly-clonal	Concentration	Company
anti–pERK	rabbit	monoclonal	1:500	Cell Signaling Technology
anti-GAD1	rabbit	monoclonal	1:1000	Cell Signaling Technology

anti- PKC γ	mouse	monoclonal	1: 400	Santa- Cruz Biotechnology
anti-D2DR	mouse	monoclonal	1:250	Santa-Cruz Biotechnology
Anti- GAPDH	rabbit	polyclonal	0.2 μg/ml	Sigma-Aldrich

33. After washing, membranes were incubated with secondary antibodies (Horseradish peroxidase conjugated 1: 5000, Sigma-aldrich, France) diluted in 5 % BSA in TBS-T at room temperature for 1 hour.

34. Densitometric quantification of the specific immunoreactive bands was done using Chemidoc imaging software (Bio-Rad).

35. The band analysis was accomplished by capturing the corresponding relative intensities using the imager ChemiDoc XRS running Chemidoc imaging software (BioRad, St Louis, USA) using Clarity Western ECL Substrate solution (Bio-Rad) {solution A: solution B 1:1, and incubation in 2 ml/ membrane was done for 5 minutes}. Colorimetric option of gel blot was used to check the molecular weight standards and chemi option for the protein bands' intensities readings.

36. Images were corrected by subtracting the background. pERK, GAD1, PKC γ and D2DR band intensities were normalized against corresponding GAPDH band intensities.

37. After that, 6-OHDA lesioned group and treated one were normalized against sham group of corresponding gel in order to be able to compare between different gels.

38. The specificity of the primary antibodies was assessed by the appearance of bands in the area corresponding to the expected specific molecular weight.

39. Results are expressed as the median ± interquartile range of expression levels of the ratio between lesioned and treated to sham group of each gel.

Material and Methods – Western Blot

Mini PROTEAN Tetra - cell gel electrophoresis
Bio-Rad

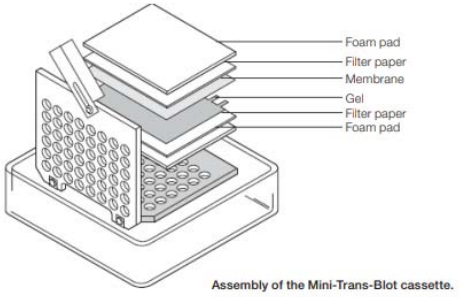

Mini-trans blot cassette assembly
Bio-Rad

Wet/ Tank Blotting system
Bio-Rad

Biorad Laboratories (2021). [Protein Electrophoresis and Blotting]. Retrieved October 1, 2021, from https://www.bio-rad.com/en-eg/category/protein-electrophoresis-blotting?ID=da4d07ba-052c-4156-89ef-16ab7b17f243.

6. Body weight analysis

Because bilateral lesions of the MFB may cause aphagia and/or adipsia, animals' weight was checked daily after surgery. 6-OHDA lesioned rats were weak and not capable of feeding themselves. They were fed (wet food pellets + water + milk) using syringe feeding two times per day, for 8–10 days.

7. Behavioral Tests

7.1. Acetone drop test (Paw cold allodynia):

The acetone test (Yoon et al., 1994) was performed to assess cold hyperalgesia-like responses in hind paw in both 6-OHDA and sham lesioned rats and after acute administration of ropinirole (dopamine agonist) in 6-OHDA lesioned rats. Rats were habituated for 15 minutes on a metal mesh floor, under small plastic cages (35x20x15 cm). An acetone drop at room temperature was formed at the tip of a 1 ml syringe and then gently applied onto the mid- plantar surface of a hind paw (without touch). Acetone-induced paw flinches were counted for 2 min. Each test consisted of applying acetone 5 times (with a 5 min interval between successive applications), and the cumulated response (total number of hind paw flinches, lifting up, scratching and touching the lifted hip/paw for the 5 successive applications) was calculated. Latency (duration between application of acetone and paw reaction) was also counted. Reaction time to acetone is by either shaking or licking paws (Barrot, 2012; Li et al., 2013; van der Wal et al., 2015).

7.2. The thermal place preference test:

The thermal place preference (TPP) test was used (Balayssac et al., 2014) one- week post-surgery. The apparatus consisted of two hot/cold plates (165X165 mm; Bioseb, Chaville, France). Every plate was regulated at ± 0.1 °C. The reference plate was set at 25 °C, while the test plate at (10-50 °C) according to the required temperature. For each session (3 minutes), the rat was positioned in the middle of the apparatus and was permitted free movement between the two plates. The time the rat passed on each test plate was calculated as a percentage. To avoid the impact of learning, reference and test plates were permuted between each session. The animals were acclimatized to the experimental conditions, using two plates settled at 25 °C, before the test.

Ugobasile (2020). [Thermal place preference]. Retrieved December 22, 2021, from https://www.ugobasile.com/products/catalogue/pain-and inflammation/item/608-thermal-place-preference-for-mice-and-rats.

7.3. Mechanical hyperalgesia (Randall test)

Hypersensitivity to mechanical stimuli was conducted by applying a gradually increasing pressure stimulus using the Ugo Basile analgesiometer (Randall-Selitto apparatus, Bioseb, France), (Randall and Selitto, 1957), at two- and four- weeks post-surgery. Rats left and right hind paws were subjected to an incremental linear mechanical force (measured in grams) until a squeak was observed marking a painful threshold. Three days before the experiment, rats were habituated by handling them by the experimenter for 20 seconds two or three times. This has also been repeated on the day of the experiment before putting the rats on the Ugo Basile apparatus. Increasing pressure was then implemented by applying the tip on the paw until the rat's vocalization was obtained. It was easier and more reliable to monitor vocalization than motor response. The vocalization threshold was measured three times to obtain two consecutive values that differed < 10 %, with a minimum of 10 minutes between each measurement and the following one. The pressure threshold of vocalization was obtained at a cut-off value of 250g.

Otto Environmenral Solutions for Animal Care (n.d.). [Ugo Basile Paw Pressure]. Retrieved December 22, 2021, from https://ottoenvironmental.com/product/ugo-basile-paw-pressure/.

Material and Methods – Behavioral Tests

7.4. Von Frey filament test

Rats were subjected to mechanical stimulation with 10 g von Frey filament to assess allodynia at hind paw. Each rat was habituated for 1 hour on a metal mesh floor, under a small plastic cage (35x20x15 cm). Tactile allodynia was determined with the use of non-noxious von Frey filament (Bioseb, Chaville, France) of 10 g (Ameyaw et al., 2014). Monofilament applied perpendicular until buckling → i.e. (applying a constant force) for 2-5 seconds (Deuis et al.,2017). Relevant behavior consisted of either paw withdrawal, paw licking or paw shaking (Li et al., 2013). Testing was avoided when animal is grooming which gives false negative responses. Consistent application was done to avoid intra and inter subject variability.

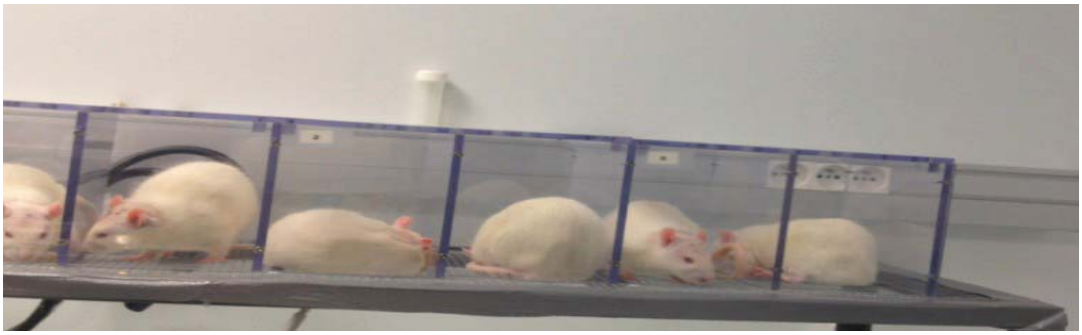

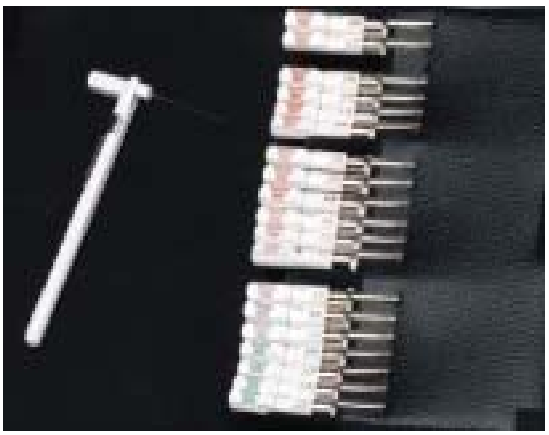

Pelvipharm (n.d.). [Von Frey Test]. Retrieved December 22, 2021, from https://www.pelvipharm.com/services,article-113,experimental-skills-behavioural-science-behavioural-science,von-frey-behavioural-test.html

7.5.Intrathecal.injection:

Intrathecal injection of ropinirole was done according to the method described by Mestre et al. (1994). Briefly, the rats were tightly restrained. Ropinirole (20 nmol) (Tang et al., 2021) or 10 µL of saline solution using a30-gauge needle was injected intrathecally (i.t.) inbetween L4 and L5 of the spinal cord. The success of the procedure was confirmed by tail-flick on injection of ropinirole as indicated by Mestre et al. (1994). Pain score (paw withdrawal after 10g von Frey filament application) was evaluated pre-injection and every 6 min up to 36 min after ropinirole injection. Spinal cord L3–L4 constitute the segments regulating the sensory processes at the level of posterior paws (Takahashi et al.,1994). In addition, acetone drop and von Frey filament were tested in the posterior paw. For these reasons, ropinirole was administered at the level of L3–L4.

7.6. Rotarod:

The rotarod test was performed 2 weeks after surgery. Locomotor impairment was determined on an accelerating rotarod treadmill (TSE systems GmbH, Bad Homburg, Germany). Before testing, the rats were habituated to the instrument at a constant (4 rpm, 5 min) and accelerated speed (40 rpm, 5 min, five times) for three consecutive half days. A testing session was performed on the fourth consecutive day. The rotarod was accelerated progressively from 4 rpm to 40 rpm over 5 min. The time that the rats remained balanced on the device was scored. The rotarod test results for each animal represent the average time (seconds) spent on the rod for the last three sequences on the testing session (mean ± SEM) (Dieb and Hafidi, 2015).

Results - 1st Paper

NEUROSCIENCE
RESEARCH ARTICLE
M. Elshennawy et al. / Neuroscience 479 (2021) 107–124

Behavioral, Cellular and Molecular Responses to Cold and Mechanical Stimuli in Rats with Bilateral Dopamine Depletion in the Mesencephalic Dopaminergic Neurons

Mennatallah Elshennawy, [a,b†] **Omar Ouachikh,** [b†] **Youssef Aissouni,** [c] **Shahira Youssef,** [a] **Shahira S. Zaki,** [a] **Franck Durif** [b] **and Aziz Hafidi** [b*]

[a] *Anatomy and Embryology Department, Faculty of Medicine, Ain Shams University, Cairo, Egypt*

[b] *Université Clermont Auvergne, CHU, CNRS, Clermont Auvergne INP, Institut Pascal, 63000 Clermont-Ferrand, France*

[c] *Université Clermont Auvergne, INSERM, NeuroDol U1107, 63000 Clermont-Ferrand, France*

Abstract—Pain is the major non-motor symptom in Parkinson's disease (PD). Preclinical studies have mostly investigated mechanical pain by considering the decrease in a nociceptive threshold. Only a few studies have focused on thermal pain in animal models of PD. Therefore, the goal of this study was to assess the thermal nociceptive behavior of rats subjected to 6-hydroxydopamine (6-OHDA) administration, which constitutes an animal model of PD. Thermal plate investigation demonstrated significant thermal sensitivity to cold temperatures of 10 °C and 15 °C, and not to higher temperatures, in 6-OHDA-lesioned rats when compared with sham. 6-OHDA-lesioned rats also showed cold allodynia as demonstrated by a significant difference in the number of flinches, latency and reaction time to acetone stimulus. Ropinirole administration, a dopamine receptor 2 (D2R) agonist, blocked the acetone-induced cold allodynia in 6-OHDA-lesioned rats. In addition, mechanical hypersensitivity and static allodynia, as demonstrated by a significant difference in the vocalization threshold and pain score respectively, were noticed in 6-OHDA-lesioned rats. Acetone stimulus induced a significant increase in extracellular signal-regulated protein kinases 1 and 2 (ERK1/2) phosphorylation, a pain process molecular marker, in the spinal dorsal horn (SDH), the insular and cingulate cortices in 6-OHDA-lesioned rats when compared to sham. In 6-OHDA-lesioned rats, there was a significant augmentation in the expression of both protein kinase C gamma (PKCγ) and glutamate decarboxylase 67 (GAD67) in the SDH. This highlighted an increase in excitation and a decrease in inhibition in the SDH. Overall, the present study demonstrated a clear cold thermal hypersensitivity, in addition to a mechanical one, in 6-OHDA-lesioned rats.

Key words: Parkinson disease, allodynia, hyperalgesia, cold, mechanical.

INTRODUCTION

Parkinson's disease (PD), which is the second most prevalent neurodegenerative disorder, results from the death of dopamine-containing cells in the substantia nigra pars compacta (SNc). The disease is characterized by motor symptoms, such as resting tremor, rigidity, akinesia and postural instability, and non-motor symptoms.

The latter are often reported by patients before the diagnosis of PD (Skogar and Lokk, 2016; Tseng and Lin, 2017; Jankovic and Tan, 2020). Pain represents the main non-motor symptom of PD and epidemiological studies have estimated its prevalence between 68% and 95% (Buhmann et al., 2020). All of the symptoms generally occurred in the off-period of the treatment (Barceló et al., 2010; Fil et al., 2013; Blanchet and Brefel-Courbon, 2018) and disappeared after levodopa treatment (Young Blood et al., 2016). A decrease in chemical, mechanical and thermal thresholds have been stated in both PD patients and animal models (Takeda et al., 2005; Chudler and Lu, 2008; Marques et al., 2013; Zenken-Toktas et al., 2013; Dieb et al., 2015, 2016a,b; Buhidma et al., 2020). After electrical stimulation, electromyogram recording showed that the heat pain threshold had decreased and the spinal nociceptive threshold had changed in PD patients (Mylius et al., 2015). The mechanism of pain is not yet well understood in PD patients, although, in different studies, (Wood, 2006; Chudler and Lu 2008; Borsook, 2012; Young Blood

*Correspondence to: Mennatallah Elshennawy, Anatomy and Embryology Department, Faculty of Medicine, Ain Shams University, Cairo, Egypt.
E-mail addresses: menna.faisal@med.asu.edu.eg (M. Elshennawy), omar.ouachikh@uca.fr (O. Ouachikh), youssef.aissouni@inserm.fr (Y. Aissouni), shahira_youssef@med.asu.edu.eg (S. Youssef), shahira_samir@med.asu.edu.eg (S. S. Zaki), franck.durif@uca.fr (F. Durif), aziz.hafidi@uca.fr (A. Hafidi).
† First and second author participated equally to the work.

https://doi.org/10.1016/j.neuroscience.2021.10.026
0306-4522/

et al., 2016), it was noted that the basal ganglia were involved in pain pathogenesis. For example, neuropathic pain (NP) was exaggerated due to the loss of dopamine (DA) in the striatum (Takeda et al., 2005; Taylor et al., 2014). On the other hand, the pain was diminished when amphetamine was infused into the nucleus accumbens (Altier and Stewart, 1999; Harris and Peng, 2020). The administration of the dopamine receptor 2 (D2R) agonist to the striatum reduced the sensation of pain (Magnusson and Fisher, 2000; Wawrzczak-Bargieła et al., 2020).

Spontaneous and evoked pains clinically characterize NP. It can occur as a dysfunction in the peripheral or the central nervous systems (Viana, 2018). NP can be characterized by allodynia or hyperalgesia (Sandkühler, 2009; Jensen and Finnerup, 2014). Only a few studies, in which the 6-hydroxydopamine (6-OHDA) rat constituted the PD model, have explored pain in bilateral denervation (Paillé et al., 2007) of the nigrostriatal pathway (Zenken-Toktas et al., 2013; Dieb et al., 2014; 2016a,b). Therefore, the present study explored mechanical and thermal hyperalgesia and cold allodynia (reduced pain threshold) in the hind paw of a rat model of PD with a bilateral 6-OHDA lesion of the medial forebrain bundle (MFB). In addition, the effect of ropinirole, a D2R agonist, was investigated pharmacologically in mechanical hyperalgesia and thermal cold allodynia. Many of the NP symptoms, such as allodynia, are a result of changes within the spinal dorsal horn (SDH) (Sandkühler, 2009). Therefore, two markers were used to investigate segmental sensitization at both the cellular and molecular levels. Protein Kinase Cγ (PKCγ), which labels cells within the SDH lamina II and plays an important function in pain chronicity (Dieb et al., 2015; Todd, 2017); and the phosphorylation of extracellular signal-regulated protein kinases 1 and 2 (ERK1/2), which is expressed under noxious stimuli in the SDH (Ji et al., 1999; Polgár et al., 2007). Active ERK1/2 (pERK1/2) represents a molecular marker for pain processes (Ji et al., 1999; Liu et al., 2012; Dieb and Hafidi, 2015). In addition, the insular and anterior cingulate cortices are involved in the neuropathic pain process (Ohara et al., 2005) and both structures receive dopaminergic projections from the SNc (Chudler and Dong, 1995; Zhang et al., 2017). Their involvement in the pain process, in the rat model of PD, has been explored by observing pERK1/2 expression.

EXPERIMENTAL PROCEDURES

Animals

Experiments were performed using 65 adult male Sprague-Dawley rats (Charles River, France) initially weighing 280–350 g. The Rats were housed three per cage in a Specific Pathogen Free facility under standard laboratory conditions (12/12 light/dark cycle, light on at 8:00 am) and were allowed free access to food pellets and water. The Rats were acclimatized for one week after transport to the animal house. 6-OHDA-lesioned rats included in the experiments were the rats showing signs of motor impairment (hind limb rigidity), aphagia, and/or adipsia. Rats with signs of deterioration, for example, having lost more than 20% of their bodyweight over the 6 days after surgery, were euthanized and excluded from the experiments. The experiments complied with the ethical guidelines of the animal ethics committee of Clermont Auvergne University (APAFIS#19965-20190325052285).

Surgery

6-OHDA lesion. The Rats were anesthetized with Ketamine 60 mg/kg and xylazine 10 mg/kg, intraperitoneal (i.p) and were positioned on a stereotaxic frame (David Kopf Instrument, CA, USA) to undergo a bilateral injection of 6-OHDA into the MFB [concentration of 3 μg/μL] with the rate (0.25 μL/min) in two deposits (2.25 and 2.85 μl). The 6-OHDA was dissolved in a vehicle solution (0.02% ascorbate saline) (Sigma-Aldrich, France, # H4381). The Injections were done at the following coordinates (Table 1) under aseptic conditions (Dieb et al., 2016b):

To protect the adrenergic neurons from 6-OHDA toxicity, the animals were injected with desipramine (25 mg/kg, i.p., Sigma-Aldrich, Saint-Quentin-Fallavier, France, # D3900) 30 min before the 6-OHDA injection. Desipramine was used in our animal model to focus on dopaminergic depletion in pain and to limit the noradrenergic effect. Sham-lesioned rats were only injected with the vehicle at the same coordinates. The injection syringe was retracted slowly 1 mm/min. The physical appearance of the rats and their body temperature were monitored regularly, as were the surgical sutures to ensure they remained in place and that the head incision was well coated. 6-OHDA-lesioned rats were fed with wet food pellets, milk, and water until they were able to feed themselves.

Study design

From our previous studies, we know that the 6-OHDA-lesioned rat had pain hypersensitivity for up to three months (Dieb et al., 2016b). To decrease the number of rats used, experiments were organized to test the same animals within a certain timeframe and add some when it was needed. Also, experiments were done over time to make sure that the animals had no effects from previous experiments. The D2R agonist was investigated in all tests when it could be done easily without harming the rats (intrathecal administration and von Frey filament test, intraperitoneal injection, and acetone test). Due to the half-life of ropinirole [30 min in rats, (Ramji et al., 1999)], we were not able to do the paw pressure test. In addition, since the thermal place preference test showed hypersensitivity to cold temperatures, the D2R was tested in the acetone drop.

The thermal place preference test

The thermal place preference (TPP) test was used (Balayssac et al., 2014) one week after surgery. The apparatus consisted of two hot/cold plates (165 × 165 mm; Bioseb, Chaville, France). Every plate was regulated

Table 1. Coordinates of the 6-OHDA lesion surgery

Deposit	Anterior	Lateral	Ventral	Tooth bar
2.25 μl,	−4.0	± 0.8	−8.0	+3.4
2.85 μl,	−4.4	± 1.2	−7.8	−2.4

at ±0.1 °C. The reference plate was set at 25 °C, while the test plate at (10–50 °C) according to the required temperature. For each session (3 min), the rat was positioned in the middle of the apparatus and was permitted free movement between the two plates. The time the rat passed on each test plate was calculated as a percentage. To avoid any possibility of habituation, the reference and test plates were permuted between each session. The animals were acclimatized to the experimental conditions, using two plates set at 25 °C, before the test.

Mechanical hyperalgesia

Hypersensitivity to mechanical stimuli was conducted by applying a gradually increasing pressure stimulus using the Ugo Basile analgesiometer (Randall-Selitto apparatus, Bioseb, France), (Randall and Selitto, 1957), at two and four weeks after surgery. The rats left and right hind paws were subjected to an incremental linear mechanical force (measured in grams) until a squeak was observed marking a painful threshold. To habituate the rats, the experimenter handled them for 20 s two or three times beginning, three days before the experiment. This was also repeated on the day of the experiment before putting the rats on the Ugo Basile apparatus. An increasing pressure was then exerted by applying the tip of the apparatus on the paw until the rat's vocalization was obtained. It was easier and more reliable to monitor vocalization than motor response. The vocalization threshold was measured three times to obtain two consecutive values that differed < 10%, with a minimum of 10 min between each measurement and the following one. The pressure threshold of vocalization was obtained at a cut-off value of 250 g.

Von Frey filament test

The rats were subjected to mechanical stimulation with a von Frey filament to test allodynia in the hind paw (Chaplan et al., 1994) at two and four weeks after surgery. Each rat was acclimatized for 1 hour on a metal mesh floor, under a small plastic cage (35 × 20 × 15 cm). Tactile allodynia was set with the use of non-noxious 10 g von Frey filament (Bioseb, Chaville, France) (Chaplan et al., 1994). Painful behavior was noted when there was paw withdrawal and/or an escape trial. All experiments were done relatively at the same time of the day. Ropinirole was injected intrathecally two weeks after surgery into a 6-OHDA-lesioned group and the pain score was calculated relative to another 6-OHDA-lesioned group, which had the saline intrathecal injection.

Intrathecal injection

Intrathecal injection of ropinirole was done according to the method described by Mestre et al. (1994). Briefly, the rats were tightly restrained. Ropinirole (20 nmol) (Tang et al., 2021) or 10 μL of saline solution using a 30-gauge needle was injected intrathecally (i.t.) in between L4 and L5 of the spinal cord. The success of the procedure was confirmed by tail-flick on injection of ropinirole as indicated by Mestre et al. (1994). Pain score (paw withdrawal) was evaluated pre-injection and every 6 min up to 36 min after ropinirole injection. Spinal cord L3–L4 constitute the segments regulating the sensory process at the level of posterior paws (Takahashi et al., 1994). In addition, acetone drop and von Frey filaments were tested in the posterior paw. For these reasons, ropinirole was administered at the level of L3–L4.

Acetone drop test

The acetone test (Choi et al., 1994) was performed at ten days after surgery for four days successively to test cold hyperalgesia-like (cold allodynia) reactions in the hind paws of three animal groups: sham, 6-OHDA-lesioned and 6-OHDA-lesioned rats with acute intraperitoneal administration (for 4 days, starting at day 10 post-surgery) of ropinirole-hydrochloride (D2R agonist, 5 mg/kg/ml, Sigma-Aldrich, Saint-Quentin-Fallavier, France, # R2530) (Mavrikaki et al., 2014, Tremblay et al., 2017). The ropinirole treated group is referred to as the 6-OHDA + D2R agonist group, a behavioral test was done after 15 min post-injection (Mavrikaki et al., 2014) for this group. The Rats were acclimatized for 15 min on a metal mesh floor, under small plastic cages (35 × 20 × 15 cm). An acetone drop from a 1 m syringe was gently applied to the hind paw plantar surface (without touch). Three parameters were tested using the acetone stimulus. Each parameter was considered after the application of acetone 5 times (with a 5 minute interval between successive applications). The first one was the number of flinches, for which the number of hind paw withdrawals was counted for five consecutive applications. The second parameter was the latency, for which the duration between the application of acetone and the hind paw reaction was measured. While the third parameter was the reaction time which was assessed for the duration of two minutes. The test was repeated for four successive days in the second week after surgery and the median + interquartile range values were calculated.

The behavioral experiments were done with a blind design so that the experimenter could not recognize the different animal groups.

Immunohistochemistry

At the end of the behavioral experiments, ketamine (60 mg/kg) and xylazine (10 mg/kg) i.p. were used to deeply anesthetise the rats which were perfused transcardially with a warm (37 °C) heparinized saline solution (25 IU heparin/ml) followed by a cold (10 °C) phosphate-buffered solution (0.1 M, pH 7.6) containing 4% paraformaldehyde and 0.03% picric acid for 15 min. Brains and spinal cords were then removed and placed in a solution of 30% sucrose and 0.05% sodium azide at 4 °C overnight. Coronal sections (40 μm) were collected with a using a freezing microtome and placed in a 0.05 M Tris-buffered saline (TBS) solution. Free-floating sections were placed in 1% normal goat serum at room temperature for 1 hour before overnight incubation in primary mouse monoclonal anti-TH antibody solution (1:5000, Sigma-Aldrich, Saint-Quentin-Fallavier, France, #T2928), rabbit monoclonal anti-pERK1/2 (1:200, Cell Signaling Technology, Ozyme Saint-Cyr-l'École, France, #4370), rabbit monoclonal anti-GAD1 (1:1000, Cell Signaling Technology, #41318) and mouse monoclonal anti-PKCγ (1:500, Santa-Cruz Biotechnology, France, #sc-166385). After several rinses, sections were incubated with a secondary antibody (1:500 for goat anti-mouse 488 #4408; goat anti-rabbit 555 #4413, goat anti-mouse 555 #4409, goat anti-rabbit 488 #4412, Cell Signaling Technology) for 2 h at room temperature. All the antibodies were diluted in TBS containing 0.25% bovine serum albumin and 0.3% TritonX-100. The sections were finally rinsed in TBS, mounted onto Thermo Scientific Superfrost Plus slides (Fisher Scientific, UK), and coverslipped with Dako Fluorescence Mounting Medium (Agilent, United States). The specificity of immunostaining was assessed by omitting the primary antibody, which resulted in the absence of the signal. Photomicrographs of immunostained sections were captured using a motorized Zeiss Axioplan 2 microscope equipped with a Hamamatsu C4742-95 digital camera (Hamamatsu Photonics France SARL, Massy, France) (switching between FITC and Texas Red filter sets) driven by MetaMorph 5.4 software. In each rat, image acquisition was done using multiple sections depending on the structure taken (Table 2). The Measurement of PKCγ positive cell number was taken from the whole lamina IIi of SDH, as it contains the majority of the PKCγ positive neurons (Dieb et al., 2016a,b), using sections that were taken from the Lumbar (L3–L6) spinal cord region. The final data were presented as a median + interquartile range value of the total sections of each group. The pERK1/2-positive cells were counted in all of the superficial laminae in the multiple sections at the level of the Lumbar (L3–L6) spinal cord region. While for the insular and cingulate cortices, rostro-caudal slices from (2.04 mm to –0.48 mm relative to Bregma) were taken, a square area of equal dimensions was applied to all counted sections. Tyrosine hydroxylase (TH) immunolabeling was quantified in the whole sections, at different slices, at the level of SNc and ventral tegmental area (VTA). Rostro-caudal sections from (−5.16 mm to −6.12 mm) were analyzed.

The cells for all PKCγ, pERK1/2, and TH were quantified using the multipoint cursor of ImageJ Software (ImageJ v1.6, National Institutes of Health, Bethesda, MD) where the numbers of cells were displayed in the results window. Cell count was done with a blind observer who did not know the different animal groups.

GAD67 and PKCγ fluorescence intensities were compared throughout different spinal cord sections at the level of the Lumbar (L3 – L6) region.

Western blot

At the end of behavioral experiments, sham, 6-OHDA-lesioned and 6-OHDA + D2R agonist groups were anesthetized with ketamine (60 mg/kg) and xylazine (10 mg/kg) and sacrificed by decapitation. Fresh spinal cord tissues (spinal cord from L3 to the end of the spinal cord) and fresh pieces from insular and cingulate

Table 2. The number of sections of each group used for each antibody

Cell Count Measurement			
Antibody	Structure	Group	Number of sections
PKCγ	Spinal cord	Sham	18
		6-OHDA-lesioned	25
		6-OHDA + D2R agonist	33
pERK1/2	Spinal cord	Sham	28
		6-OHDA-lesioned	32
		6-OHDA + D2R agonist	38
	Insular cortex	Sham	9
		6-OHDA-lesioned	10
		6-OHDA + D2R agonist	18
	Cingulate cortex	Sham	10
		6-OHDA-lesioned	16
		6-OHDA + D2R agonist	24
TH	SNc and VTA	Sham	27
		6-OHDA-lesioned	13

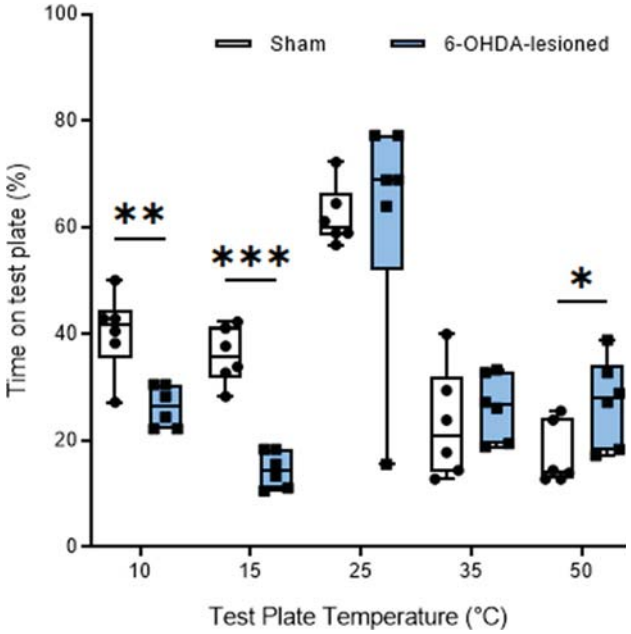

Fig. 1. Thermal place preference behavioral test. The graph represents time spent on thermal test plates of the sham and 6-OHDA-lesioned groups. There were significant differences; Student's *t*-test, between the groups for temperatures 10 °C (t_{10} = 4.02, p = 0.002, $^{**}P \leq 0.01$), 15 °C (t_{10} = 8.31, p = 0.00001, $^{***}P \leq 0.001$) and a non-significant difference for 35 °C (t_{10} = 0.66, p = 0.53, $p > 0.05$). While Mann–Whitney *U* test was used for 25 °C ($U_{6,6}$ = 10, p = 0.22, $p > 0.05$) and 50 °C ($U_{6,6}$ = 4, p = 0.03, $^{*}P \leq 0.05$). Data are represented as a box-and-whiskers plot, where the box depicts the median and the 25th and 75th quartiles and the whiskers show the 5th and 95th percentile of the sham (n = 6) and 6-OHDA-lesioned groups (n = 6).

cortices bilaterally (2 mm) were punched, snap-frozen in liquid nitrogen, and stored at −80 °C until use. Each sample was homogenized with a glass homogenizer in 200 μl of lysis buffer (50 mM HEPES, pH 7.5, 1% TritonX-100, 10 mM EDTA, 150 mM NaCl, 10 mM Na4P2O7, 0.1 M NaF, 2 mM vanadate) supplemented with PMSF 0.5 mM, complete™, Protease Inhibitor Cocktail (Sigma Aldrich, #5892970001) and Triton 1%, sonicated for 3 min and incubated on ice for 20 min. 100-μl of extraction buffer was added to each sample before centrifugation at 14,000 g for 15 min at 4 °C. The supernatants were collected in clean tubes and stored at −80 °C until use. The total amount of protein in each sample was measured using the BCA Protein Assay Kit (Pierce-Thermo Scientific, Illkirch-Graffenstaden, France) before loading on polyacrylamide gels. Samples (40 μg) were separated using 4–20% Mini-PROTEAN TGX polyacrylamide gels (BioRad, Roanne, France) and transferred to nitrocellulose membranes using the Wet/Tank Blotting System (BioRad). After the blots had been washed with TBS-T (10 mM Tris-HCl, pH 7.6, 150 mM NaCl, 0.01% Tween-20), they were blocked with 5% BSA in TBS-T for 1 h at room temperature. Then the membranes were incubated at 4 °C overnight with primary antibodies diluted in 5% BSA in TBS-T. The Primary antibodies used were rabbit monoclonal anti-pERK1/2 (1:500, Cell Signaling Technology, #4370), rabbit monoclonal anti-GAD1 (1:1000, Cell Signaling Technology, #41318), mouse monoclonal anti-PKCγ (1:400, Santa-Cruz Biotechnology, France, #sc-166385) and rabbit polyclonal anti-GAPDH (0.2 μg/ml, Sigma-Aldrich, #G9545). After washing with TBS-T, membranes were incubated for 1 h with HRP-

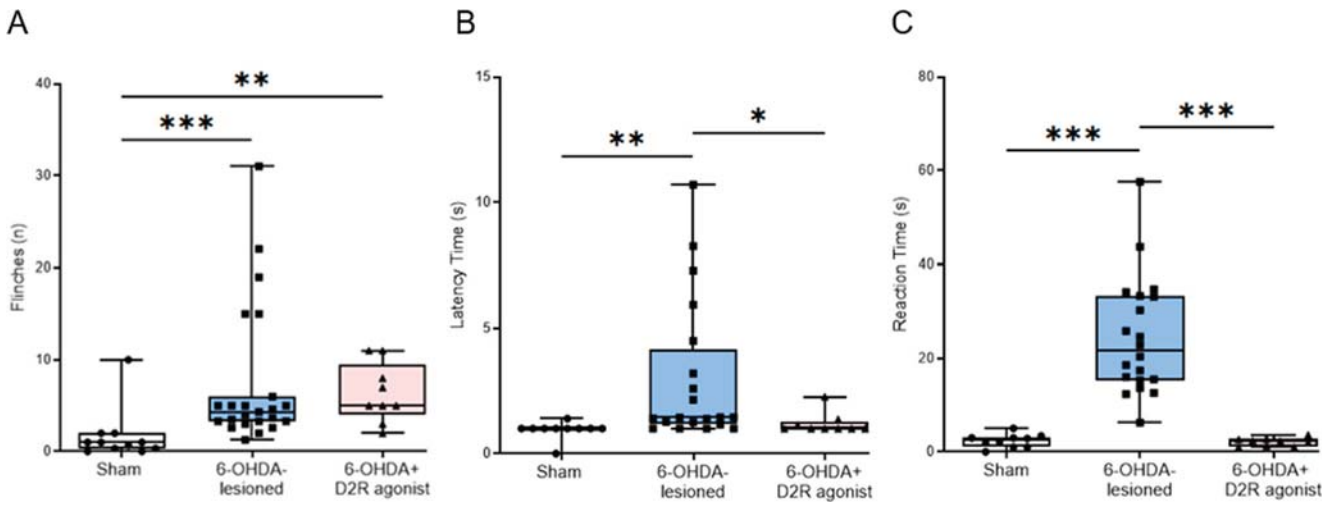

Fig. 2. Acetone cold allodynia behavioral test (Intraperitoneal administration of Ropinirole for 6-OHDA + D2R agonist group). Graph **(A)** represents the number of flinches for the three groups; Kruskal–Wallis *H* test (H_2 = 17.23, p = 0.0002, $^{***}P \leq 0.001$): 6-OHDA-lesioned rats had more significant numbers than the sham ones (Dunn's multiple comparisons test, p = 0.001, $^{***}P \leq 0.001$) also, the 6-OHDA + D2R agonist group had an increase in significance over the sham group (Dunn's multiple comparisons test, p = 0.01, $^{**}P \leq 0.01$). Graph **(B)** represents the latency time of the three groups; Kruskal–Wallis *H* test (H_2 = 15.13, p = 0.0004, $^{***}P \leq 0.001$), the 6-OHDA-lesioned rats had a more significant increase in latency time than both the sham and 6-OHDA + D2R agonist groups (Dunn's multiple comparisons tests, p = 0.006, p = 0.04, respectively, $^{**}P \leq 0.01$, $^{*}P \leq 0.05$ respectively). Graph **(C)** represents the reaction time of the three groups; Kruskal–Wallis *H* test (H_2 = 28.58, $p < 0.0001$, $^{***}P \leq 0.001$): the 6-OHDA-lesioned group had a more significant increase in reaction time than both the sham and 6-OHDA + D2R agonist groups (Dunn's multiple comparisons test, $p < 0.0001$, $^{***}P \leq 0.001$). Data are represented as box-and-whiskers plots, where the box depicts the median and the 25th and 75th quartiles and the whiskers show the 5th and 95th percentile of the sham (n = 11), 6-OHDA-lesioned (n = 23), and 6-OHDA + D2R agonist groups (n = 9).

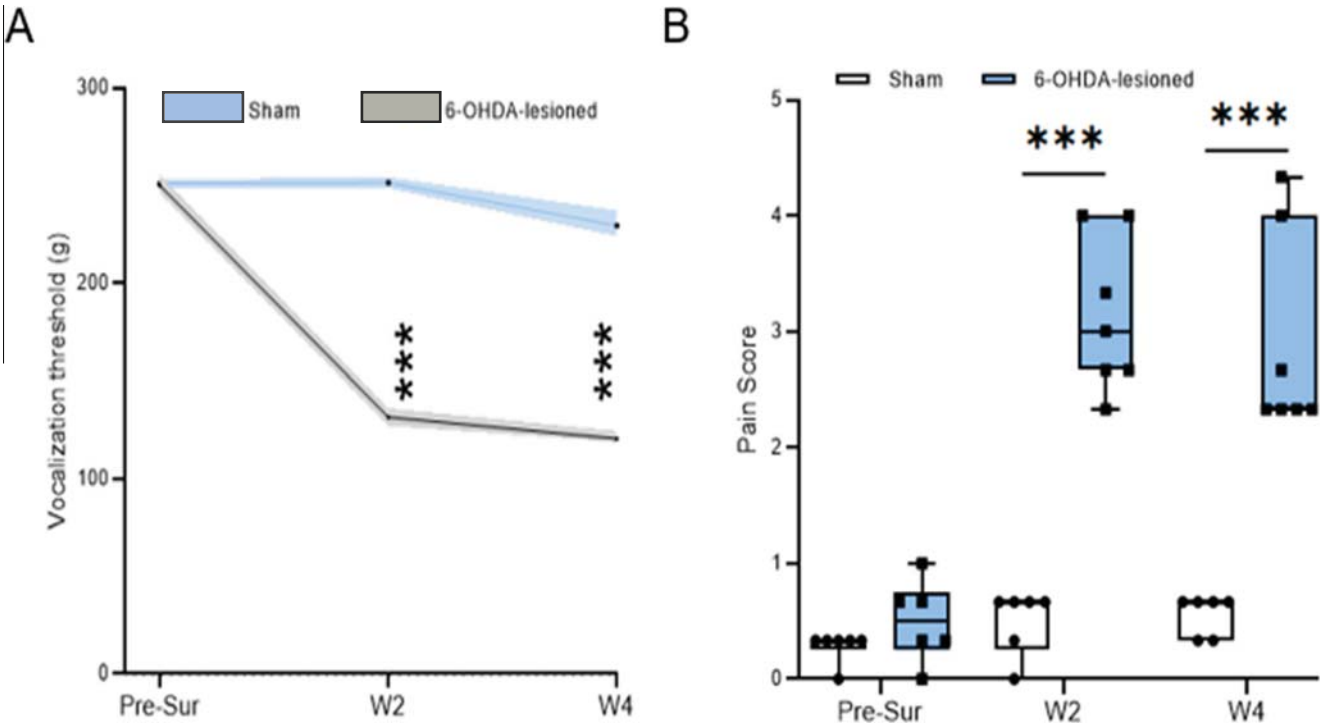

Fig. 3. Graph **(A)** represents mechanical hyperalgesia (Randall-test) at two and four weeks after surgery; Two-way ANOVA test with significant interaction, row and column factors ($F_{2,\ 30}$ = 479.6, $F_{2,\ 30}$ = 695.4, $F_{1,\ 30}$ = 197 respectively, $p < 0.0001$, ***$P \leq 0.001$): followed by (Sidak's multiple comparisons test, $p < 0.0001$, ***$P \leq 0.001$). Data are represented as a line plot of the median ± interquartile range of sham (n = 6) and 6-OHDA-lesioned rats (n = 6). Graph **(B)** shows similar results using the non-noxious 10 g von Frey filament test at two and four weeks after surgery; Friedman's test ($\chi 2_2$ = 16.84, $p < 0.001$, ***$P \leq 0.001$) followed by (Wilcoxon Signed-Rank Test, $p < 0.0001$, ***$P \leq 0.001$). Data are represented as a box-and-whiskers plot, where the box depicts the median and the 25th and 75th quartiles and the whiskers show the 5th and 95th percentile of the sham (n = 6) and 6-OHDA-lesioned groups (n = 6).

conjugated anti-rabbit and anti-mouse IgG secondary antibodies (1:5000, Invitrogen-Thermo Scientific #31460, #31430, respectively) diluted in 5% BSA in TBS-T. The bands were visualized with Clarity™ western ECL substrate solution (Bio-Rad, USA) and the positive pixel areas of specific bands were measured with a computer-assisted image analysis system (ChemiDoc XRS, Bio-Rad, USA) and normalized against the corresponding GAPDH loading control bands. The 6-OHDA-lesioned group and the 6-OHDA + D2R agonist one were normalized against the sham group of the corresponding gel to be able to compare the different gels. Results are expressed as the median ± interquartile range of expression levels of the ratio between 6-OHDA-lesioned and 6-OHDA + D2R agonist to the sham group of each gel.

Body weight analysis

Because bilateral lesions of the MFB may cause aphagia and/or adipsia, the animals' weight was checked daily after surgery. 6-OHDA-lesioned rats were not able to self-feed. They were fed (wet food pellets + milk + wat er) by syringe feeding twice a day, for 8 to 10 days.

Statistical analysis

The results are expressed as median ± interquartile range. Statistical analysis was performed using one-way ANOVA to compare the three groups, followed by Tukey's posthoc multiple comparisons test for parametric data and the Kruskal–Wallis test, followed by Dunn's posthoc multiple comparisons test for non-parametric data. Normality tests were done using the Shapiro–Wilk normality test, if parametric, Levene's test was done to check for equal variances (supplementary material). Two-way ANOVA, followed by Sidak's posthoc multiple comparisons test and Friedman's test were used when convenient. In addition, Student's *T*-test was used when the comparison between only two groups was required for parametric data and the Mann–Whitney test for non-parametric data. The level of significance was determined at a *P*-value ≤0.05. Data were analyzed using GraphPad Prism Software (v.8.0.2) and SPSS (v. 1.0.0.1447). Fixed-effect model ANOVA was used as variables were fixed factors in the experiment. Also, in the two-way ANOVA analysis, variables were fixed factors in both rows and columns factors.

RESULTS

Thermal hyperalgesia (Fig. 1)

Thermal sensitivity was tested one week after surgery; the rats were tested for thermal place preference (Fig. 1) at different temperature degrees (10 °C, 15 °C, 25 °C, 35 °C, and 50 °C). The 6-OHDA-lesioned rats showed a significantly higher thermal sensitivity when compared with the sham ones. This increase was

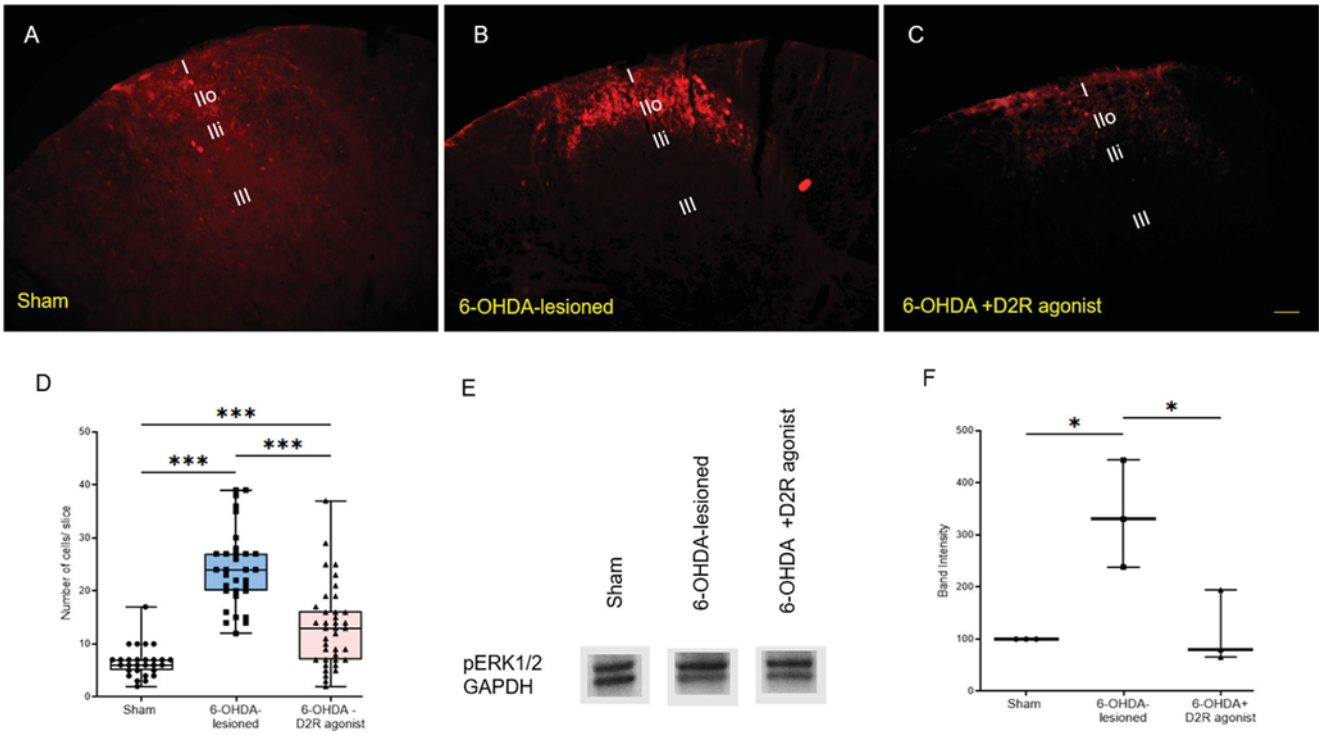

Fig. 4. pERK1/2 protein expression. The Figure shows pERK expression in the SDH of the sham **(A)**, 6-OHDA-lesioned **(B)**, and 6-OHDA + D2R agonist groups **(C)**. Graph **(D)** represents pERK1/2 positive cells within the SDH superficial laminae; Kruskal–Wallis H test ($H_2 = 55.64$, $p < 0.0001$, $^{***}P \leq 0.001$): 6-OHDA-lesioned rats had a more significant number than both the sham and 6-OHDA + D2R agonist groups (Dunn's multiple comparisons test, $p < 0.0001$, $^{***}P \leq 0.001$) also, the 6-OHDA + D2R agonist group had an increase in significance over the sham (Dunn's multiple comparisons test, $p < 0.0001$, $^{***}P \leq 0.001$). Data are represented as a box-and-whiskers plot, where the box depicts the median and the 25th and 75th quartiles and the whiskers show the 5th and 95th percentile of the sham ($n = 5$), 6-OHDA-lesioned ($n = 6$), and D2R agonist groups ($n = 6$). The Scale bar = 50 μm. Figure **(E)** shows Western blot bands of pERK1/2 for the three groups. Graph **(F)** represents Western blot band intensities for the three groups; one-way ANOVA ($F_{2,\ 6} = 10.29$, $p = 0.012$, $^{*}P \leq 0.05$): The 6-OHDA-lesioned rats had a more significant increase in expression than both the sham and 6-OHDA + D2R agonist groups (Tukey's multiple comparisons test, $p = 0.02$, $p = 0.02$ respectively, $^{*}P \leq 0.05$). Data are represented as a barplot of the median ± interquartile range of the sham ($n = 3$), 6-OHDA-lesioned ($n = 3$) and 6-OHDA + D2R agonist groups ($n = 3$), GAPDH was used as the loading control.

observed with the temperatures 10 °C and 15 °C, as the 6-OHDA-lesioned rats spent less time on the test plate than sham ones. While at 50 °C, the sham rats spent less time than 6-OHDA-lesioned rats on the plate. For the other temperatures, 25 °C and 35 °C; there was no significant difference observed between the groups.

Cold allodynia (Acetone test, Fig. 2)

Cold allodynia was tested during the second week in the three groups; sham, 6-OHDA-lesioned, and 6-OHDA + D2R agonist. 6-OHDA-lesioned rats had a significant increase in cold allodynic behavior, which was shown by an increasing number of flinches, the reaction time and latency in comparison with the sham group. Ropinirole had a significant role in decreasing allodynic behavior, which was evident from the significant decreases of reaction time and latency between the 6-OHDA + D2R agonist group and the 6-OHDA lesioned one.

Mechanical hyperalgesia and static allodynia (Fig. 3)

Mechanical hyperalgesia and mechanical static allodynia were tested at two and four weeks after surgery using the Randall-test (Fig. 3A) and non-noxious 10 g von Frey filament (Fig. 3B), respectively. The 6-OHDA-lesioned rats had greater mechanical hyperalgesia and mechanical static allodynia than the sham group, as was substantiated by the increase in vocalization at 50% of the baseline score and the increase in paw withdrawals at two and four weeks after surgery, respectively.

pERK1/2 expression in the SDH (Fig. 4)

pERK1/2 labeling expression upon paw acetone stimulus was observed in the superficial laminae of the SDH in the sham (Fig. 4A), 6-OHDA-lesioned (Fig. 4B), and 6-OHDA + D2R agonist rats (Fig. 4C). pERK1/2-positive cells were quantified in the SDH superficial laminae in the three animal groups. The 6-OHDA-lesioned rats had a significant increase in pERK1/2 in comparison with both the sham and 6-OHDA + D2R agonist groups. Ropinirole intraperitoneal administration led to a significant decrease in pERK1/2 in the 6-OHDA + D2R agonist rats when compared with the 6-OHDA-lesioned ones, while the sham group showed a less significant decrease. Western blot (Fig. 4E) revealed a significant pERK1/2 protein difference between the 6-OHDA-lesioned rats and both the sham and 6-OHDA + D2R agonist rats (Fig. 4F).

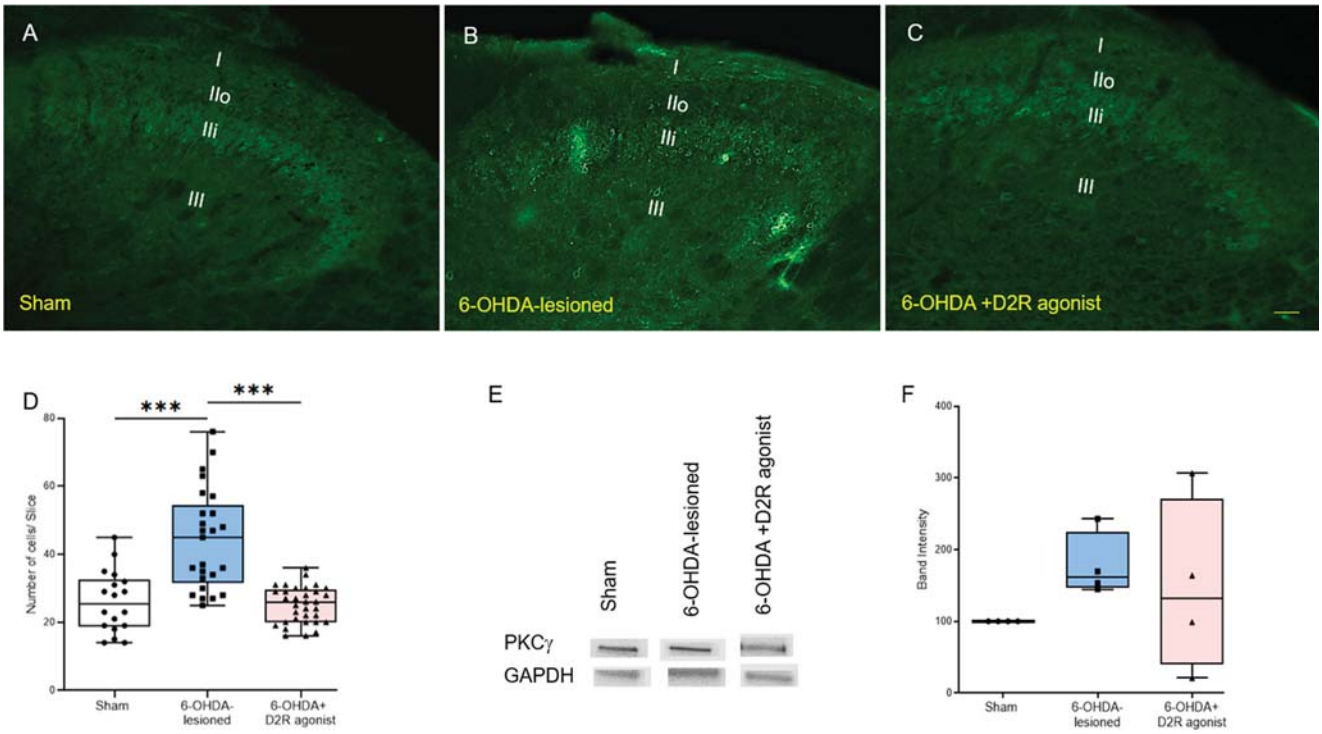

Fig. 5. PKCγ protein expression. The Figure shows PKCγ expression in the SDH of the sham **(A)**, 6-OHDA-lesioned **(B)** and 6-OHDA + D2R agonist groups **(C)**. PKCγ positive cells were observed within the SDH mostly in cells of lamina IIi and scattered cells within lamina III. Figure **(B)** has more intense fluorescent labeling than both Figures **(A)** and **(C)**. The Scale bar = 50 μm. Graph **(D)** represents PKCγ cell number count; Kruskal–Wallis H test ($H_2 = 29.42$, $p < 0.0001$, $^{***}P \leq 0.001$): the 6-OHDA-lesioned rats had a higher significant number than both the sham and 6-OHDA + D2R agonist groups (Dunn's multiple comparisons test, $p = 0.0001$, $p < 0.0001$ respectively, $^{***}P \leq 0.001$). Data are represented as a box-and-whiskers plot, where the box depicts the median and the 25th and 75th quartiles, and the whiskers show the 5th and 95th percentile of the sham ($n = 6$), 6-OHDA-lesioned ($n = 7$), and D2R agonist group ($n = 6$). Figure **(E)** shows the Western blot bands of PKCγ for the three groups. Graph **(F)** represents Western blot band intensities for the three groups, one-way ANOVA ($F_{2, 9} = 1.11$, $p = 0.37$, $p > 0.05$): the 6-OHDA-lesioned group had a less significant increase in expression than both the sham and 6-OHDA + D2R agonist groups (Tukey's multiple comparisons tests, $p = 0.35$, $p = 0.65$, respectively, $p > 0.05$). Data are represented as a barplot of the median ± interquartile range of the sham ($n = 4$), 6-OHDA-lesioned ($n = 4$) and 6-OHDA + D2R agonist groups ($n = 4$), GAPDH was used as the loading control.

PKCγ expression in the SDH (Fig. 5)

PKCγ labeling is localized in the SDH superficial laminae cells in the sham (Fig. 5A), 6-OHDA-lesioned (Fig. 5B), and 6-OHDA + D2R agonist rats (Fig. 5C). PKCγ labeling was quantified using the number of positive cells (Fig. 5D). The 6-OHDA-lesioned rats had more PKCγ expression than both the sham and 6-OHDA + D2R agonist groups regarding the number of cells. Also, the 6-OHDA-lesioned rats had more intense fluorescent labeling than both the sham and 6-OHDA + D2R agonist rats. Ropinirole intraperitoneal administration led to a significant decrease in PKCγ expression in the 6-OHDA + D2R agonist rats when compared with the 6-OHDA-lesioned ones regarding the fluorescence intensity and the number of cells. While there was a non-significant increase in Western blot band intensities between the 6-OHDA-lesioned and both the sham and 6-OHDA + D2R agonist groups.

GAD67 expression in the SDH (Fig. 6)

GAD67 labeling was expressed throughout the SDH laminae in the sham (Fig. 6A), 6-OHDA-lesioned (Fig. 6B), and 6-OHDA + D2R agonist animals (Fig. 6C). The 6-OHDA-lesioned groups demonstrated more of an augmentation in the GAD67 expression more than either of the sham or 6-OHDA + D2R agonist groups did, as shown by the increase in fluorescence intensity of the 6-OHDA-lesioned group over the other two groups. In addition, there was an increase in the Western blot band intensity of the 6-OHDA lesioned group in comparison with the sham and 6-OHDA + D2R agonist animals. Ropinirole intraperitoneal administration led to a significant decrease in GAD67 expression in the 6-OHDA + D2R agonist rats in relation to the 6-OHDA-lesioned ones.

pERK1/2 expression in the insular and the cingulate cortices (Figs. 7 and 8)

In the insular cortex, pERK1/2 labeling was expressed in the cell bodies and dendrites of somata located across the different cortical layers in the sham (Fig. 7A), 6-OHDA-lesioned (Fig. 7B), and 6-OHDA + D2R agonist (Fig. 7C) groups. These cells had mostly pyramidal cell morphology. The 6-OHDA-lesioned group showed an increase in pERK1/2 as revealed by its quantification and the increase in Western blot band intensity when compared with both the sham and the 6-OHDA + D2R agonist rats. Ropinirole intraperitoneal administration led

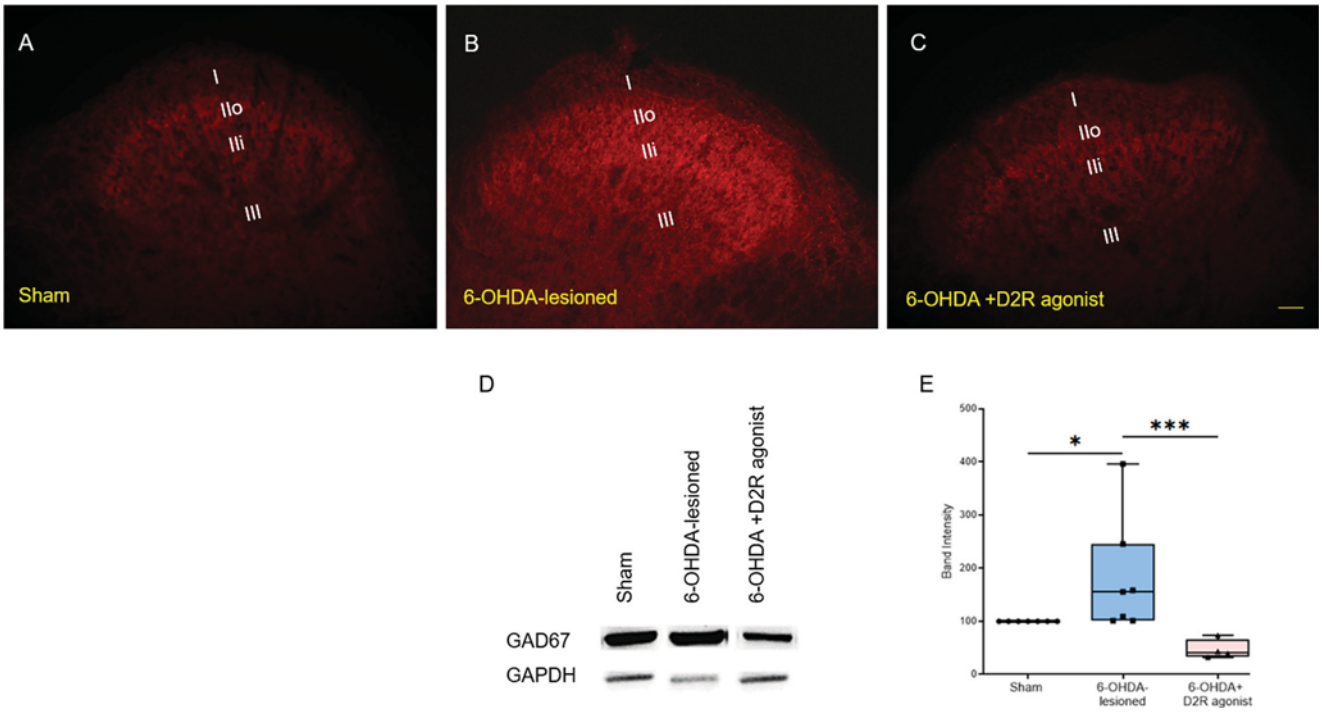

Fig. 6. GAD67 protein expression. The Figure shows GAD67 expression in the SDH of the sham **(A)**, 6-OHDA-lesioned **(B)**, and 6-OHDA + D2R agonist groups **(C)**. Figure **(B)** has more intense fluorescent labeling than both figures **(A)** and **(C)**. The Scale bar = 50 μm. Figure **(D)** shows the Western blot bands of GAD67 for the three groups. Graph **(E)** represents Western blot band intensities for the three groups; Kruskal–Wallis test ($H_2 = 15.79$, $p < 0.0001$, $^{***}P \leq 0.001$): The 6-OHDA-lesioned rats had a more significant increase in expression than both the sham and 6-OHDA + D2R agonist groups (Dunn's multiple comparisons test, $p = 0.03$, $p = 0.0004$, respectively, $^{*}P \leq 0.05$, $^{***}P \leq 0.001$). Data are represented as a barplot of the median ± interquartile range of the sham ($n = 4$), 6-OHDA-lesioned ($n = 8$) and 6-OHDA + D2R agonist groups ($n = 8$), GAPDH was used as the loading control.

to a significant decrease in pERK1/2, as was substantiated by the diminution in pERK1/2 expression in the 6-OHDA + D2R agonist rats more than in the 6-OHDA lesioned ones, when taking into account the number of cells and band intensity.

In the cingulate cortex, pERK1/2 labeling was observed in the cell bodies and dendrites of the cells located mostly within the deep layers in the sham (Fig. 8A), 6-OHDA-lesioned (Fig. 8B), and 6-OHDA + D2R agonist groups (Fig. 8C). The 6-OHDA-lesioned group showed a significant increase in pERK1/2, as was revealed by the increase in pERK1/2 quantification when compared with both the sham and 6-OHDA + D2R agonist rats, in addition to its increase in Western blot band intensity in the 6-OHDA-lesioned group compared with the sham rats. Ropinirole intraperitoneal administration led to a significant decrease in pERK1/2 expression in the 6-OHDA + D2R agonist rats more than in the 6-OHDA-lesioned ones, when taking into account the number of cells and band intensity.

Intrathecal ropinirole administration (Fig. 9)

To test segmental involvement in the pain process, ropinirole was intrathecally administered and the rats were then subjected to a non-noxious 10 g von Frey filament test. Intrathecal administration of ropinirole led to a decreasing pain score (paw withdrawal) in the 6-OHDA-lesioned rats in comparison with saline-injected, 6-OHDA-lesioned rats. The pain score decrease remained evident for up to 25 min.

TH immunostaining in the 6-OHDA-lesioned rats (Fig. 10)

TH labeling was explored in the SNc and ventral tegmental area (VTA) in both the sham (Fig. 10A) and 6-OHDA-lesioned groups (Fig. 10B) in order to highlight the effects of 6-OHDA toxin in the MFB lesion. TH labeling was observed in the somata and processes in the SNc and VTA. A general extreme significant decrease in the TH staining was observed in the 6-OHDA-lesioned rats when compared to sham confirming the degeneration of dopaminergic cells. The Quantification of TH cells in SNc and VTA (Fig. 10C) demonstrated a 67.8 % decrease in cell number between the 6-OHDA-lesioned and sham groups. A significant 56.7 % decrease in TH positive cell number was also observed between the 6-OHDA-lesioned and sham rats in the VTA (Fig. 10D). As well, a significant 89.9 % decrease was obtained in TH positive cell number between the 6-OHDA-lesioned and sham groups in the SNc (Fig. 10E).

Body weight

After surgery, the 6-OHDA-lesioned group had a significantly decreased body weight due to aphagia and adipsia. A considerable weight difference was observed

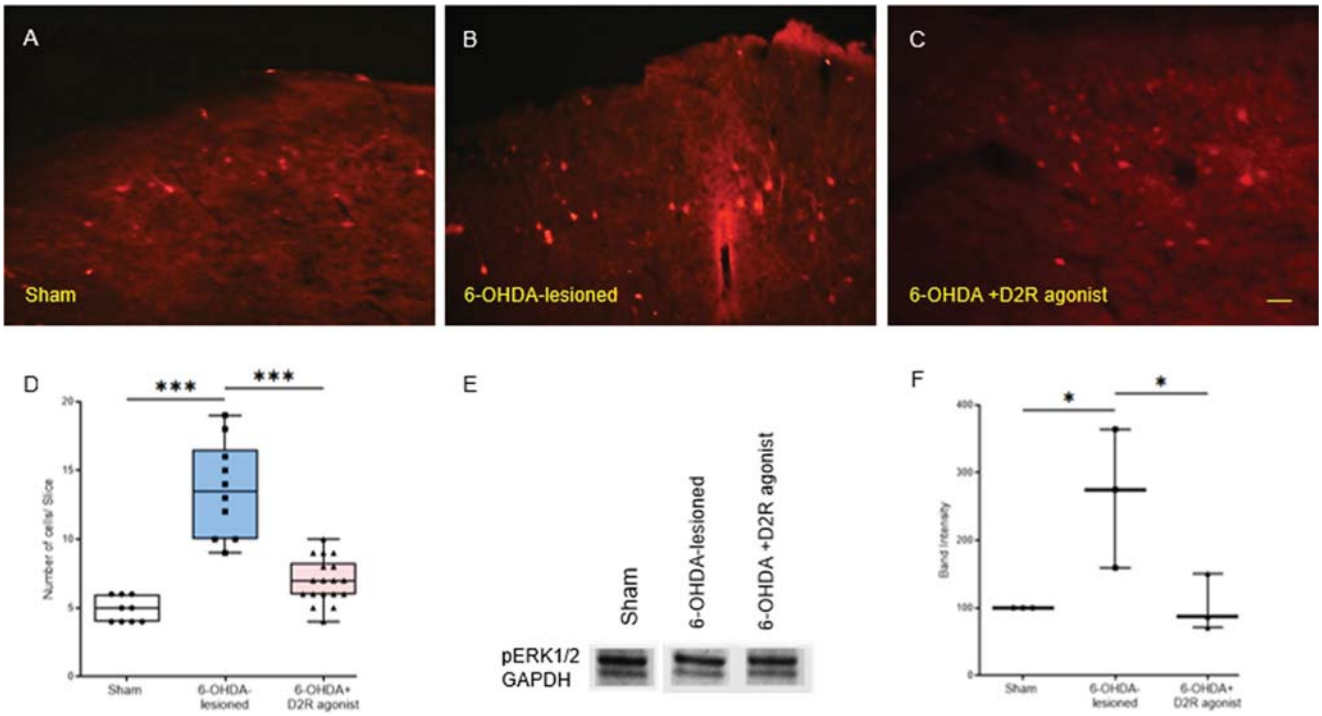

Fig. 7. pERK1/2 protein expression. The Figure shows pERK expression in the insular cortex of the sham **(A)**, 6-OHDA-lesioned **(B)**, and 6-OHDA + D2R agonist groups **(C)**. Graph **(D)** represents pERK1/2 positive cells within the insular cortex; Kruskal–Wallis test ($H_2 = 25.71$, $p < 0.0001$, $^{***}P \leq 0.001$): the 6-OHDA-lesioned animals had more significant numbers than both the sham and 6-OHDA + D2R agonist groups (Tukey's multiple comparisons test, $p < 0.0001$, $^{***}P \leq 0.001$). Data are represented as a box-and-whiskers plot, where the box depicts the median and the 25th and 75th quartiles and the whiskers show the 5th and 95th percentile of the sham ($n = 6$), 6-OHDA-lesioned ($n = 6$), and 6-OHDA + D2R agonist groups ($n = 7$). The Scale bar = 50 μm. Figure **(E)** shows Western blot bands of pERK1/2 for the three groups. Graph **(F)** represents Western blot band intensities for the three groups; one-way ANOVA ($F_{2, 6} = 6.60$, $p = 0.031$, $^{*}P \leq 0.05$): The 6-OHDA-lesioned group had a more significant increase in expression than both the sham and 6-OHDA + D2R agonist groups (Tukey's multiple comparisons test, $p = 0.044$, $p = 0.046$ respectively, $^{*}P \leq 0.05$). Data are represented as a barplot of the median ± interquartile range of the sham ($n = 3$), 6-OHDA-lesioned ($n = 3$) and 6-OHDA + D2R agonist groups ($n = 3$), GAPDH was used as the loading control.

in the 6-OHDA-lesioned rats in comparison with the sham ones (Fig. 10F).

DISCUSSION

The main results of this study showed that bilateral 6-OHDA-lesioned rats demonstrated an increase in thermal sensitivity to cold temperatures. This sensitivity was supported by the presence of cold allodynia, which was exhibited by the acetone test. In addition, lesioned rats demonstrated the presence of both mechanical hyperalgesia and mechanical static allodynia. Acetone stimulation promoted the expression of pERK1/2 in the SDH, the insular, and cingulate cortices, thus implicating these structures in the pain-process in both 6-OHDA-lesioned rats and sham ones, nevertheless, pERK1/2 expression in the 6-OHDA-lesioned rats was considerably elevated when compared with the sham ones. In addition, the 6-OHDA lesion induced an increase in the expression of PKCγ and GAD67 (glutamate decarboxylase) in the SDH. These two proteins may highlight an increase in excitation (PKCγ) and a decrease in inhibition (GABA), respectively. Moreover, the use of ropinirole, a D2R agonist, reversed the expression of PKCγ and GAD67 in the SDH and alleviated the pain sensitivity. These results demonstrated a clear implication of the SDH and dopamine in the pain process in 6-OHDA-lesioned rats (Fig. 11).

Although a study has shown that ketamine had a neuroprotective role in the 6-OHDA PD model (Ferro et al., 2007), according to our previous work, (Ouachikh et al., 2013; Ouachikh et al., 2014; Dieb et al., 2014; Dieb et al., 2016a,b), there was always a neuronal cell death percentage over 60% while using ketamine. This allowed us to consider that we are in an animal model of PD. Therefore, the use of ketamine as an anesthetic did not constitute an obstacle to neuronal degeneration.

Pain is measured through the motor and non-motor reflexes. Different studies using 6-OHDA-lesioned animals showed a reduction in mechanical and thermal nociceptive thresholds or allodynia in both hind paws without the affection of their motor functions (Saadé et al., 1997; Takeda et al., 2005; Paillé et al., 2007; Dieb et al., 2015, 2016a,b; Campos et al., 2019; Tang et al., 2021). In addition, 6-OHDA lesions generally showed a contralateral motor deficit along with bilateral pain (Chudler and Lu, 2008; Dieb et al., 2015; 2016a,b). After the lesion, while there was motor improvement, pain scores remained similar over time. This showed the probable occurrence of compensatory modulation in motor circuits, which did not apply to the pain pathway. In PD

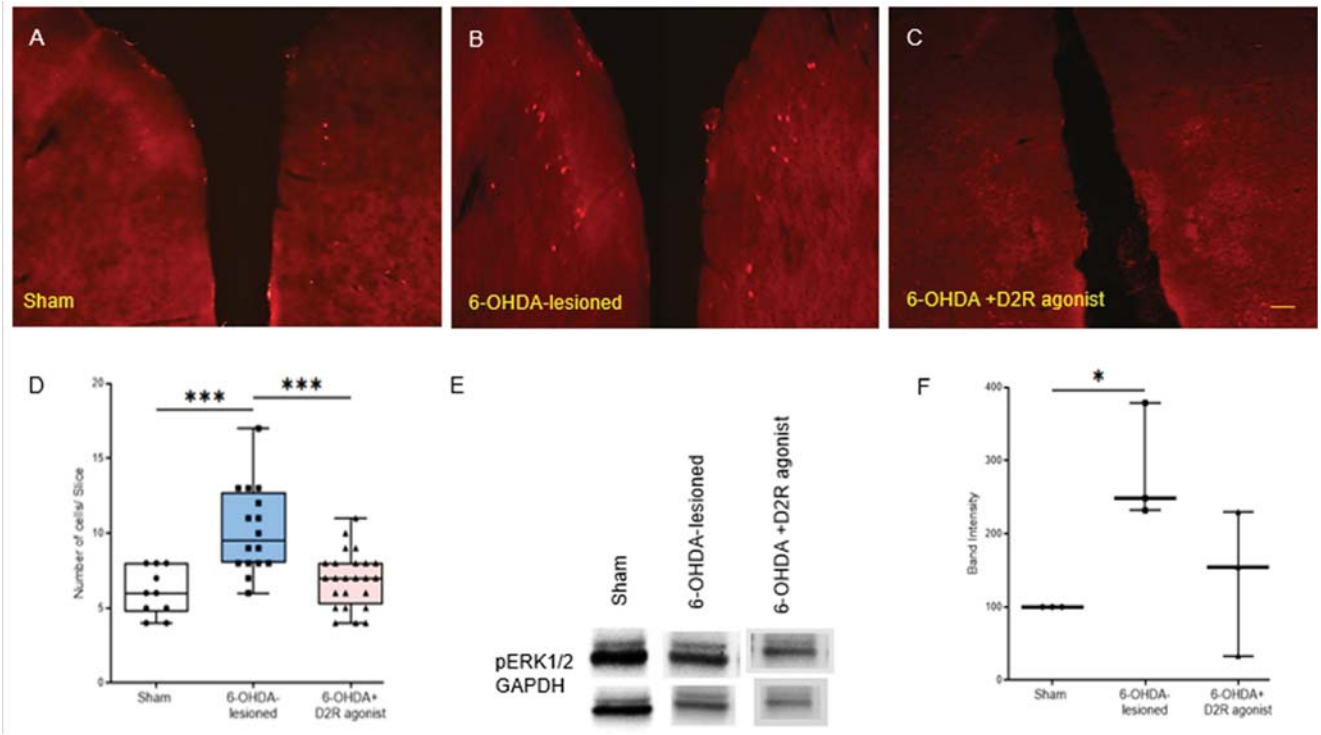

Fig. 8. pERK1/2 protein expression. The Figure shows pERK expression in the cingulate cortex of the sham **(A)**, 6-OHDA-lesioned **(B)**, and 6-OHDA + D2R agonist groups **(C)**. Graph **(D)** represents pERK1/2 positive cells within the cingulate cortex; one-way ANOVA ($F_{2, 47} = 14.36$, $p < 0.0001$, $^{***}P \leq 0.001$): the 6-OHDA-lesioned rats had more significant numbers than both the sham and 6-OHDA + D2R agonist groups (Tukey's multiple comparisons test, $p < 0.0001$, $^{***}P \leq 0.001$). Data are represented as a box-and-whiskers plot, where the box depicts the median and the 25th and 75th quartiles and the whiskers show the 5th and 95th percentile of the sham ($n = 6$), 6-OHDA lesioned ($n = 6$), and 6-OHDA + D2R agonist groups ($n = 7$). The Scale bar = 100 μm. Figure **(E)** shows Western blot bands of pERK1/2 for the three groups. Graph **(F)** represents Western blot band intensities for the three groups; one-way ANOVA ($F_{2, 6} = 5.34$, $p = 0.047$, $^{*}P \leq 0.05$): the 6-OHDA-lesioned group had a more significant increase in expression than the sham group (Tukey's multiple comparisons test, $p = 0.048$, $^{*}P \leq 0.05$). Data are represented as a barplot of the median ± interquartile range of the sham ($n = 4$), 6-OHDA-lesioned ($n = 4$) and 6-OHDA + D2R agonist groups ($n = 4$), GAPDH was used as the loading control.

patients, pain occurs before the onset of motor symptoms (O'Sullivan et al., 2008; Tseng and Lin, 2017), and increases with disease progression (Stamey et al., 2008; Barone et al., 2009). Together, these data infer that in the 6-OHDA-lesioned animal, pain may be associated with dopamine depletion rather than motor deficit.

The 6-OHDA-lesioned rats developed sensitivity to cold temperature (TPP test) and cold allodynia (acetone test). In addition, these rats also developed mechanical hyperalgesia and allodynia. Noxious cold stimuli activate nociceptive C and Aδ afferents, some of which are of a polymodal subtype and respond to a mechanical stimulus (Simone and Kajander, 1996; Dubin and Patapoutian 2010; Sneddon, 2018). These afferent subtypes are probably under central dopaminergic regulation and may be involved in both the mechanical and cold sensitizations observed in 6-OHDA-lesioned rats. SNc probably modulates pain through the inhibition of nociceptive inputs at the spinal cord neuron level (Pasquier et al., 1977; Barnes et al., 1979; Beckstead et al., 1979; Von Krosigk and Smith, 1991) or ascending projections to cortical areas such as insular and/or cingulate cortices (Beckstead et al., 1979; Burkey et al., 1999; Ohara et al., 2003). This is highlighted here by the expression of pERK1/2 at the level of the SDH and the insular and cingulate cortices. pERK1/2 was expressed under noxious and not non-noxious stimuli (Ji et al., 1999; Dieb et al., 2015; 2016a,b). pERK1/2 was highly expressed in these structures in the 6-OHDA-lesioned rats and the administration of D2R agonist ropinirole decreased its expression. This result agrees with previous studies showing an elevation of pERK1/2 expression and its decrease using bromocriptine, another D2R agonist in 6-OHDA-lesioned rats (Dieb et al., 2016a,b). Although the intraperitoneal administration of ropinirole may have affected a variety of brain structures, here, it is demonstrated to affect pain processing structures such as insular and cingulate cortices, in addition to SDH. The latter is clearly involved in the pain process as demonstrated by the changes in the different markers at this level. In addition, the effect of intrathecal ropinirole administration on pain (von Frey test) is in support of the segmental involvement of the pain process in 6-OHDA-lesioned rats.

Most of the data in animals (Domenici et al., 2019; Tang et al., 2021) and humans (Brefel-Courbon et al., 2005) showed that dopamine or dopamine agonists did not affect pain in the control or sham animals. For this reason, and to decrease the number of animals needing to be

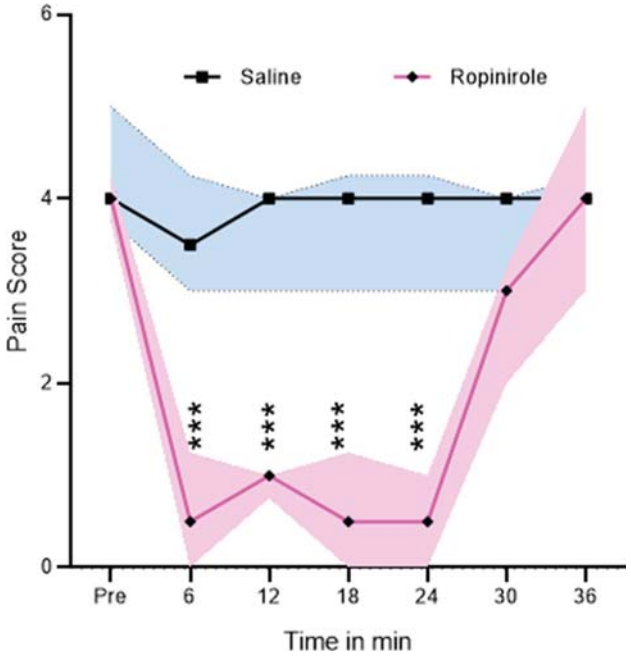

Fig. 9. A significant allodynic behavior was observed in the hind paws in the 6-OHDA-lesioned rats. The allodynic behavior decreased almost immediately with the intrathecal administration of ropinirole in the 6-OHDA-lesioned rats; two-way ANOVA test with significant interaction, row and column factors ($F_{6,\ 70}$ = 14.08, $F_{6,\ 70}$ = 17.80, $F_{1,\ 70}$ = 147.9, respectively, $p < 0.0001$, ***$P \leq 0.001$): followed by (Sidak's multiple comparisons test: $p < 0.0001$, ***$P \leq 0.001$). This effect lasted for almost 25 min. Data are represented as a line plot of the median ± interquartile range of the sham (n = 6) and 6-OHDA-lesioned rats (n = 6).

used, a dopamine agonist was not tested on the sham animals.

The use of specific inhibitors of ERK phosphorylation demonstrated that ERK played a role in allodynia and hyperalgesia caused by spinal cord injury or chronic inflammatory and neuropathic pain (Cruz and Cruz, 2007). Since the question here was the phosphorylation of pre-existing ERK and not the expression of ERK, the total ERK (phosphorylated and non-phosphorylated) was not taken into consideration. In addition, if the total ERK/pERK had been taken into consideration a difference might not have been obtained between the groups. Also, the time between stimulus and sacrifice of the animal was too short for protein synthesis. ERK phosphorylation is induced because of glutamate release (English and Sweatt 1996, 1997), and its binding to both NMDA and metabotropic receptors. It is also induced by neurotrophins through their binding to their tyrosine kinase receptors and by neurotransmitters, such as NPY. Phosphorylation of ERK modulates glutamate receptor and potassium channel activities (Adams et al., 2000; Hu et al., 2006) leading to increased neuronal excitability (Hu and Gereau, 2003). ERK phosphorylation contributes to LTP (Jones et al., 1999; Martin et al., 2000; Schafe et al., 2000; Wei et al., 2006) probably through the expression of different NMDA subunits. Phosphorylation of ERK mediates the windup phenomenon, which is a kind of central sensitization evoked during repetitive C-fiber stimulation (Fukui et al., 2007). More recent studies have also demonstrated a decrease in the mechanical and thermal thresholds in 6-OHDA-lesioned rats, thus implying a segmental pain process (Dieb et al., 2016b; Charles et al., 2018; Campos et al., 2019). Moreover, the windup was higher in the 6-OHDA-lesioned when compared to the sham rats (Charles et al., 2018). The windup is modified by an endogenous opioid mechanism at the level of the SDH (Guan et al., 2006). This opioidergic system has been involved in the mechanical allodynia observed in the 6-OHDA model of PD (Campos et al., 2019). Together, these data imply a segmental pain process in PD animal models.

The present study also demonstrated an increase in the expression of PKCγ, a protein that is involved in pain chronicity (Malmberg et al., 1997; Dieb and Hafidi, 2015; Dieb et al., 2016a,b). Inhibiting PKCγ also depressed the expression of pERK1/2 in the superficial laminae of the medullary dorsal horn and alleviated the pain in the rats (Dieb and Hafidi, 2015). pERK1/2 positive cells receive PKCγ ending innervations (Dieb and Hafidi, 2015). In the present study, ropinirole administration decreased both PKCγ and pERK1/2 expressions. Therefore, dopamine depletion in 6-OHDA-lesioned rats produced sensitization (increase in excitation) at the SDH level (Charles et al., 2018) increasing PKCγ cells excitation (increase in PKCγ staining) leading to the activation of pERK1/2 cells. The latter transfer non-painful stimuli to the pain processing pathway (Dieb and Hafidi, 2015). It is to be noted that, in our case, we have never found pERK1/2 or PKCγ in glial cells. A previous report of double immunostaining using NeuN antibody and pERK1/2 showed that they both colocalize in the same neurons (Dieb et al., 2015).

The administration of the D2R agonist, bromocriptine, lowered the expression of PKCγ, decreased the expression of pERK1/2 in the superficial laminae of the medullary dorsal horn, and alleviated the pain in 6-OHDA-lesioned rats (Dieb et al., 2016a,b). Although the present study confirmed the important role of ropinirole (intraperitoneal and intrathecal administrations) in the pain process, other non-dopaminergic processes should not be excluded. Ropinirole is D3/D2 receptor agonist with very little affinity for D4 and no affinity for D1/D5, serotonin, histamine, acetylcholine, muscarinic, opioids, or adrenergic receptors (Wood, 2008). Ropinirole binds to D2 like receptors with avoiding ergot–like side effects. Ropinirole activates D2 receptors in the central and peripheral nervous systems. The efficiency of ropinirole was better than that of bromocriptine after 3 years of treatment. In different animal models, ropinirole had an antiparkinsonian effect (Fukuzaki et al., 2000). The ropinirole antiparkinsonian effect depends on both D2R and D3R (Matsukawa et al., 2007). To sum up, Ropinirole - as dopamine agonist- is effective as a therapy for early and progressing PD symptoms. This includes pain, as some studies have shown that, in PD models, unilateral injury led to bilateral dorsal horn spinal cord neuron hyperexcitability and augmented D2R function bilaterally (Shill & Stacy, 2009; Tang et al., 2021).

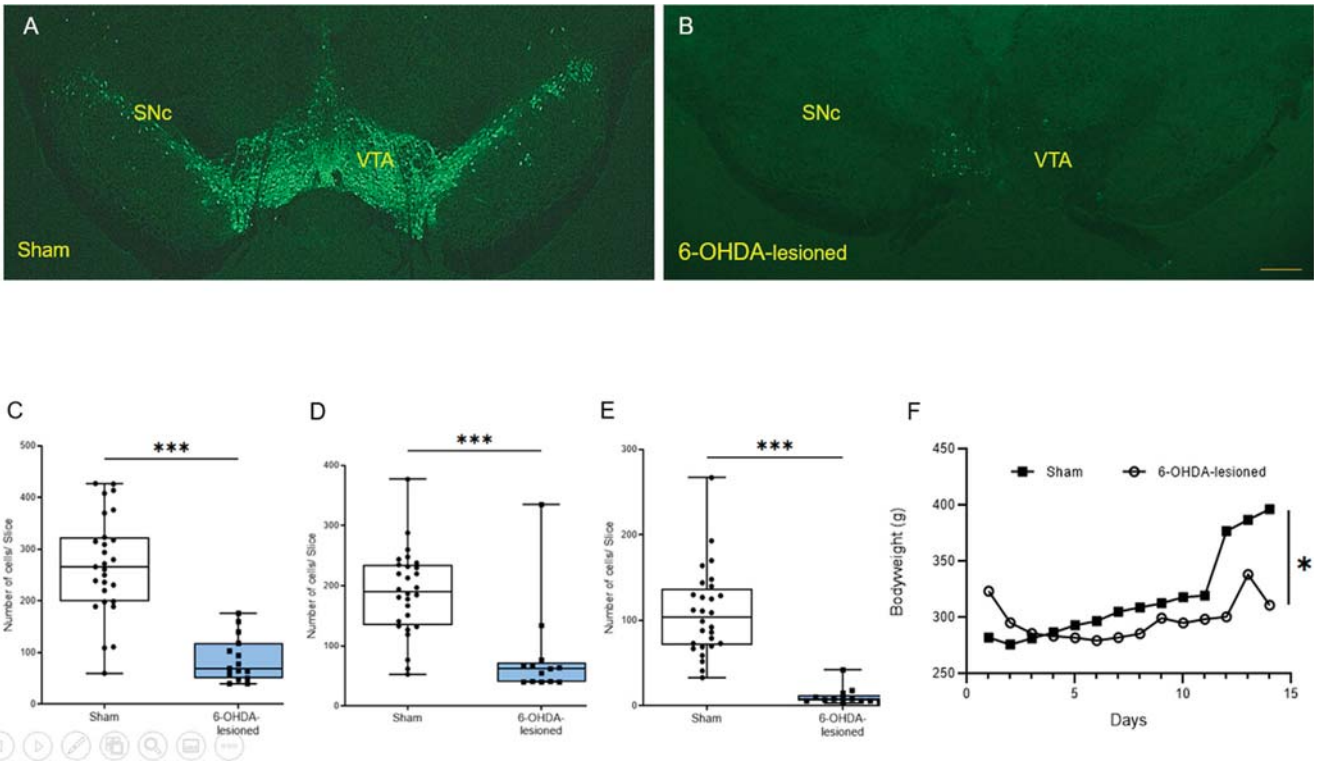

Fig. 10. TH immunostaining in the sham **(A)** and 6-OHDA-lesioned animals **(B)** shows a profound decrease in the intensity of staining, in both the SNc and the VTA in the 6-OHDA-lesioned rats when compared with the sham ones. The Cell count of the TH positive cells in both the SNc and the VTA together; Mann–Whitney test ($U_{27,15} = 18$, $p < 0.0001$, $^{***}P \leq 0.001$) **(C)** or in the VTA only; Mann–Whitney test ($U_{28,13} = 45$, $p < 0.0001$, $^{***}P \leq 0.001$) **(D)** or in the SNc only; Mann–Whitney test ($U_{28,13} = 2$, $p < 0.0001$, $^{***}P \leq 0.001$) **(E)** revealed a significant difference between the 6-OHDA-lesioned and the sham groups. Cell death percentage in both the SNc and the VTA was 67.8%, in VTA only, it was 56.7% and in the SNc, it only was 89.9% after 6-OHDA lesion. Data are represented as a box-and-whiskers plot, where the box depicts the median and the 25th and 75th quartiles and the whiskers show the 5th and 95th percentile of the sham ($n = 5$) and 6-OHDA-lesioned groups ($n = 6$). The Scale bar = 200 μm. The graph **(F)** represents data from two animal groups: sham ($n = 11$) and 6-OHDA-lesioned ($n = 18$). A significant decrease in weight difference (Student's *T*-test) was observed in the 6-OHDA-lesioned group in comparison to the sham rats after surgery ($p = 0.027$, $^{*}P \leq 0.05$).

The present study confirms that of Dieb and Hafidi (2015), except that, here, the stimulus is acetone. Although, to date, there is no proof in the literature of direct projections from SNc/VTA to the spinal cord. There is, however, some evidence that SNc/VTA may influence brainstem descending inhibitory pathways (Beckstead et al., 1979; Commissiong et al., 1979; Loughlin and Fallon, 1984; Ikemoto, 2007; Halliday et al., 2012). For example, the stimulation of SNc inhibits nociceptive input by activating spinal cord neurons through dopaminergic descending pathways (Barnes et al., 1979; Burkey et al., 1999).

Together, these data indicate that dopamine probably regulates the pain process by decreasing excitation in the dorsal horn PKCγ cells. PKCγ cells represent a key cell for switching non-noxious stimuli to the nociceptive pathway (Dieb and Hafidi, 2015; Dieb et al., 2015, 2016a,b).

PKCγ is expressed only in the excitatory interneurons in the rat spinal cord (Todd, 2017) and these neurons contribute to the SDH sensitization. PKCγ protein expression up-regulation was observed in different pain models (Zou et al., 2012; Dieb et al., 2014, 2016b). PKCγ mutant mice displayed normal responses to acute painful stimuli but did not display the exaggerated response to noxious stimuli usually seen after partial sciatic nerve section (Malmberg et al., 1997). Glutamate release and the activation of NMDA receptor-induced both upregulation of PKCγ protein and its translocation from the plasma membrane to the cytosol. PKCγ positive cells project endings to pERK1/2 positive cells within the medullary dorsal horn (Dieb et al., 2015). The inhibition of PKCγ decreased the expression of pERK1/2 and alleviated the allodynia (Dieb et al., 2015). Moreover, several studies have shown that repetitive morphine exposure increased the level of PKCγ protein in the SDH (Mao et al., 1995). PKCγ mutant mice failed to exhibit opioid tolerance (Zeitz et al., 2001).

Another way of increasing excitation at the level of SDH is by decreasing the inhibition or, by disinhibition. Such mechanisms have been described in medullary and SDHs where a decrease in GABA transmission promoted pain (Castro-Lopes et al., 1993; Ibuki et al., 1997; Eaton et al., 1998; Dieb and Hafidi, 2015). In the present study, both immunohistochemistry and Western blots demonstrated an increase in GAD67. There is a converse correlation between the synthesis of GABA and the expression of GAD67 (Rimvall and Martin, 1992). GAD67 activity is regulated by GABA feedback, and this activity declined when GABA levels were elevated. Therefore, the high expression of GAD67 in the

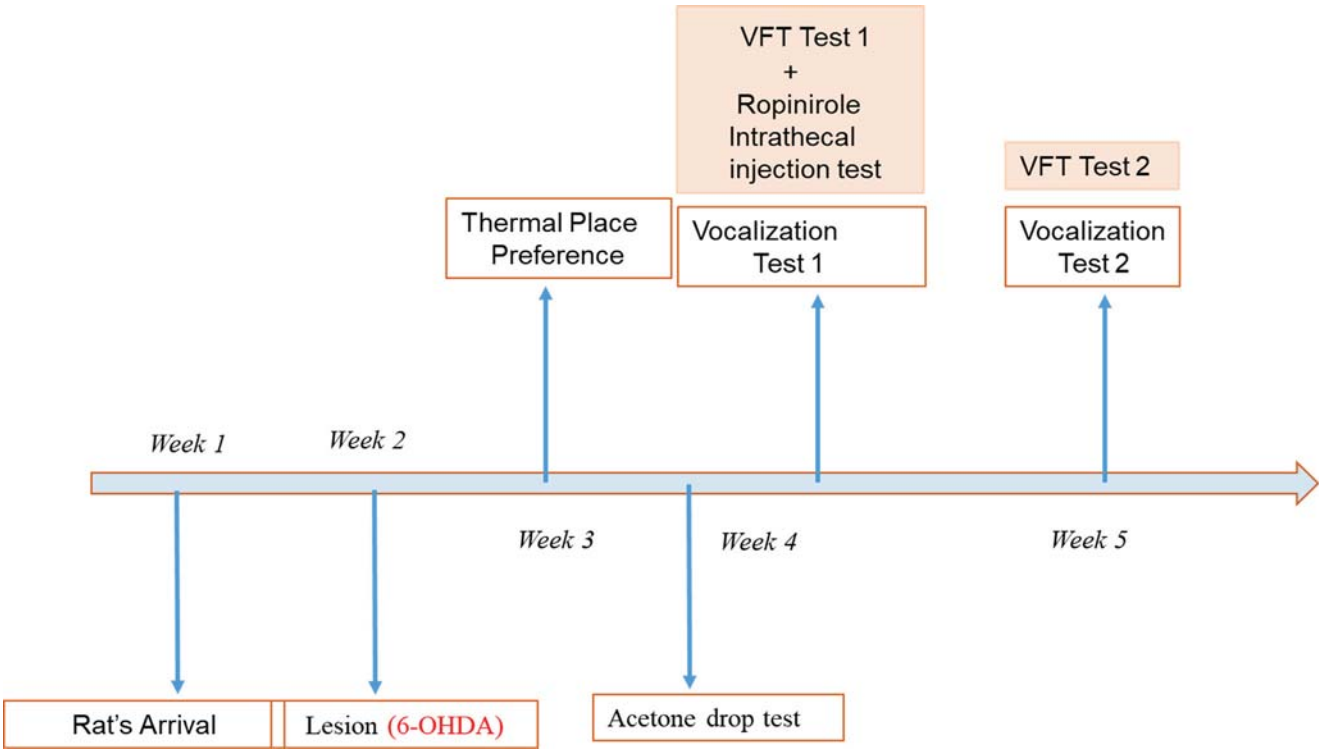

Fig. 11. Behavioral experiments time course. 6-OHDA (6-hydroxydopamine) and VFT (von Frey test).

dorsal horn of 6-OHDA-lesioned rats may have reflected a decrease in GABA levels. This decrease, in turn, increased the excitation of PKCγ cells as reported previously (Dieb and Hafidi, 2015). The 6-OHDA-lesioned rats presented both mechanical allodynia and hyperalgesia, in addition to thermal hyperalgesia.

GAD67 expression is controlled by dopamine. For example, dopamine depletion or D2R antagonists produced an increase in GAD67 expression (Soghomonian and Chesselet, 1992; Périer et al., 2003; Winkler et al., 2003; Billings and Marshall, 2004). Moreover, levodopa treatment reversed GAD67 mRNA overexpression in 6-OHDA-lesioned rats (Bacci et al., 2002; Périer et al., 2003). Although there is no previous report in the literature on this at the spinal cord level, to the best of our knowledge, the administration of ropinirole decreased GAD67 expression in the SDH, as demonstrated by immunohistochemistry and Western blot. Dopamine depletion (SNc/VTA) could regulate GAD67 expression via brainstem descending inhibitory pain pathways or, directly, via dopaminergic hypothalamic nuclei (A11). SNc/VTA project to A11 nucleus. The latter is known to project directly to the spinal cord (Björklund and Skagerberg, 1979; Hokfelt et al., 1979; Skagerberg and Lindvall, 1985; Ozawa et al., 2017).

In the present study, 6-OHDA targeted both SNc and VTA, two nuclei that almost project to similar ascending (cortical and subcortical) or descending (brainstem) structures (Beckstead et al., 1979; Loughlin and Fallon 1984; Ikemoto, 2007; Halliday et al., 2012), which are part of the medial pain system. The neuronal activity in this system is regulated by nociceptive stimuli (Chudler and Dong, 1995; Cortelli et al., 2013) and by dopamine (Schultz and Romo, 1987; Mitsi and Zachariou, 2016). Therefore, the impact of the SNc/VTA lesion on pain is considered as a whole and not each nucleus separately. Both nuclei are affected by the 6-OHDA injection to the MFB. First, the primary target of these structures is the striatum (dorsal and ventral) which plays an important role in pain regulation. Striatal administration of D2R agonists had an anti-nociceptive effect (Lin et al., 1981; Cobacho et al., 2010) mediated by the rostral ventromedial medulla (RVM) (Ansah et al., 2007). Insular and cingulate cortices regulate pain (Chudler and Dong, 1995; Mitsi and Zachariou, 2016; Alles and Smith, 2018). However, a major difference between the SNc and the VTA is that the latter modulates the perception of the affective pain and the reward related pain (Chudler and Dong 1995). Acetone stimulation increased the expression of pERK1/2 in the insular and cingulate cortices, hence demonstrating their implication in the pain process in 6-OHDA-lesioned rats. The administration of ropinirole significantly decreased the number of pERK1/2 positive cells in both structures, demonstrating the role of dopamine regulation in this expression. A decreased cold pain threshold has been shown in PD patients, and Levodopa administration normalized it (Brefel-Courbon et al., 2005, 2013). Similarly, over-activation in the insular and cingulate cortices was observed in pain-free PD subjects who were off levodopa at the time in comparison to healthy subjects (Brefel-Courbon et al., 2005).

In conclusion, the present study demonstrated cold and mechanical allodynia and mechanical hyperalgesia in 6-OHDA-lesioned rats. Acetone stimulus activated neurons within superficial spinal dorsal laminae, cingulate and insular cortices.

ACKNOWLEDGMENTS

The Missions Sector of the Ministry of Higher Education and Scientific Research in Egypt; Ain Shams University, Egypt and Clermont Auvergne University, France funded this study, and all authors declare that there is no conflict of interest. This study has been funded by France Parkinson.

AUTHOR CONTRIBUTIONS

All authors contributed substantially to this study: conception and design of the study (M.E, O.O., A.H); acquisition and interpretation of data (M.E., O.O, A.H., Y.A); drafting of the article (F.D., S.Y., S.S.Z), intellectual revision of the article (M.E., O.O., A.H); and approval of the last version of the manuscript (M.E., O. O., A.H., F.D., S.S.Z., S.Y., Y.A).

FUNDING

The Missions Sector of the Ministry of Higher Education and Scientific Research of the Arab Republic of Egypt; Ain Shams University, Egypt and Clermont Auvergne University, France funded this study, and all authors declare that there is no conflict of interest. This study was funded by France Parkinson.

DECLARATIONS OF INTEREST

None.

REFERENCES

Adams JP, Anderson AE, Varga AW, Dineley KT, Cook RG, Pfaffinger PJ, Sweatt JD (2000) The A-type potassium channel Kv4.2 is a substrate for the mitogen-activated protein kinase ERK. J Neurochem 75:2277–2287.

Alles SRA, Smith PA (2018) Etiology and pharmacology of neuropathic pain. Pharmacol Rev 70(2):315–347.

Altier N, Stewart J (1999) The role of dopamine in the nucleus accumbens in analgesia. Life Sci 65:2269–2287.

Ansah OB, Leite-Almeida H, Wei H, Pertovaara A (2007) Striatal dopamine D2 receptors attenuate neuropathic hypersensitivity in the rat. Exp Neurol 205(2):536–546.

Bacci J-J, Salin P, Kerkerian-Le Goff L (2002) Systemic administration of dizocilpine maleate (MK-801) or L-dopa reverses the increases in GAD65 and GAD67 mRNA expression in the globus pallidus in a rat hemiparkinsonian model. Synapse 46(4):224–234.

Balayssac D, Ling B, Ferrier J, Pereira B, Eschalier A, Authier N (2014) Assessment of thermal sensitivity in rats using the thermal place preference test: description and application in the study of oxaliplatin-induced acute thermal hypersensitivity and inflammatory pain models. Behav Pharmacol 25(2):99–111.

Barceló AC, Fillipini B, Pazo JH (2010) Study of the neural basis of striatal modulation of the jaw-opening reflex. J Neural Transm 117 (2):171–181.

Barnes CD, Fung SJ, Adams WL (1979) Inhibitory effects of substantia nigra on impulse transmission from nociceptors. Pain 6(2):207–215.

Barone P, Antonini A, Colosimo C, Marconi R, Morgante L, Avarello TP, Bottacchi E, Cannas A, Ceravolo G, Ceravolo R, Cicarelli G, Gaglio RM, Giglia RM, Iemolo F, Manfredi M, Meco G, Nicoletti A, Pederzoli M, Petrone A, Pisani A, Pontieri FE, Quatrale R, Ramat S, Scala R, Volpe G, Zappulla S, Bentivoglio AR, Stocchi F, Trianni G, Dotto PD (2009) The PRIAMO study: A multicenter assessment of nonmotor symptoms and their impact on quality of life in Parkinson's disease. Mov Disord 24(11):1641–1649.

Beckstead RM, Domesick VB, Nauta WJH (1979) Efferent connections of the substantia nigra and ventral tegmental area in the rat. Brain Res 175(2):191–217.

Billings LM, Marshall JF (2004) Glutamic acid decarboxylase 67 mRNA regulation in two globus pallidus neuron populations by dopamine and the subthalamic nucleus. J Neurosci 24 (12):3094–3103.

Björklund A, Skagerberg G (1979) Evidence for a major spinal cord projection from the diencephalic A 11 dopamine cell group in the rat using transmitter-specific fluorescent retrograde tracing. Brain Res 177(1):170–175.

Blanchet PJ, Brefel-Courbon C (2018) Chronic pain and pain processing in Parkinson's disease. Prog Neuropsychopharmacol Biol Psychiatry 87(Pt B):200–206.

Borsook D (2012) Neurological diseases and pain. Brain 135:320–344.

Brefel-Courbon C, Payoux P, Thalamas C, Ory F, Quelven I, Chollet F, Montastruc JL, Rascol O (2005) Effect of levodopa on pain threshold in Parkinson's disease: a clinical and positron emission tomography study. Mov Disord 20(12):1557–1563.

Brefel-Courbon C, Ory-Magne F, Thalamas C, Payoux P, Rascol O (2013) Nociceptive brain activation in patients with neuropathic pain related to Parkinson's disease. Parkinsonism Relat Disord 19 (5):548–552.

Buhidma Y, Rukavina K, Chaudhuri KR, Duty S (2020) Potential of animal models for advancing the understanding and treatment of pain in Parkinson's disease. NPJ Parkinsons Dis 6:1.

Buhmann C, Kassubek J, Jost WH, Bloem BR, Brundin P (2020) Management of pain in Parkinson's disease. J Parkinson's Dis 10 (s1):S37–S48.

Burkey AR, Carstens E, Jasmin L (1999) Dopamine reuptake inhibition in the rostral agranular insular cortex produces antinociception. J Neurosci 19(10):4169–4179.

Campos ACP, Berzuino MB, Hernandes MS, Fonoff ET, Pagano RL (2019) Monoaminergic regulation of nociceptive circuitry in a Parkinson's disease rat model. Exp Neurol 318:12–21.

Castro-Lopes JM, Tavares I, Coimbra A (1993) GABA decreases in the spinal cord horn after peripheral neurectomy. Brain Res 620:287–291.

Chaplan SR, Bach FW, Pogrel JW, Chung JM, Yaksh TL (1994) Quantitative assessment of tactile allodynia in the rat paw. J Neurosci Methods 53(1):55–63.

Charles K-A, Naudet F, Bouali-Benazzouz R, Landry M, De Deurwaerdère P, Fossat P, Benazzouz A (2018) Alteration of nociceptive integration in the spinal cord of a rat model of Parkinson's disease. Mov Disord 33(6):1010–1015.

Choi Y, Yoon YW, Na HS, Kim SH, Chung JM (1994) Behavioral signs of ongoing pain and cold allodynia in a rat model of neuropathic pain. Pain 59:369–376.

Chudler EH, Dong WK (1995) The role of the basal ganglia in nociception and pain. Pain 60:3–38.

Chudler EH, Lu Y (2008) Nociceptive behavioral responses to chemical, thermal and mechanical stimulation after unilateral, intrastriatal administration of 6-hydroxydopamine. Brain Res 1213:41–47.

Cobacho N, De la Calle JL, González-Escalada JR, Paíno CL (2010) Levodopa analgesia in experimental neuropathic pain. Brain Res Bull 83(6):304–309.

Commissiong JW, Gentleman S, Neff NH (1979) Spinal cord dopaminergic neurons: evidence for an uncrossed nigrospinal pathway. Neuropharmacology 18(6):565–568.

Cortelli P, Giannini G, Favoni V, Cevoli S, Pierangeli G (2013) Nociception and autonomic nervous system. Neurol Sci 34 (S1):41–46.

Cruz CD, Cruz F (2007) The ERK 1 and 2 pathway in the nervous system: from basic aspects to possible clinical applications in pain and visceral dysfunction. Curr Neuropharmacol 5(4):244–252.
Dieb W, Ouachikh O, Durif F, Hafidi A (2014) Lesion of the dopaminergic nigrostriatal pathway induces trigeminal dynamic mechanical allodynia. Brain Behav 4(3):368–380.
Dieb W, Alvarez P, Hafidi A (2015) PKC gamma-positive neurons gate light tactile inputs to pain pathway through pERK1/2 neuronal network in trigeminal neuropathic pain model. J Oral Fac Pain Headache 29:70–82.
Dieb W, Hafidi A (2015) Mechanism of GABA-involvement in posttraumatic trigeminal neuropathic pain: Activation of neuronal circuitry composed by PKC γ interneurons, and pERK1/2 expressing neurons. Eur J Pain 19:85–96.
Dieb W, Ouachikh O, Alves S, Boucher Y, Durif F, Hafidi A (2016a) Nigrostriatal dopaminergic depletion increases static orofacial allodynia. J Headache Pain 17:11.
Dieb W, Ouachikh O, Durif F, Hafidi A (2016b) Nigrostriatal dopaminergic depletion produces orofacial static mechanical allodynia. Eur J Pain 20(2):196–205.
Domenici RA, Campos ACP, Maciel ST, Berzuino MB, Hernandes MS, Fonoff ET, Pagano RL (2019) Parkinson's disease and pain: Modulation of nociceptive circuitry in a rat model of nigrostriatal lesion. Exp Neurol 315:72–81.
Dubin AE, Patapoutian A (2010) Nociceptors: the sensors of the pain pathway. J Clin Invest 120(11):3760–3772.
Eaton MJ, Plunkett JA, Karmally S, Martinez MA, Montanez K (1998) Changes in GAD- and GABA-immunoreactivity in the spinal dorsal horn after peripheral nerve injury and promotion of recovery by lumbar transplant of immortalized serotonergic precursors. J Chem Neuroanat 16(1):57–72.
English JD, Sweatt JD (1996) Activation of p42 mitogen-activated protein kinase in hippocampal long term potentiation. J Biol Chem 271(40):24329–24332.
English JD, Sweatt JD (1997) A requirement for the mitogen-activated protein kinase cascade in hippocampal long term potentiation. J Biol Chem 272(31):19103–19106.
Ferro MM, Angelucci ME, Anselmo-Franci JA, Canteras NS, Da Cunha C (2007) Neuroprotective effect of ketamine/xylazine on two rat models of Parkinson's disease. Braz J Med Biol Res 40 (1):89–96.
Fil A, Cano-de-la-Cuerda R, Muñoz-Hellín E, Vela L, Ramiro-González M, Fernández-de-las-Peñas C (2013) Pain in Parkinson disease: A review of the literature. Parkinsonism Relat Disord 19(3):285–294.
Fukui T, Dai Y, Iwata K, Kamo H, Yamanaka H, Obata K, Kobayashi K, Wang S, Cui X, Yoshiya S, Noguchi K (2007) Frequency-dependent ERK phosphorylation in spinal neurons by electric stimulation of the sciatic nerve and the role in the electrophysiological activity. Mol Pain 16:3–18.
Fukuzaki K, Kamenosono T, Nagata R (2000) Effects of ropinirole on various parkinsonian models in mice, rats, and cynomolgus monkeys. Pharmacol Biochem Behav 65(3):503–508.
Guan Y, Borzan J, Meyer RA, Raja SN (2006) Windup in dorsal horn neurons is modulated by endogenous spinal mu-opioid mechanisms. J Neurosci 26(16):4298–4307.
Halliday G, Reyes S, Double K (2012) Substantia Nigra, Ventral Tegmental Area, and Retrorubral Fields. In: The human nervous system, ed. 3 (Mai JK, Paxinos G), ch 13, pp 439-455. Academic Press.
Harris HN, Peng YB (2020) Evidence and explanation for the involvement of the nucleus accumbens in pain processing. Neural Regen Res 15(4):597–605.
Hokfelt T, Phillipson O, Goldstein M (1979) Evidence for a dopaminergic pathway in the rat descending from the A11 cell group to the spinal cord. Acta Physiol Scand 107:393–395.
Hu H-J, Carrasquillo Y, Karim F, Jung WE, Nerbonne JM, Schwarz TL, Gereau RW (2006) The kv4.2 potassium channel subunit is required for pain plasticity. Neuron 50(1):89–100.
Hu H-J, Gereau RW (2003) ERK integrates PKA and PKC signaling in superficial dorsal horn neurons II. Modulation of neuronal excitability. J Neurophysiol 90(3):1680–1688.
Ibuki T, Hama AT, Wang X-T, Pappas GD, Sagen J (1997) Loss of GABA-immunoreactivity in the spinal dorsal horn of rats with peripheral nerve injury and promotion of recovery by adrenal medullary grafts. Neuroscience 76(3):845–858.
Ikemoto S (2007) Dopamine reward circuitry: two projection systems from the ventral midbrain to the nucleus accumbens-olfactory tubercle complex. Brain Res Rev 56(1):27–78.
Jankovic J, Tan EK (2020) Parkinson's disease: etiopathogenesis and treatment. J Neurol Neurosurg Psychiatry 91(8):795–808.
Jensen TS, Finnerup NB (2014) Allodynia and hyperalgesia in neuropathic pain: Clinical manifestations and mechanisms. Lancet Neurol 13(9):924–935.
Ji R-R, Baba H, Brenner GJ, Woolf CJ (1999) Nociceptive-specific activation of ERK in spinal neurons contributes to pain hypersensitivity. Nat Neurosci 2(12):1114–1119.
Jones MW, French PJ, Bliss TV, Rosenblum K (1999) Molecular mechanisms of long-term potentiation in the insular cortex. J Neurosci 19(RC36):1–8.
Lin MT, Wu JJ, Chandra A, Tsay BL (1981) Activation of striatal dopamine receptors induces pain inhibition in rats. J Neural Trans 51(3-4):213–222.
Liu MG, Matsuura S, Shinoda M, Honda K, Suzuki I, Shibuta K, Tamagawa T, Katagiri A, Kiyomoto M, Ohara K, Furukawa A, Urata K, Iwata K (2012) Metabotropic glutamate receptor 5 contributes to inflammatory tongue pain via extracellular signal-regulated kinase signaling in the trigeminal spinal subnucleus caudalis and upper cervical spinal cord. J Neuroinflamm 9:258.
Loughlin SE, Fallon JH (1984) Substantia nigra and ventral tegmental area projections to cortex: topography and collateralization. Neuroscience 11(2):425–435.
Magnusson JE, Fisher K (2000) The involvement of dopamine in nociception: The role of D(1) and D(2) receptors in the dorsolateral striatum. Brain Res 855(2):260–266.
Malmberg AB, Chen C, Tonegawa S, Basbaum AI (1997) Preserved acute pain and reduced neuropathic pain in mice lacking PKCgamma. Science 278:279–283.
Mao J, Price DD, Phillips LL, Lu J, Mayer DJ (1995) Increases in protein kinase C gamma immunoreactivity in the spinal cord of rats associated with tolerance to the analgesic effects of morphine. Brain Res 677(2):257–267.
Marques A, Chassin O, Morand D, Pereira B, Debilly B, Derost P, Ulla M, Lemaire JJ, Durif F (2013) Central pain modulation after subthalamic nucleus stimulation: A crossover randomized trial. Neurology 81(7):633–640.
Martin SJ, Grimwood PD, Morris RGM (2000) Synaptic plasticity and memory: an evaluation of the hypothesis. Annu Rev Neurosci 23 (1):649–711.
Matsukawa N, Maki M, Yasuhara T, Hara K, Yu G, Xu L, Kim KM, Morgan JC, Sethi KD, Borlongan CV (2007) Overexpression of D2/D3 receptors increases the efficacy of ropinirole in chronically 6-OHDA-lesioned Parkinsonian rats. Brain Res 1160:113–123.
Mavrikaki M, Schintu N, Nomikos GG, Panagis G, Svenningsson P (2014) Ropinirole regulates emotionality and neuronal activity markers in the limbic forebrain. Int J Neuropsychopharmacol 17 (12):1981–1993.
Mestre C, Pélissier T, Fialip J, Wilcox G, Eschalier A (1994) A method to perform direct transcutaneous intrathecal injection in rats. J Pharmacol Toxicol Methods 32(4):197–200.
Mitsi V, Zachariou V (2016) Modulation of pain, nociception, and analgesia by the brain reward center. Neuroscience 338:81–92.
Mylius V, Ciampi de Andrade D, Cury RG, Teepker M, Ehrt U, Eggert KM, Beer S, Kesselring J, Stamelou M, Oertel WH, Möller JC, Lefaucheur J-P (2015) Pain in Parkinson's disease: current concepts and a new diagnostic algorithm. Mov Disord Clin Pract 2(4):357–364.

Ohara PT, Granato A, Moallem TM, Wang B-R, Tillet Y, Jasmin L (2003) Dopaminergic input to GABAergic neurons in the rostral agranular insular cortex of the rat. J Neurocytol 32(2):131–141.
Ohara PT, Vit J-P, Jasmin L (2005) Cortical modulation of pain. Cell Mol Life Sci 62(1):44–52.
Ouachikh O, Dieb W, Durif F, Hafidi A (2013) Differential behavioral reinforcement effects of dopamine receptor agonists in the rat with bilateral lesion of the posterior ventral tegmental area. Behav Brain Res 1(252):24–31.
Ouachikh O, Dieb W, Durif F, Hafidi A (2014) Anterior ventral tegmental area dopaminergic neurons are not involved in the motivational effects of bromocriptine, pramipexole, and cocaine in drug-free rats. Behav Brain Res 1(262):1–7.
Ozawa H, Yamaguchi T, Hamaguchi S, Yamaguchi S, Ueda S (2017) Three types of A11 neurons project to the rat spinal cord. Neurochem Res 42(8):2142–2153.
O'Sullivan SS, Williams DR, Gallagher DA, Massey LA, Silveira-Moriyama L, Lees AJ (2008) Nonmotor symptoms as presenting complaints in Parkinson's disease: a clinicopathological study. Mov Disord 23(1):101–106.
Paillé V, Henry V, Lescaudron L, Brachet P, Damier P (2007) Rat model of Parkinson's disease with bilateral motor abnormalities, reversible with levodopa, and dyskinesias. Mov Disord 22 (4):533–539.
Pasquier DA, Kemper TL, Forbes WB, Morgane PJ (1977) Dorsal raphe, substantia nigra and locus coeruleus: interconnections with each other and the neostriatum. Brain Res Bull 2(5):323–339.
Périer C, Marin C, Jimenez A, Bonastre M, Tolosa E, Hirsch EC (2003) Effect of subthalamic nucleus or entopeduncular nucleus lesion on levodopa-induced neurochemical changes within the basal ganglia and on levodopa-induced motor alterations in 6-hydroxydopamine-lesioned rats: STN or EP lesion on levodopa-induced changes. J Neurochem 86(6):1328–1337.
Polgár E, Campbell AD, MacIntyre LM, Watanabe M, Todd AJ (2007) Phosphorylation of ERK in neurokinin 1 receptor-expressing neurons in laminae III and IV of the rat spinal dorsal horn following noxious stimulation. Mol Pain 3:4.
Ramji JV, Keogh JP, Blake TJ, Broom C, Chenery RJ, Citerone DR, Lewis VA, Taylor AC, Yeulet SE (1999) Disposition of ropinirole in animals and man. Xenobiotica 29(3):311–325.
Randall LO, Selitto JJ (1957) A method for measurement of analgesic activity on inflamed tissue. Arch Int Pharmacodyn Ther 111 (4):409–419.
Rimvall K, Martin DL (1992) Increased intracellular gamma-aminobutyric acid selectively lowers the level of the larger of two glutamate decarboxylase proteins in cultured GABAergic neurons from rat cerebral cortex. J Neurochem 58(1):158–166.
Saadé NE, Atweh SF, Bahuth NB, Jabbur SJ (1997) Augmentation of nociceptive reflexes and chronic deafferentation pain by chemical lesions of either dopaminergic terminals or midbrain dopaminergic neurons. Brain Res 751(1):1–12.
Sandkühler J (2009) Models and mechanisms of hyperalgesia and allodynia. Physiol Rev 89(2):707–758.
Schafe GE, Atkins CM, Swank MW, Bauer EP, Sweatt JD, LeDoux JE (2000) Activation of ERK/MAP kinase in the amygdala is required for memory consolidation of pavlovian fear conditioning. J Neurosci 20(21):8177–8187.
Shill HA, Stacy M (2009) Update on ropinirole in the treatment of Parkinson's disease. Neuropsychiatr Dis Treat 5:33–36.
Schultz W, Romo R (1987) Responses of nigrostriatal dopamine neurons to high-intensity somatosensory stimulation in the anesthetized monkey. J Neurophysiol 57(1):201–217.
Simone DA, Kajander KC (1996) Excitation of rat cutaneous nociceptors by noxious cold. Neurosci Lett 213(1):53–56.
Skagerberg G, Lindvall O (1985) Organization of diencephalic dopamine neurons projecting to the spinal cord in the rat. Brain Res 342:340–351.
Skogar O, Lokk J (2016) Pain management in patients with Parkinson's disease: challenges and solutions. J Multidisc Healthc 9:469–479.
Sneddon LU (2018) Comparative physiology of nociception and pain. Physiology (Bethesda) 33(1):63–73.
Soghomonian JJ, Chesselet MF (1992) Effects of nigrostriatal lesions on the levels of messenger RNAs encoding two isoforms of glutamate decarboxylase in the globus pallidus and entopeduncular nucleus of the rat. Synapse 11(2):124–133.
Stamey W, Davidson A, Jankovic J (2008) Shoulder pain: a presenting symptom of Parkinson disease. J Clin Rheumatol 14:253–254.
Takahashi Y, Nakajima Y, Sakamoto T (1994) Dermatome mapping in the rat hindlimb by electrical stimulation of the spinal nerves. Neurosci Lett 168(1-2):85–88.
Takeda R, Ikeda T, Tsuda F, Abe H, Hashiguchi H, Ishida Y, Nishimori T (2005) Unilateral lesions of mesostriatal dopaminergic pathway alters the withdrawal response of the rat hind paw to mechanical stimulation. Neurosci Res 52(1):31–36.
Dl T, Yw L, Cy Z, Xiao C (2021) D2 receptor activation relieves pain hypersensitivity by inhibiting superficial dorsal horn neurons in parkinsonian mice. Acta Pharmacol Sin 42:189–198.
Taylor AMW, Murphy NP, Evans CJ, Cahill CM (2014) Correlation between ventral striatal catecholamine content and nociceptive thresholds in neuropathic mice. J Pain 15(8):878–885.
Todd AJ (2017). Identifying functional populations among the interneurons in laminae I-III of the spinal dorsal horn. Mol Pain 13:1744806917693003.
Tremblay M, Silveira MM, Kaur S, Hosking JG, Adams WK, Baunez C, Winstanley CA (2017) Chronic $D_{2/3}$ agonist ropinirole treatment increases preference for uncertainty in rats regardless of baseline choice patterns. Eur J Neurosci 45:159–166.
Tseng MT, Lin CH (2017) Pain in early-stage Parkinson's disease: Implications from clinical features to pathophysiology mechanisms. J Formosan Med Assoc 116(8):571–581.
Viana F (2018) Nociceptors: thermal allodynia and thermal pain. Handb Clin Neurol 156:103–119.
Krosigk M, Smith AD (1991) Descending projections from the substantia nigra and retrorubral field to the medullary and pontomedullary reticular formation. Eur J Neurosci 3(3):260–273.
Wawrzczak-Bargieła A, Ziółkowska B, Piotrowska A, Starnowska-Sokół J, Rojewska E, Mika J, Przewłocka B, Przewłocki R (2020) Neuropathic pain dysregulates gene expression of the forebrain opioid and dopamine systems. Neurotox Res 37(4):800–814.
Wei F, Vadakkan KI, Toyoda H, Wu LJ, Zhao MG, Xu H, Shum FW, Jia YH, Zhuo M (2006) Calcium calmodulin-stimulated adenylyl cyclases contribute to activation of extracellular signal-regulated kinase in spinal dorsal horn neurons in adult rats and mice. J Neurosci 26:851–861.
Winkler C, Bentlage C, Cenci MA, Nikkhah G, Björklund A (2003) Regulation of neuropeptide mRNA expression in the basal ganglia by intrastriatal and intranigral transplants in the rat Parkin-son model. Neuroscience 118(4):1063–1077.
Wood PB (2006) Mesolimbic dopaminergic mechanisms and pain control. Pain 120:230–234.
Wood PB (2008) Role of central dopamine in pain and analgesia. Expert Rev Neurother 8(5):781–797.
Young Blood MR, Ferro MM, Munhoz RP, Teive HAG, Camargo CHF (2016) Classification and characteristics of pain associated with Parkinson's disease. Parkinsons Dis 2016:6067132.
Zeitz KP, Malmberg AB, Gilbert H, Basbaum AI (2001) Reduced development of tolerance to the analgesic effects of morphine and clonidine in PKC gamma mutant mice. Pain 94:245–253.
Zenken-Toktas Y, Authier N, Denizot H, Chassain C, Hafidi A, Llorca PM, Durif F (2013) Motivational properties of D2 and D3 dopamine receptors agonists and cocaine, but not with D1 dopamine receptors agonist and L-dopa, in bilateral 6-OHDA lesioned rat. Neuropharmacology 70:74–82.
Zhang Y, Larcher KM, Misic B, Dagher A (2017) Anatomical and functional organization of the human substantia nigra and its connections. Elife 6:e26653.
Zou W, Zhan X, Li M, Song Z, Liu C, Peng F, Guo Q (2012) Identification of differentially expressed proteins in the spinal cord

of neuropathic pain models with PKCgamma silence by proteomic analysis. Brain Res 1440:34–46.

APPENDIX A. SUPPLEMENTARY DATA

Supplementary data to this article can be found online at https://doi.org/10.1016/j.neuroscience.2021.10.026.

(Received 2 May 2021, Accepted 26 October 2021)
(Available online 6 November 2021)

Table (3): Shows the normality test used, followed by measurement of equal variances (Levene's test) in case of parametric data, in addition to final statistical tests used in accordance.

Experimental Test	Normality Test used			Parametric/ Non-parametric	If parametric equal variances testing (Levene's test p-value)	Final Test to be used (Parametric/ non-parametric)
	Test name	group	P-value			
TPP	Shapiro-Wilk test	10 °C Sham	0.507	Parametric	0.480	Student's T-test
		10 °C Lesioned	0.129			
		15 °C Sham	0.758	Parametric	0.214	Student's T-test
		15 °C Lesioned	0.297			
		25 °C Sham	0.012	Non- Parametric		Mann-Whitney U Test
		25 °C Lesioned	0.005			
		35 °C Sham	0.717	Parametric	0.184	Student's T-test
		35 °C Lesioned	0.303			
		50 °C Sham	0.021	Non- Parametric		Mann-Whitney U Test
		50 °C Lesioned	0.681			
Acetone Drop Test	Shapiro-Wilk test	*Number of flinches*		Non- Parametric		Kruskal - Walllis Test
		Sham	<0.0001			
		6-OHDA-lesioned	<0.0001			
		6-OHDA +D2R agonist	0.377			
		Latency time		Non- Parametric		Kruskal - Wallis Test
		Sham	<0.0001			
		6-OHDA-lesioned	<0.0001			
		6-OHDA +D2R agonist	<0.0001			

		Reaction time Sham 6-OHDA-lesioned 6-OHDA +D2R agonist	 0.863 0.118 0.575	Parametric	<0.001 Thus, switching to Non- parametric test	Kruskal - Wallis Test
Vocalization Threshold	Shapiro-Wilk test	*Pre-surgery* Sham 6-OHDA-lesioned *Week 1* Sham 6-OHDA-lesioned *Week 2* Sham 6-OHDA-lesioned	 0.441 0.331 0.860 0.900 0.037 0.928	Parametric	 0.248 0.328 0.334	Two–way ANOVA
Pain Score (VFT)	Shapiro-Wilk test	*Pre-surgery* Sham 6-OHDA-lesioned	 < 0.001 0.482	Non- Parametric		Friedman's Test

		Week 1 Sham 6-OHDA-lesioned *Week 2* Sham 6-OHDA-lesioned	0.006 0.048 < 0.001 0.255			
pERK SC	Shapiro-Wilk test	*Immunohisto-chemistry* Sham 6-OHDA-lesioned 6-OHDA +D2R agonist	<0.0001 0.479 0.010	Non- Parametric		Kruskal - Walllis Test
		Western Blot Sham 6-OHDA-lesioned 6-OHDA +D2R agonist	0.886 0.190	Parametric	0.311	One–way ANOVA
PKCγ SC	Shapiro-Wilk test	*Immunohisto-chemistry*		Parametric	< 0.001	Kruskal - Wallis Test

		Sham 6-OHDA-lesioned 6-OHDA +D2R agonist	0.464 0.114 0.352		Thus, switching to Non- parametric test	
		Western Blot Sham 6-OHDA-lesioned 6-OHDA +D2R agonist	 0.145 0.878	Parametric	0.057	One–way ANOVA
GAD67		*Western Blot* Sham 6-OHDA-lesioned 6-OHDA +D2R agonist	 0.034 0.210	Non- Parametric		Kruskal - Wallis Test
pERK IC	Shapiro-Wilk test	*Immunohisto-chemistry* Sham 6-OHDA-lesioned	 0.012 0.690	Non- Parametric		Kruskal - Wallis Test

		6-OHDA +D2R agonist	0.507			
		Western Blot Sham 6-OHDA-lesioned 6-OHDA +D2R agonist	 0.860 0.366	Parametric	0.366	One–way ANOVA
pERK CC	Shapiro-Wilk test	*Immunohisto-chemistry* Sham 6-OHDA-lesioned 6-OHDA +D2R agonist	 0.145 0.289 0.376	Parametric	0.081	One–way ANOVA
		Western Blot Sham 6-OHDA-lesioned 6-OHDA +D2R agonist	 0.200 0.744	Parametric	0.366	One–way ANOVA
Ropinirole-Saline	Shapiro-Wilk test	*Pre-injection* Sham	 0.212	Parametric		Two–way ANOVA

(intrathecal injection)		6-OHDA-lesioned	0.101		0.599	
		6 minutes				
		Sham	0.091		1.000	
		6-OHDA-lesioned	0.091			
		12 minutes				
		Sham	0.001			
		6-OHDA-lesioned	< 0.001		0.549	
		18 minutes				
		Sham	0.212			
		6-OHDA-lesioned	0.091		0.563	
		24 minutes				
		Sham	0.212			
		6-OHDA-lesioned	0.004		1.000	
		30 minutes				
		Sham				
		6-OHDA-lesioned	0.001		0.599	

		36 minutes Sham 6-OHDA-lesioned	0.212 0.212 0.167		0.599	
TH SN+VTA	Shapiro-Wilk test	Sham 6-OHDA-lesioned	0.564 0.069	Parametric	0.016 Thus, switching to Non- parametric test	Mann-Whitney U Test
TH VTA only	Shapiro-Wilk test	Sham 6-OHDA-lesioned	0.590 <0.0001	Non- Parametric		Mann-Whitney U Test
TH SN only	Shapiro-Wilk test	Sham 6-OHDA-lesioned	0.072 0.0002	Non- Parametric		Mann-Whitney U Test

Results – 2nd Paper

Neuroscience Letters 762 (2021) 136135

Contents lists available at ScienceDirect

Neuroscience Letters

journal homepage: www.elsevier.com/locate/neulet

Research article

Nigrostriatal dopamine depletion promoted an increase in inhibitory markers (parvalbumin, GAD67, VGAT) and cold allodynia

Mennatallah Elshennawy [a,b], Omar Ouachikh [b], Shereen Adel Saad [a], Yasmin Ramadan [a], Franck Durif [b], Aziz Hafidi [b,*]

[a] Anatomy and Embryology Department, Faculty of Medicine, Ain Shams University, Cairo, Egypt
[b] Université Clermont Auvergne, CHU, CNRS, Clermont Auvergne INP, Institut Pascal, Clermont-Ferrand 63000, France

ARTICLE INFO

Keywords:
Parkinson's disease
Allodynia
Hyperalgesia
Cold

ABSTRACT

Pain constitutes the major non-motor symptom in Parkinson's disease (PD). Its mechanism is still poorly understood although an increase in excitation or a decrease in inhibition have been reported in preclinical studies. The aim of this study was to investigate gamma aminobutyric acid (GABA) inhibition in the 6-hydroxydopamine (6-OHDA) PD rat model. Therefore, the expression of three inhibitory markers parvalbumin, glutamate decarboxylase 67 (GAD67) and vesicular GABA transporter (VGAT) was evaluated, besides cold allodynia, in bilateral 6-OHDA lesioned rat. There was a significant increase in the expression of the three markers labeling within the spinal dorsal horn (SDH) of 6-OHDA lesioned rats. In parallel, there was also an increase of the excitatory marker protein kinase C gamma (PKCγ) . PKCγ cells have a crucial role in pain chronicity and are regulated by GABAergic influences. Central dopamine depletion induced an increase in excitation as reveled by an increase in cFOS expression upon acetone stimulus and the presence of cold allodynia. In addition, dopamine depletion induced increased expression in inhibitory markers, which may reflect a disinhibition or a decreased inhibition in 6-OHDA lesioned rats.

1. Introduction

Parkinson's disease (PD), which is a neurodegenerative pathology occurring due to loss of dopaminergic neurons in the substantia nigra pars compacta (SNc), entails both motor and non-motor symptoms. PD patients complain of motor symptoms such as resting tremor, rigidity, akinesia and postural instability; while non– motor symptoms are usually stated earlier before PD diagnosis [1,2]. The major non-PD symptom is pain, which constitutes around *68*–95% [3]. Symptoms of pain happen commonly in the off phase of treatment [4] and pain was alleviated on treatment using Levodopa [5]. In PD patients and animal models, many studies have confirmed the decrease in chemical, mechanical and thermal pain thresholds [6,7,8,9]. Although basal ganglia have been implicated in pain, nevertheless, the exact mechanisms integrated in pain pathology are not yet fully discovered [5,6]. In addition, the diminution of dopamine (DA) in striatal pathway has enhanced neuropathic pain [10], while injecting Dopamine receptor 2 (D2R) agonist in the striatum has relieved pain [11,12]. Also, when DA was increased by amphetamine instillation into the nucleus accumbens, pain has been lessened [13].

Neuropathic pain (NP) can be either spontaneous or evoked. Either primary malfunction of the peripheral or central nervous systems may cause NP [14]. It can be manifested as allodynia or hyperalgesia [15,16]. The most common cellular mechanism is an imbalance in neurotransmission with an increase in excitation or disinhibition and/or a decrease in inhibition [15]. Therefore, the goal of the present study was to explore gamma aminobutyric acid (GABA) inhibition in the 6-hydroxydopamine (6-OHDA) rat, which is extensively used as a model of PD [8,17]. Also, two inhibitory markers were explored at the level of the spinal dorsal horn (SDH): vesicular GABA transporter (VGAT) and parvalbumin. VGAT is present in both glycinergic and GABAergic terminals [18], while parvalbumin is present in neurons that co-release GABA and Glycine in the SDH [19,20]. At last, we explored cold allodynia in this model using acetone stimulus.

* Corresponding author.
E-mail addresses: menna.faisal@med.asu.edu.eg (M. Elshennawy), omar.ouachikh@uca.fr (O. Ouachikh), drshereen_youssef@med.asu.edu.eg (Shereen Adel Saad), ramdan_yasmin@med.asu.edu.eg (Y. Ramadan), franck.durif@uca.fr (F. Durif), aziz.hafidi@uca.fr (A. Hafidi).

https://doi.org/10.1016/j.neulet.2021.136135
Received 26 May 2021; Received in revised form 21 July 2021; Accepted 21 July 2021
Available online 24 July 2021

2. Materials and methods

2.1. Animals

24 adult male Sprague-Dawley rats (Charles River, France) were used in these experiments. The weight of rats was ranging from 280 to 350 g. Three rats/cage were housed in each cage subjected to optimum laboratory environmental conditions (12/12 light/dark cycle, light on at 7:00 am). Free access to water and food pellets was offered. The experiments followed the animal committee ethical guidelines of Clermont Auvergne University (APAFIS#19965-20190325052285).

2.2. Surgery

6-OHDA lesion

After anesthesia using intraperitoneal injections of (Ketamine 60 mg/kg and xylazine 10 mg/kg), rats have undergone stereotaxic surgery using stereotaxic frame (David Kopf Instrument, CA, USA). Medial Forebrain Bundle was injected bilaterally with 6-OHDA (with rate 0.25 µl/min) in two deposits (2.25 and 2.85 µl, respectively). Vehicle saline solution (0.02% ascorbic acid) was used to dissolve 6-OHDA (6-hydroxydopamine hydrochloride) neurotoxin which was injected at a concentration of 3 µg/µL (Sigma-Aldrich, France). Injections were performed at the following coordinates: For 2.25 µl deposit; anterior (A) −4.0; lateral (L) ± 0.8; ventral (V) −8.0; tooth bar at + 3.4 and for 2.85 µl deposit: A −4.4; L ± 1.2; V −7.8; tooth bar at −2.4 [8]. Desipramine hydrochloride (25 mg/kg, i.p., Sigma-Aldrich) was injected to save adrenergic neurons from degeneration 30 min before 6-OHDA injection. Vehicle -only- was injected in sham rats using similar coordinates. The syringe used for injection was retracted with a rate 1 mm/minute. Bilateral 6-OHDA Medial Forebrain Bundle lesion results in rats' aphagia and adipsia, therefore, rats' weight was observed daily. They were syringe fed using wet food pellets, milk and water twice daily until they became independent.

2.3. Study groups

There are 3 groups included in this study. Sham, 6-OHDA lesioned and 6-OHDA lesioned rats with acute intraperitoneal administration of D2R agonist which is ropinirole hydrochloride. Ropinirole hydrochloride was given for four days starting at day ten after 6-OHDA lesion surgery. The concentration of ropinirole used was 5 mg/Kg/ml (Sigma-Aldrich), (Elshennawy et al., Submitted). The ropinirole treated group is stated as 6-OHDA + D2R agonist group. Tests were done after two weeks of surgery.

2.4. Immunohistochemistry

Rats were deeply anesthetized using ketamine (60 mg/kg) and xylazine (10 mg/kg) intraperitoneal. Acetone stimulus was used as cold allodynic stimulus; acetone drop was gently applied onto the plantar surface of hind paw bilaterally (without touch). Methodology details are modified from (Dieb et al., 2016) [8]: Frozen coronal sections (40 µm) were cut with a microtome. Spinal cord segments used were lumbar ones (L3–L6). Primary antibodies solutions used were: rabbit monoclonal anti-cFOS (1:2000 Cell Signaling, France), rabbit polyclonal anti-VGAT (1:100 Sigma-Aldrich), mouse monoclonal anti-Parvalbumin (1:200 Sigma-Aldrich), rabbit monoclonal anti-GAD1 (1:1000, Cell Signaling), mouse monoclonal anti-PKCγ (1: 500, Santa- Cruz, France) and mouse monoclonal anti-TH antibody (1:5000, Sigma-Aldrich), which were incubated overnight. After multiple washes, sections were incubated with a secondary antibody solution (1:500 for goat anti-mouse 488; goat anti-rabbit 555, Cell Signaling) for 2 h at room temperature. At the end, sections were washed and mounted onto Thermo Scientific Superfrost Plus slides (Fisher Scientific, UK), and cover slipped with Dako Fluorescence Mounting Medium (Agilent, USA). Primary antibodies were omitted and there were no signals confirming their specificity of the immunostaining. Immuno-stained sections were photographed using a motorized Zeiss Axioplan 2 microscope. Same area of the spinal cord was used to lessen staining variability among different sections for fluorescent signal quantification. Measurement of cFOS positive cell number was taken from the SDH. A square area of equal dimensions **(2x2″)** was applied for all sections. The Parvalbumin positive cells were counted in Laminae II of SDH. Tyrosine hydroxylase (TH) immunolabeled cells were quantified in the whole sections at different slices at the level of Substantia nigra pars compacta (SNc) and Ventral tegmental area (VTA) {Rostro-caudal sections from (-5.16 mm to −6.12 mm) were analyzed}. cFOS, Parvalbumin and TH cells were quantified using multipoint cursor in ImageJ Software (ImageJ v1.6, National Institutes of Health). Parvalbumin, VGAT, GAD67 and PKCγ fluorescence intensities were measured throughout different spinal cord slices. The number of sections used for each group and each antibody was eight. Fluorescence intensity was measured using Image J software. The RGB image was converted to a grayscale 16-bit image, then the image was duplicated. After that, a threshold was assigned to create a binary image where sliders were adjusted to highlight the expression. The assigned pixels range was used to compare between all groups' sections. Image analysis took place and mean pixels intensity was measured. Cell counting and fluorescence quantification were done by a blind observer.

2.5. Western Blot

Fresh spinal cord tissues (from L3 to the end of spinal cord) were snap frozen and homogenized with lysis buffer (50 mM HEPES, pH 7.5, 1% Triton X-100, 10 mM EDTA, 150 mM NaCl, 10 mM Na4P2O7, 0.1 M NaF, 2 mM vanadate), extraction buffer was added then centrifuged and supernatants were collected. Samples' proteins amount was assessed using BCA Protein Assay Kit (Pierce-Thermo Scientific, France) and equal amount (40µg) was loaded on 4–20% Mini-PROTEAN TGX polyacrylamide gels (BioRad, France) and transferred using wet blotting system (BioRad). After washing blots with TBS-T (10 mM Tris-HCl, pH 7.6, 150 mM NaCl, 0.01% Tween-20), they were blocked with 5% BSA in TBS-T for 1 h at room temperature. Then incubated at 4°C overnight with primary antibodies diluted in 5 % BSA in TBS-T; mouse monoclonal anti-D2DR (1:250, Santa-Cruz) and rabbit polyclonal anti-GAPDH (0.2 µg/ml, Sigma-Aldrich). Membranes were incubated for 1 h with HRP-conjugated anti-rabbit and anti-mouse IgG secondary antibodies (1:5000, Pierce-Thermo Scientific) diluted in 5% BSA in TBS-T. Clarity Western ECL Substrate solution (Bio-Rad) was used to visualize the different bands using ChemiDoc XRS (Bio-Rad, USA).

2.6. Statistical analysis

The results are expressed as mean ± SEM. Statistical analysis was performed using one-way ANOVA to compare between the three groups, followed by post-hoc Tukey's multiple comparisons test for parametric data and Kruskal-Wallis test, followed by post-hoc Dunn's multiple comparisons test for non-parametric data. Student's T-test was used when the comparison between two groups only was required for parametric data. Normality tests were done using D'Agostino-Pearson normality test. The level of significance was determined at P value $\leq$ 0.05. Data were analyzed using GraphPad Prism Software (v.8.0.2).

3. Results

3.1. cFOS expression in the spinal dorsal horn upon acetone stimulation

cFOS labeling expression upon paw acetone stimulus was observed in superficial and deep laminae of the SDH in sham (Fig. 1A), 6-OHDA lesioned (Fig. 1B) and 6-OHDA + D2R agonist rats (Fig. 1C). cFOS-positive cells were quantified in the SDH laminae in the three animal groups. Pain marker, cFOS positive cells number (Fig. 1D), was

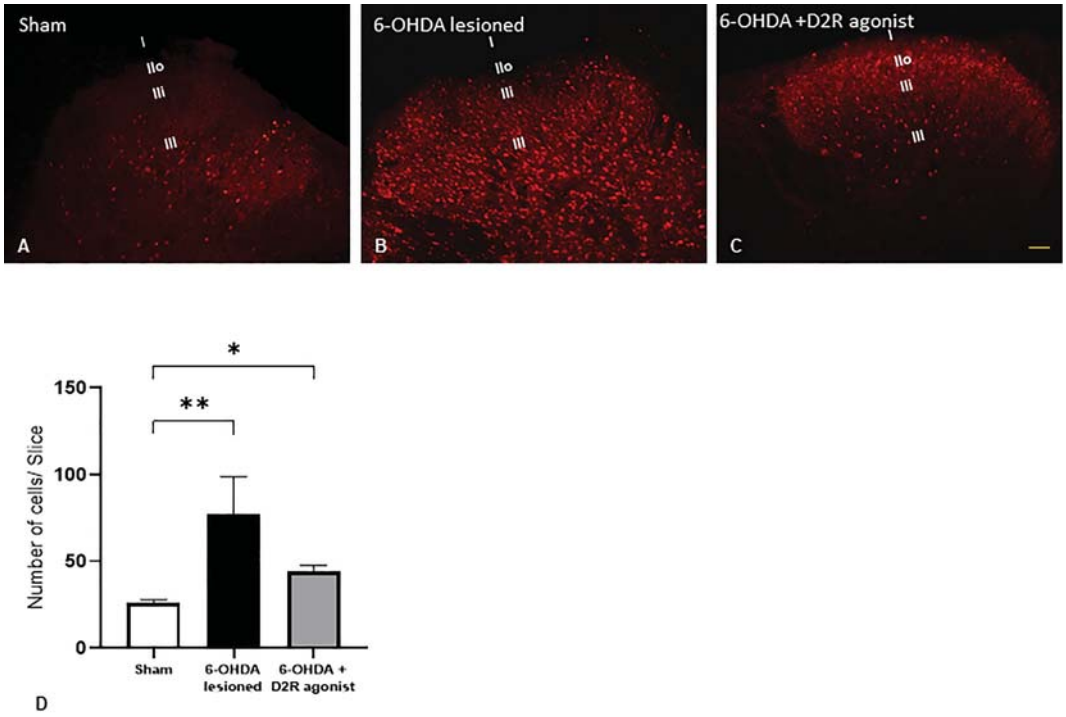

Fig. 1. cFOS protein expression upon acetone stimulus. Figure shows cFOS expression in SDH of sham (A), 6-OHDA lesioned (B) and 6-OHDA + D2R agonist group (C). Graph (D) represents cFOS positive cells within SDH superficial and deep laminae (Kruskal-Wallis test, $p = 0.0016$): 6-OHDA lesioned had more significant number than sham (Dunn's multiple comparisons test, $p = 0.0019$); $^{**}p \leq 0.01$. Also, there was an increase in significance (Dunn's multiple comparisons test, $p = 0.0249$) of 6-OHDA + D2R agonist group more than sham; $^{*}p \leq 0.05$. Data are means ± SEM of 4 animals/group. Scale bar represents 50 μm.

increased significantly ($P \leq 0.01$) in 6-OHDA lesioned group than sham. There was also a significant ($P \leq 0.05$) difference between 6-OHDA + D2R agonist rats and sham. There was no significant difference between 6-OHDA lesioned and 6-OHDA + D2R agonist groups.

3.2. VGAT expression in the spinal dorsal horn

VGAT labeling was expressed throughout the SDH laminae in sham (Fig. 2A), 6-OHDA lesioned (Fig. 2B) and 6-OHDA + D2R agonist animals (Fig. 2C). VGAT was observed across superficial and deep SDH laminae. Intense VGAT staining was observed in the SDH of 6-OHDA

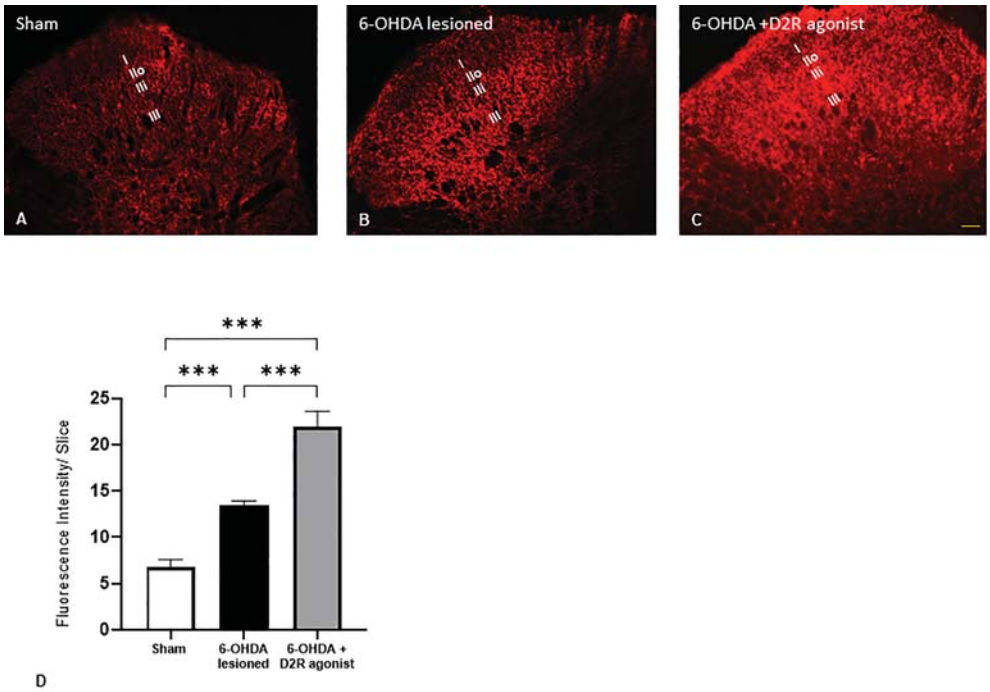

Fig. 2. The figure shows VGAT immunolabeling in the SDH of sham (A), 6-OHDA lesioned (B) and 6-OHDA + D2R agonist group (C). Graph (D) represents VGAT fluorescence quantification within SDH superficial and deep laminae (one-way ANOVA, $p < 0.0001$, $F(2, 21) = 46.35$): 6-OHDA lesioned had more significant number than sham (Tukey's multiple comparisons test, $p = 0.0010$); $^{***}p \leq 0.001$. Also, there was an intense increase in significance (Tukey's multiple comparisons test, $p < 0.0001$) of 6-OHDA + D2R agonist group more than both sham and 6-OHDA lesioned; $^{***}p \leq 0.001$. Data are means ± SEM of 4 animals/group. Scale bar represents 50 μm.

lesioned when compared to sham. While more intense VGAT staining was observed in 6-OHDA + D2R agonist compared to 6-OHDA lesioned and sham rats. VGAT staining fluorescence comparison (Fig. 2D) revealed a highly significant ($P \leq 0.001$) difference between the 6-OHDA lesioned and sham. Ropinirole has augmented significantly VGAT; a high level of significance ($P \leq 0.001$) was observed between 6-OHDA + D2R agonist and both 6-OHDA lesioned and sham.

3.3. Parvalbumin expression in the spinal dorsal horn

In the present study, Parvalbumin labeling is localized in SDH superficial laminae cells in the sham (Fig. 3A), 6-OHDA lesioned (Fig. 3B) and 6-OHDA + D2R agonist rats (Fig. 3C). Within the SDH of all groups, Parvalbumin immunolabeling was observed mostly in cells of lamina II and in scattered cells within lamina III. Parvalbumin labeling was measured using both fluorescence quantification (Fig. 3D) and the number of positive cells (Fig. 3E). 6-OHDA lesioned has an intense significant ($P \leq 0.001$) increase of Parvalbumin expression more than sham regarding both fluorescence quantification and number of positive cells. Ropinirole decreased the Parvalbumin expression significantly ($P \leq 0.001$) in 6-OHDA + D2R agonist rats compared to 6-OHDA lesioned one regarding both fluorescence quantification and number of positive cells too.

3.4. VGAT and parvalbumin co-labeling in the spinal dorsal horn

Double labeling using VGAT and parvalbumin antibodies, (Fig. 4A–D) show the presence of VGAT in parvalbumin cells (Fig. 4C–D). VGAT staining had a broader cell localization (Fig. 4A) than the more restricted parvalbumin one (Fig. 4B) within the SDH.

3.5. GAD67 expression in the spinal dorsal horn

GAD67 labeling was expressed throughout the SDH laminae in sham (Fig. 5A), 6-OHDA lesioned (Fig. 5B) and 6-OHDA + D2R agonist animals (Fig. 5C). GAD67 expression was measured using fluorescence quantification (Fig. 5D). 6-OHDA lesioned rats showed a significant increase ($P \leq 0.001$) in GAD67 fluorescence intensity more than both sham and 6-OHDA + D2R agonist. Ropinirole intraperitoneal administration led to a significant diminution ($P \leq 0.001$) of GAD67 expression in 6-OHDA + D2R agonist group compared to 6-OHDA lesioned one.

3.6. D2DR expression in the spinal dorsal horn

Western blot bands (Fig. 6A) revealed a significant D2DR protein increase in 6-OHDA lesioned group more than both sham ($P \leq 0.05$) and 6-OHDA + D2R agonist ($P \leq 0.01$) groups (Fig. 6B).

3.7. PKC gamma expression in the spinal dorsal horn

PKCγ labeling is localized in SDH superficial laminae cells in sham (Fig. 7A), 6-OHDA lesioned (Fig. 7B) and 6-OHDA + D2R agonist rats (Fig. 7C). PKCγ positive cells were observed within SDH mostly in cells of lamina IIi and in scattered cells within lamina III. PKCγ expression was measured using fluorescence quantification (Fig. 7D). 6-OHDA lesioned rats had significant ($P \leq 0.001$) increase in PKCγ fluorescence quantification compared to both sham and 6-OHDA + D2R agonist groups regarding fluorescence intensity. Ropinirole intraperitoneal administration resulted in a significant decrease ($P \leq 0.001$) of PKCγ expression in 6-OHDA + D2R agonist rats when compared to 6-OHDA lesioned ones.

3.8. TH expression in SNc and VTA

TH labeling was expressed in SNc and VTA in both sham (Fig. 8A) and 6-OHDA lesioned groups (Fig. 8B) to verify the effect of 6-OHDA toxin in the bilateral MFB lesion. TH labeling was seen in cell bodies and processes of the dopaminergic cells in the SNc and VTA. A remarked severe decrease in the TH staining was present in the 6-OHDA lesioned rats in relation to sham validating dopaminergic cells' degeneration. Quantification of TH cells in both SNc and VTA (Fig. 8C) showed an enormous significant decrease in cell number between the 6-OHDA

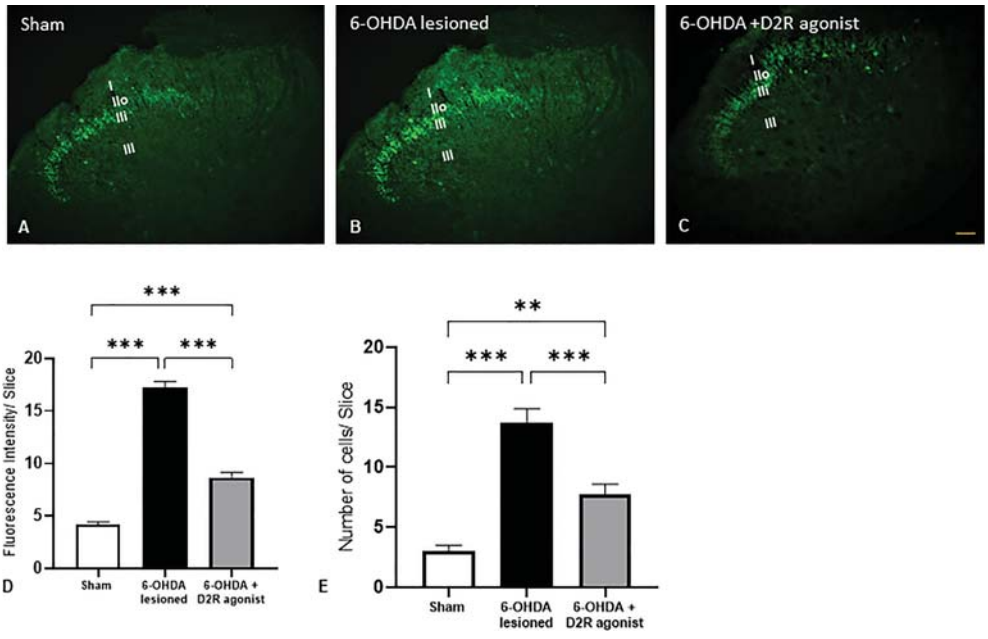

Fig. 3. The figure shows Parvalbumin immunolabeling in sham (A), 6-OHDA lesioned (B) and 6-OHDA + D2R agonist group (C). Graph (D) represents Parvalbumin fluorescence quantification within cells of lamina II and in scattered cells within lamina III (one-way ANOVA, $p < 0.0001$, $F(2, 37) = 92.97$): 6-OHDA lesioned had more significant intensity than both sham and 6-OHDA + D2R agonist groups (Tukey's multiple comparisons test, $p < 0.0001$); ***$p \leq 0.001$. Also, there was an increase in significance of 6-OHDA + D2R agonist group more than sham (Tukey's multiple comparisons test, $p < 0.0001$); ***$p \leq 0.001$. Ropinirole administration decreased dramatically the expression of Parvalbumin; where 6-OHDA + D2R agonist group had less fluorescence quantification than 6-OHDA lesioned one (***$p \leq 0.001$). Graph (E) represents Parvalbumin number of cells (one-way ANOVA, $p < 0.0001$, $F(2, 21) = 38.39$): 6-OHDA lesioned had more significant number than both sham and 6-OHDA + D2R agonist groups (Tukey's multiple comparisons test, $p < 0.0001$, 0.0002 respectively); ***$p \leq 0.001$. Also, there was an increase in significance of 6-OHDA + D2R agonist group more than sham (Tukey's multiple comparisons test, $p = 0.0025$); **$p \leq 0.01$. Ropinirole administration decreased the expression of Parvalbumin; where 6-OHDA + D2R agonist group had less number of cells than 6-OHDA lesioned one (***$p \leq 0.001$). Data are means ± SEM of 4 animals/group. Scale bar represents 50 μm.

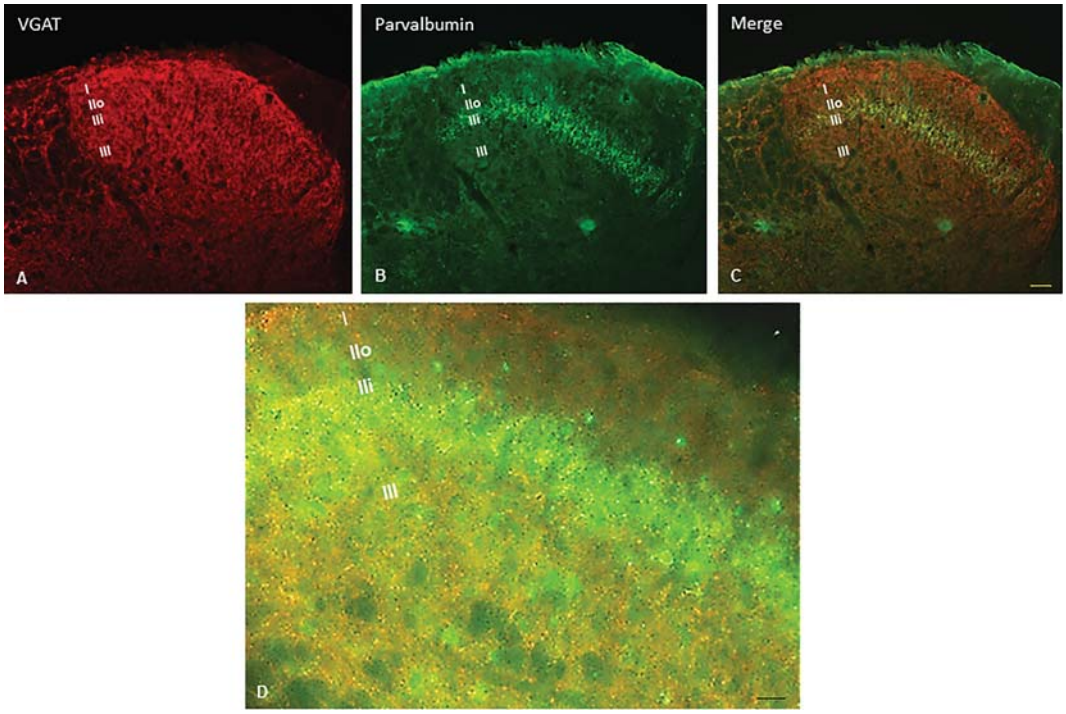

Fig. 4. Co-labeling of VGAT and parvalbumin antibodies, (Fig. 4A–D) reveal the expression of VGAT in parvalbumin cells (Fig. 4C–D). VGAT labelling had a wider cell localization (Fig. 4A) than the more restricted parvalbumin one (Fig. 4B) within the SDH lamina II and in scattered cells within lamina III. Scale bar represents 50 μm for A–C and 20 μm for D.

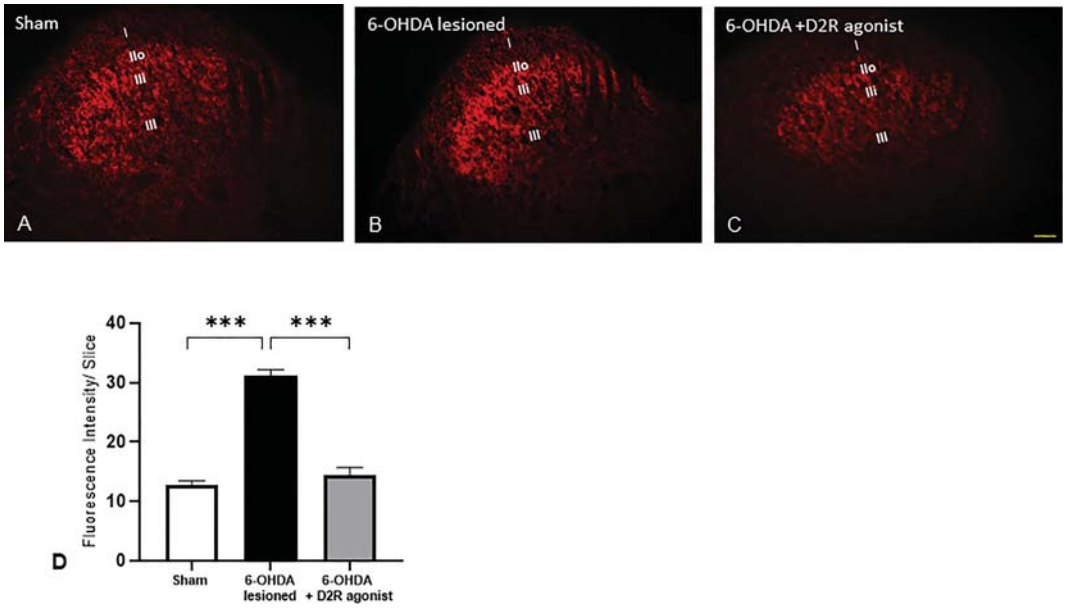

Fig. 5. GAD67 protein expression. The figure shows GAD67 expression in SDH of sham (A), 6-OHDA lesioned (B) and 6-OHDA + D2R agonist group (C). Graph (D) represents GAD67 fluorescence quantification within SDH (one-way ANOVA, $p < 0.0001$, $F(2, 21) = 97.18$): 6- OHDA lesioned had increased significance than both sham and 6-OHDA + D2R agonist groups (Tukey's multiple comparisons test, $p < 0.0001$); ***$P \leq 0.001$. Data are means ± SEM of 4 animals/group. Scale bar represents 50 μm.

lesioned and sham ($P \leq 0.001$).

Thus, our 6-OHDA lesioned model was validated by the high dopaminergic cells' degeneration in SNc and VTA using TH labeling. Upon applying a cold stimulus, the expression of CFOS (pain) increased in 6-OHDA lesioned when compared to sham. Also, there was an increase in PKCγ (chronic pain) and inhibitory markers (VGAT, Parvalbumin and GAD67) in the 6-OHDA lesioned rats when compared to sham. The markers' increase was diminished upon intraperitoneal ropinirole administration, except for the VGAT. D2DR protein is more expressed in the 6-OHDA lesioned when compared to sham.

4. Discussion

The main result of this study shows that bilateral 6-OHDA lesion induced an increase in the expression of inhibitory cell markers parvalbumin, VGAT and GAD67 in the SDH. These proteins highlighted an

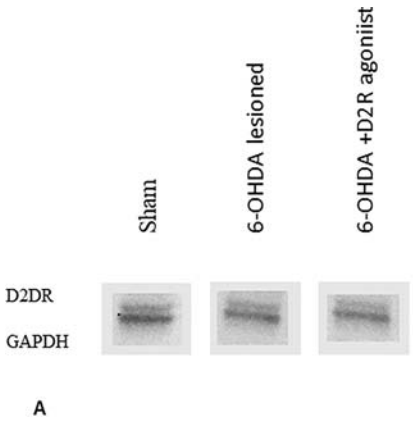

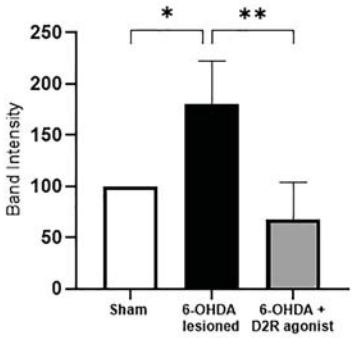

Fig. 6. Figure (A) represents western blot bands of D2R expression of sham, 6-OHDA lesioned and 6-OHDA + D2R agonist group. Graph (B) shows relative intensities of bands of the three groups (one-way ANOVA test, $p = 0.0021$, $F(2, 9) = 13.17$): 6-OHDA lesioned had more significant increase in expression than both sham and 6-OHDA + D2R agonist groups (Tukey's multiple comparisons test, $p = 0.0154$, $p = 0.0019$ respectively); *P ≤ 0.05, **P ≤ 0.01. Data are means ± SEM of 4 animals/group, GAPDH was used as the loading control.

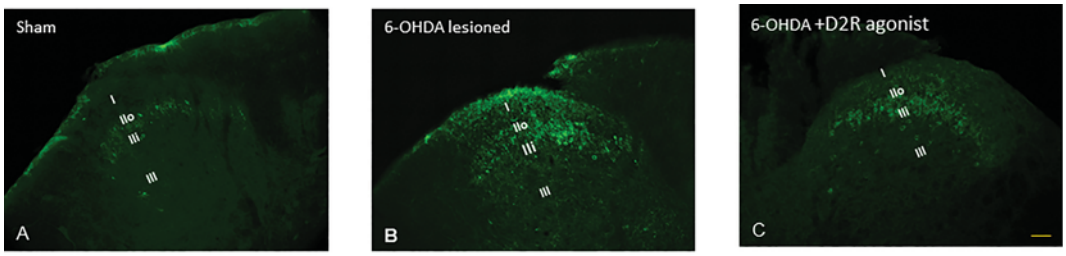

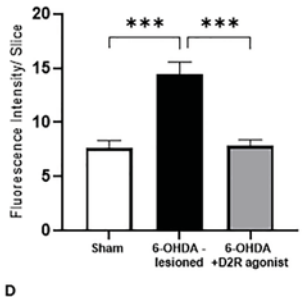

Fig. 7. PKCγ protein expression. Figure shows PKCγ expression in SDH of sham (A), 6- OHDA lesioned (B) and 6-OHDA + D2R agonist group (C). PKCγ positive cells were located within SDH in cells of lamina IIi and in scattered cells within lamina III. Graph (D) represents PKCγ fluorescence quantification (one-way ANOVA, $p < 0.0001$, $F(2, 21) = 22.43$): 6-OHDA lesioned had more significance than both sham and 6-OHDA + D2R agonist groups (Tukey's multiple comparisons test, $p < 0.0001$); ***P ≤ 0.001. Data are means ± SEM of 4 animals/group. Scale bar represents 50 μm.

increase in excitation at the level of GABA cells. The increase in their expressions is regulated by cell activity [21,22]. In addition, cold allodynia is demonstrated by the increase in cFOS expression in the SDH upon acetone stimulation of the paw. Moreover, the use of ropinirole, a D2R agonist, reversed the expression of parvalbumin, GAD67, PKCγ and cFOS in the SDH. The use of ropinirole has also been demonstrated to alleviate pain sensitivity in this model (Elshennawy et al., Submitted). The present study showed a clear implication of the dopaminergic system in the changes in inhibitory markers in the SDH and the consequent cold pain sensitivity. In parallel, there was an increase in excitation, which is highlighted, by the increase of PKCγ protein in the SDH of 6-OHDA lesioned rats as it was also demonstrated in the medullary dorsal horn [7,8,23]. PKCγ protein plays an important role in pain chronicity [8,24]. PKCγ cells also play an important role in the transfer of non-noxious stimuli to pain processing pathway through polysynaptic pathway [7]. Parvalbumin cells represent gatekeepers of touch-evoked pain after nerve injury and their ablation in naive mice produce neuropathic pain-like mechanical allodynia via disinhibition of PKCγ excitatory interneurons [25]. In addition, PKCγ cells receive parvalbumin innervation at both medullary [26] and spinal [25] dorsal horns. The present study showed an increase in excitation at both parvalbumin and PKCγ cells as highlighted by the increase in the expression of parvalbumin and PKCγ proteins respectively in these cell types.

Parvalbumin cells expressed both GABAergic and Glycinergic subtypes [19,20]. In the medullary dorsal horn, parvalbumin subtypes were shown to be electrically connected through electrical synapses [26]. Parvalbumin cells might exercise their influences on PKCγ cells through a disinhibition (through inhibitory cells that are in direct contact with PKCγ cells). Therefore, the decrease in the descending pain control, such as in the 6-OHDA conditions, increases excitation in parvalbumin cells hence disinhibiting PKCγ cells. Therefore, both parvalbumin and PKCγ are highly activated and their respective expressions of parvalbumin and PKCγ proteins are increased. Both parvalbumin [22] and PKCγ [7,8] proteins are activity-dependent expressed.

A converse correlation exists between the synthesis of GABA and the expression of GAD67 [27]. GAD67 activity declined when GABA levels were elevated. Therefore, the high expression of GAD67 in the dorsal horn of 6-OHDA lesioned rats may reflect a decrease in GABA level. In addition, GAD67 expression is under dopamine control. For example, dopamine depletion or the use of D2R antagonists produced an increase

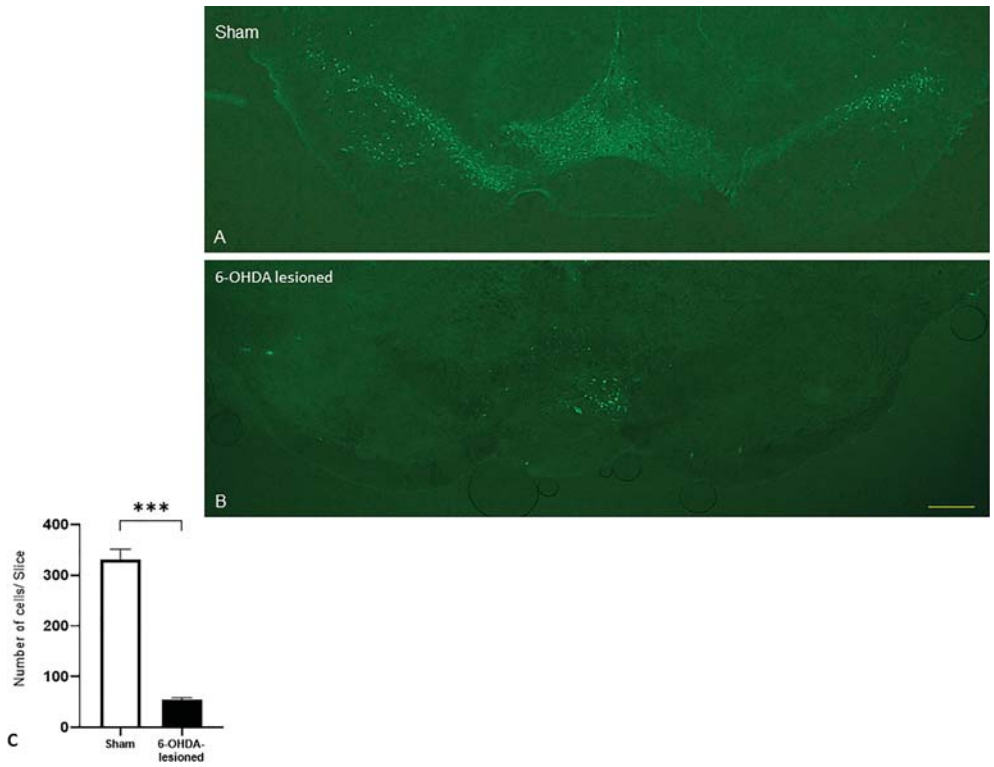

Fig. 8. TH immunolabeling in sham (A) and 6-OHDA lesioned animals (B) indicates an extreme decrease in the intensity of labeling, in both SNc and VTA in 6-OHDA lesioned animals in comparison to sham ones. Graph (C) shows cell count of TH immunolabeled cells in both SNc and VTA together (student's T-test, $p < 0.001$); ***$P \leq 0.001$. Data are means ± SEM of 5 animals/group. Scale bar represents 200 μm.

in GAD67 expression [28]. Moreover, levodopa treatment reversed GAD67 mRNA overexpression in 6-OHDA lesioned rats [29,30]. Although there is no previous report on this at the spinal cord level in the literature to the best of our knowledge, the administration of ropinirole decreased GAD67 expression in the SDH as demonstrated here by immunohistochemistry.

The high increase of VGAT observed in the 6-OHDA-lesioned rat may reflect an increase in excitation at the level of GABA cells within the SDH. Indeed, VGAT expression is activity dependent [31]. The increase in VGAT expression in the SDH did not reflect an increase in inhibition (GABA release); otherwise, the rats would not have had allodynic behavior. A more recent study using unilateral 6-OHDA lesion showed both an increase and a decrease in VGAT in different GABAergic striatal cell subtypes [32]. Ropinirole increased the VGAT labeling expression in the SDH of 6-OHDA lesioned rats. This result is in accordance with a previous report demonstrating an ipsilateral increase of VGAT mRNA in case of L-Dopa administration in unilateral 6-OHDA lesioned rats [32]. It is clear that dopamine agonists increase the expression of VGAT in the SDH; however, the mechanism involved is still to be determined.

cFOS expression significantly increased in the 6-OHDA lesioned SDH upon acetone stimulation and was present in both SDH superficial and deep laminae. Conversely, ropinirole decreased cFOS expression in the SDH although it was still above the sham level (low expression). The present result shows that central dopaminergic regulation is involved in cold sensitization observed in 6-OHDA lesioned rats. SNc modulated pain through the inhibition of nociceptive inputs at spinal cord neurons [33,34] or ascending projections to cortical areas such as insular or cingulate cortices [34,35]. Although, to date, there is no evidence in literature of direct projections from the SNc/VTA to the spinal cord, there is some evidence that the SNc/VTA may influence brainstem descending inhibitory pathways [34,36]. The stimulation of SNc inhibited nociceptive input by activation of spinal cord neurons through dopaminergic descending pathways [33,35]. The high expression of D2R protein in the 6-OHDA lesioned rats when compared to sham may probably reveal the lack of dopamine secretion at the level of the SDH.

5. Conclusion

The present study demonstrated that central dopamine depletion promoted disinhibition at the SDH level. This change was responsible for the observed cold allodynia in 6-OHDA lesioned rats.

Declaration of Competing Interest

The authors declare that they have no known competing financial interests or personal relationships that could have appeared to influence the work reported in this paper.

Acknowledgements

The Missions Sector of the Ministry of Higher Education and Scientific Research of the Arab Republic of Egypt; Ain Shams University, Egypt and Clermont Auvergne University, France funded this study, and all authors declare that there is no conflict of interest.

References:

[1] O. Skogar, J. Lokk, Pain management in patients with Parkinson's disease: challenges and solutions, J. of multidisciplinary healthcare 9 (2016) 469–479.
[2] M.T. Tseng, C.H. Lin, Pain in early-stage Parkinson's disease: Implications from clinical features to pathophysiology mechanisms, J. of the Formosan Medical Association 116 (8) (2017) 571–581.
[3] C. Buhmann, J. Kassubek, W.H. Jost, B.R. Bloem, P. Brundin, Management of Pain in Parkinson's Disease, J. of Parkinson's disease 10 (s1) (2020) S37–S48.
[4] A. Fil, R. Cano-de-la-Cuerdab, E. Muñoz-Hellínb, L. Velac, M. Ramiro-Gonzálezd, C. Fernández-de-las-Peñasb, Pain in Parkinson disease: A review of the literature, Parkinsonism Relat. Disord. 19 (3) (2013) 285–294.
[5] M.R. Young Blood, M.M. Ferro, R.P. Munhoz, H.A. Teive, C.H. Camargo, Classification and Characteristics of Pain Associated with Parkinson's Disease, Parkinson's disease (2016, 2016,) 6067132.

[6] E.H. Chudler, Y. Lu, Nociceptive behavioral responses to chemical, thermal and mechanical stimulation after unilateral, intrastriatal administration of 6-hydroxydopamine, Brain Res. 1213 (2008) 41–47.
[7] W. Dieb, P. Alvarez, A. Hafidi, PKC gamma-positive neurons gate light tactile inputs to pain pathway through pERK1/2 neuronal network in trigeminal neuropathic pain model, J. of oral & facial pain and headache 29 (2015) 70-82.
[8] W. Dieb, O. Ouachikh, S. Alves, Y. Boucher, F. Durif, A. Hafidi, Nigrostriatal dopaminergic depletion increases static orofacial allodynia, J. Headache Pain 17 (2016) 11.
[9] Y. Buhidma, K. Rukavina, K.R. Chaudhuri, S. Duty, Potential of animal models for advancing the understanding and treatment of pain in Parkinson's disease, npj, Parkinsons Dis. 6 (2020) 1.
[10] R. Takeda, T. Ikeda, F. Tsuda, H. Abe, H. Hashiguchi, Y. Ishida, T. Nishimori, Unilateral lesions of mesostriatal dopaminergic pathway alters the withdrawal response of the rat hindpaw to mechanical stimulation, Neurosci. Res. 52 (1) (2005) 31–36.
[11] J.E. Magnusson, K. Fisher, The involvement of dopamine in nociception: The role of D(1) and D(2) receptors in the dorsolateral striatum, Brain Res. 855 (2) (2000) 260–266.
[12] A. Wawrzczak-Bargieła, B. Ziółkowska, A. Piotrowska, J. Starnowska-Sokół, E. Rojewska, J. Mika, B. Przewłocka, R. Przewłocki, Neuropathic Pain Dysregulates Gene Expression of the Forebrain Opioid and Dopamine Systems, Neurotox. Res. 37 (4) (2020) 800–814.
[13] H.N. Harris, Y.B. Peng, Evidence and explanation for the involvement of the nucleus accumbens in pain processing, Neural Regen. Res. 15 (4) (2020) 597–605.
[14] F. Viana, Nociceptors: thermal allodynia and thermal pain, Handb. Clin. Neurol. 156 (2018) 103–119.
[15] J. Sandkühler, Models and mechanisms of hyperalgesia and allodynia, Physiol. Rev. 89 (2) (2009) 707–758.
[16] T.S. Jensen, N.B. Finnerup, Allodynia and hyperalgesia in neuropathic pain: Clinical manifestations and mechanisms, The Lancet Neurology 13 (9) (2014) 924–935.
[17] W. Dieb, O. Ouachikh, F. Durif, A. Hafidi, Lesion of the dopaminergic nigrostriatal pathway induces trigeminal dynamic mechanical allodynia, Brain Behav. 4 (3) (2014) 368–380.
[18] A. Dumoulin P. Rostaing C. Bedet S. Levi M.F. Isambert J.P. Henry A. Triller B. Gasnier Presence of the vesicular inhibitory amino acid transporter in GABAergic and glycinergic synaptic terminal boutons 112 6 1999 811 823.
[19] A.J. Todd, A.C. Sullivan, Light microscope study of the coexistence of GABA-like and glycine-like immunoreactivities in the spinal cord of the rat, J. Comp. Neurol. 296 (3) (1990) 496–505.
[20] I. Laing, A.J. Todd, C.W. Heizmann, H.H.H.W. Schmidt, Subpopulations of GABAergic neurons in laminae I-III of rat spinal dorsal horn defined by coexistence with classical transmitters, peptides, nitric oxide synthase or parvalbumin, Neuroscience 61 (1) (1994) 123–132.
[21] J. Van Liefferinge, A. Massie, J. Portelli, G. Di Giovanni, I. Smolders, Are vesicular neurotransmitter transporters potential treatment targets for temporal lobe epilepsy? Front. Cell. Neurosci. 7 (2013) 139.
[22] J.B. Ruden, L.L. Dugan, C. Konradi, Parvalbumin interneuron vulnerability and brain disorders, Neuropsychopharmacology 46 (2) (2021) 279–287.
[23] W. Dieb, A. Hafidi, Astrocytes are involved in trigeminal dynamic mechanical allodynia: potential role of D-serine, J. Dent. Res. 92 (9) (2013) 808–813.
[24] W. Dieb, A. Hafidi, Mechanism of GABA-involvement in posttraumatic trigeminal neuropathic pain: Activation of neuronal circuitry composed by PKC γ interneurons and pERK1/2 expressing neurons, Eur. J. Pain 19 (2015) 85–96.
[25] H. Petitjean, S.A. Pawlowski, S.L. Fraine, B. Sharif, D. Hamad, T. Fatima, J. Berg, C. M. Brown, L.-Y. Jan, A. Ribeiro-da-Silva, J.M. Braz, A.I. Basbaum, R. Sharif-Naeini, Dorsal Horn Parvalbumin Neurons Are Gate-Keepers of Touch-Evoked Pain after Nerve Injury, Cell Rep. 13 (6) (2015) 1246–1257.
[26] O. Ouachikh, A. Hafidi, Y. Boucher, W. Dieb, Electrical Synapses are Involved in Orofacial Neuropathic Pain, Neuroscience 382 (2018) 69–79.
[27] K. Rimvall, D.L. Martin, Increased intracellular gamma-aminobutyric acid selectively lowers the level of the larger of two glutamate decarboxylase proteins in cultured GABAergic neurons from rat cerebral cortex, J. Neurochem. 58 (1) (1992) 158–166.
[28] J.-J. Soghomonian, M.-F. Chesselet, Effects of nigrostriatal lesions on the levels of messenger RNAs encoding two isoforms of glutamate decarboxylase in the globus pallidus and entopeduncular nucleus of the rat, Synapse 11 (2) (1992) 124–133.
[29] C. Périer, C. Marin, A. Jimenez, M. Bonastre, E. Tolosa, E.C. Hirsch. Effect of subthalamic nucleus or entopeduncular nucleus lesion on levodopa-induced neurochemical changes within the basal ganglia and on levodopa-induced motor alterations in 6-hydroxydopamine-lesioned rats: STN or EP lesion on levodopa-induced changes Journal of Neurochemistry 86 6 2003 1328 1337.
[30] Jean-Jacques Bacci, Pascal Salin, Lydia Kerkerian-Le Goff, Systemic administration of dizocilpine maleate (MK-801) or L-dopa reverses the increases in GAD65 and GAD67 mRNA expression in the globus pallidus in a rat hemiparkinsonian model, Synapse 46 (4) (2002) 224–234.
[31] Rafael Gutiérrez, Activity-dependent expression of simultaneous glutamatergic and GABAergic neurotransmission from the mossy fibers in vitro, J. Neurophysiol. 87 (5) (2002) 2562–2570.
[32] H. Wang, J. Katz, P. Dagostino, J.-J. Soghomonian, Unilateral 6-hydroxydopamine lesion of dopamine neurons and subchronic L-DOPA administration in the adult rat alters the expression of the vesicular GABA transporter in different subsets of striatal neurons and in the substantia nigra, pars reticulata, Neuroscience 145 (2) (2007) 727–737.
[33] Charles D. Barnes, Simon J. Fung, William L. Adams, Inhibitory effects of substantia nigra on impulse transmission from nociceptors, Pain 6 (2) (1979) 207–215.
[34] Robert M. Beckstead, Valerie B. Domesick, Walle J.H. Nauta, Efferent connections of the substantia nigra and ventral tegmental area in the rat, Brain Res. 175 (2) (1979) 191–217.
[35] Adam R. Burkey, Earl Carstens, Luc Jasmin, Dopamine reuptake inhibition in the rostral agranular insular cortex produces antinociception, J. Neurosci. 19 (10) (1999) 4169–4179.
[36] G. Halliday, S. Reyes, K. Double, Substantia Nigra, Ventral Tegmental Area, and Retrorubral Fields, In: The human nervous system, ed. 3 (J.K. Mai, G. Paxinos), Academic press, (2012), ch 13, pp. 439-455.

Third part: Fluororuby

Third part - Fluororuby

1. Introduction

Many studies, included those from our laboratory, demonstrated the influence of SNpc in pain process. SNpc neuronal stimulation or neuronal degeneration within this structure demonstrated different physiological, cellular and molecular modifications at the spinal cord level. However, to date to our knowledge, no studies in the literature reported a direct projection from the SNpc to the spinal cord (Beckstead et al., 1978). On the other hand, there is important dopaminergic projection from A11 dopaminergic neurons to the spinal cord (Skagerberg et al., 1982; Qu et al., 2006, Domenici et al., 2019). Two studies demonstrated connection between the SNpc and the PAG. One study using the injection of tritiated leucine and proline to the SNpc demonstrated axonal projections to the PAG (Beckstead et al., 1978). A second study used the horseradish injection to the SNpc demonstrated also afferent projections to the PAG (Hopkins and Niessen, 1976). PAG constitutes a key structure of the descending pain inhibitory system. It receives inputs from brainstem and higher central structures such as cortex and amygdala. It contains both dopaminergic and GABAergic neurons. The goal of our study, using a more sensitive marker Fluororuby, is to demonstrate if the SNpc projects to descending inhibitory pain structures within the brainstem in the rat. Fluororuby is an anterograde tetramethylrhodamine dextran that labels neuronal structures (cell body, axons and dendrites). It is transported within 3-14 days to the target structures (Nance & Burns, 1990; Bowyer & Schmued, 2006).

2. Material and Methods

Please see fluorescent tracing technique in the material and methods section. FR was injected in various parts of the SNpc and traced in PAG and the spinal cord. The structures which were examined, were co-labelled with Tyrosine Hydroxylase immunohistochemically to check if the traced neurons and fibers were of dopaminergic origin or not.

3. Results

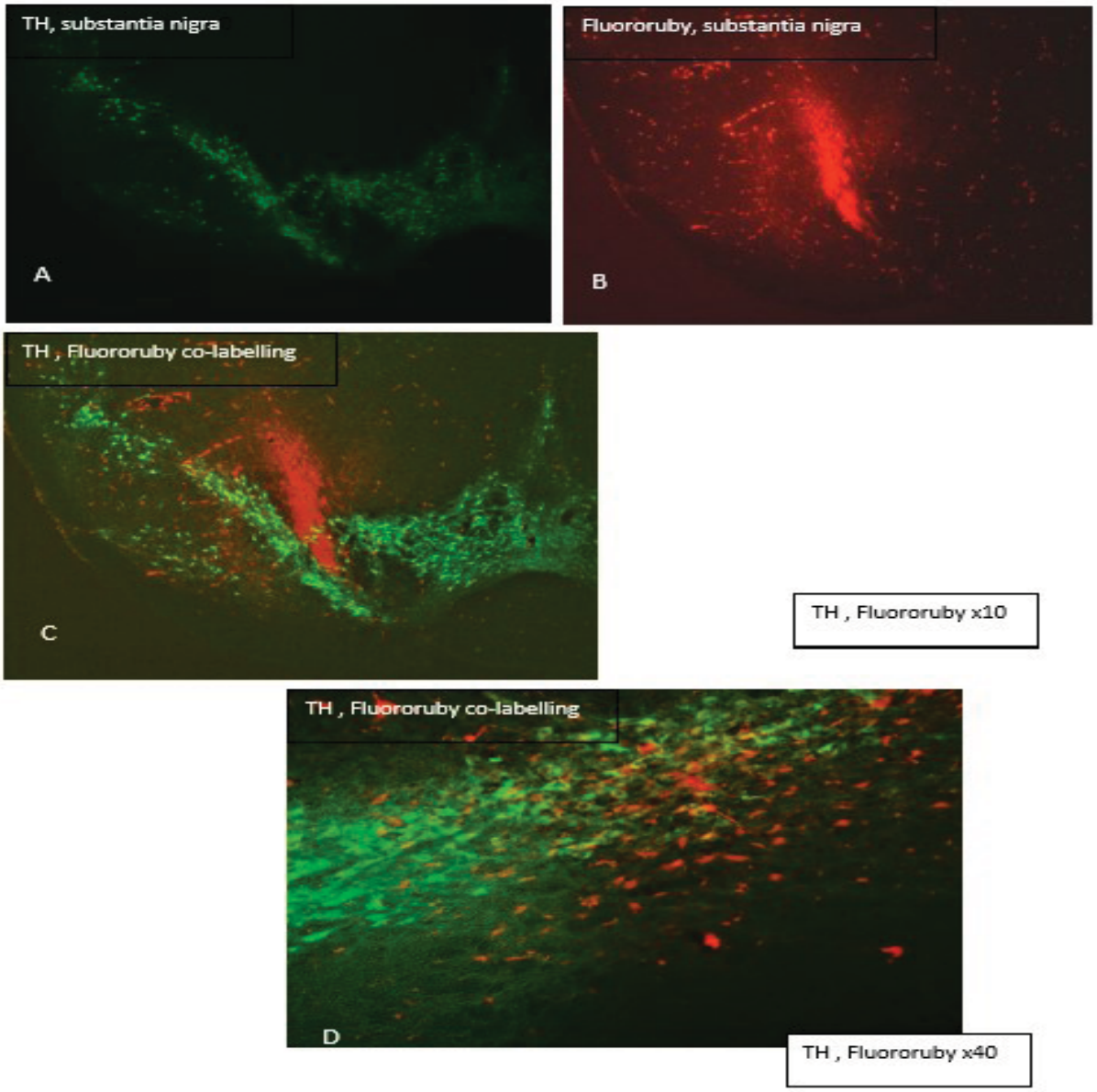

Figure (10): TH and Fluororuby. Figure (A) shows Tyrosine Hydroxylase staining dopaminergic neurons in substantia nigra and ventral tegmental area. Figure (B) shows injection site of Fluororuby tracer in substantia nigra pars compacta. Figure (C) shows TH + Fluororuby co-labelling in substantia nigra. Figure (D) shows a focus on dopaminergic neuronal cells (TH) co-labelled with Fluororuby tracer (yellow color).

Third part - Fluororuby

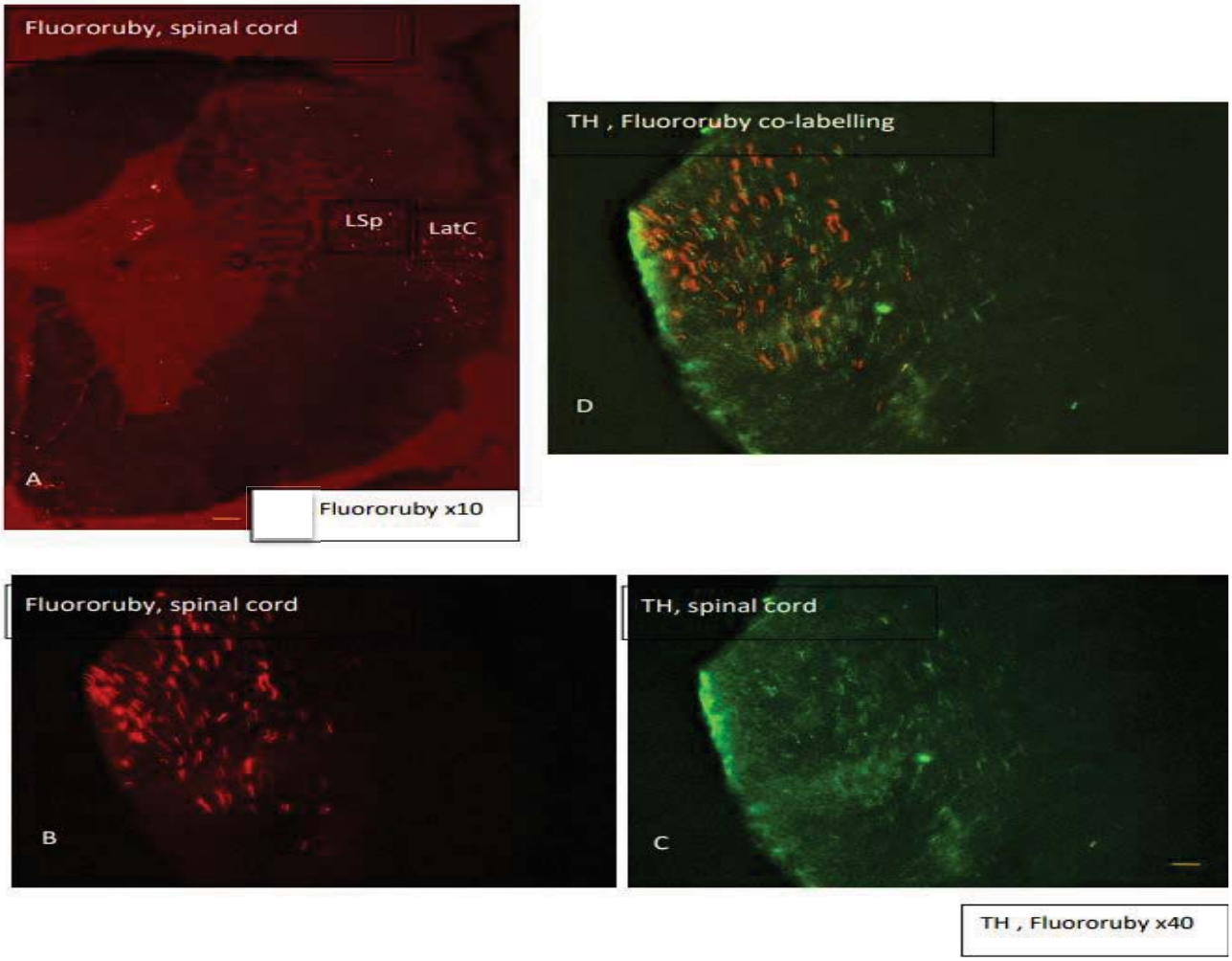

Figure (11): TH and Fluororuby. Figure (A) shows Fluororuby tracer staining LSp (lateral spinal nucleus) and LatC (lateral cervical nucleus of the spinal cord). Figure (B) shows Fluororuby tracer in LSp and LatC. Figure (C) shows Tyrosine Hydroxylase staining dopaminergic neurons in LSp and LatC. Figure (D) shows dopaminergic fibers (TH) co-labelled with Fluororuby tracer (yellow color).

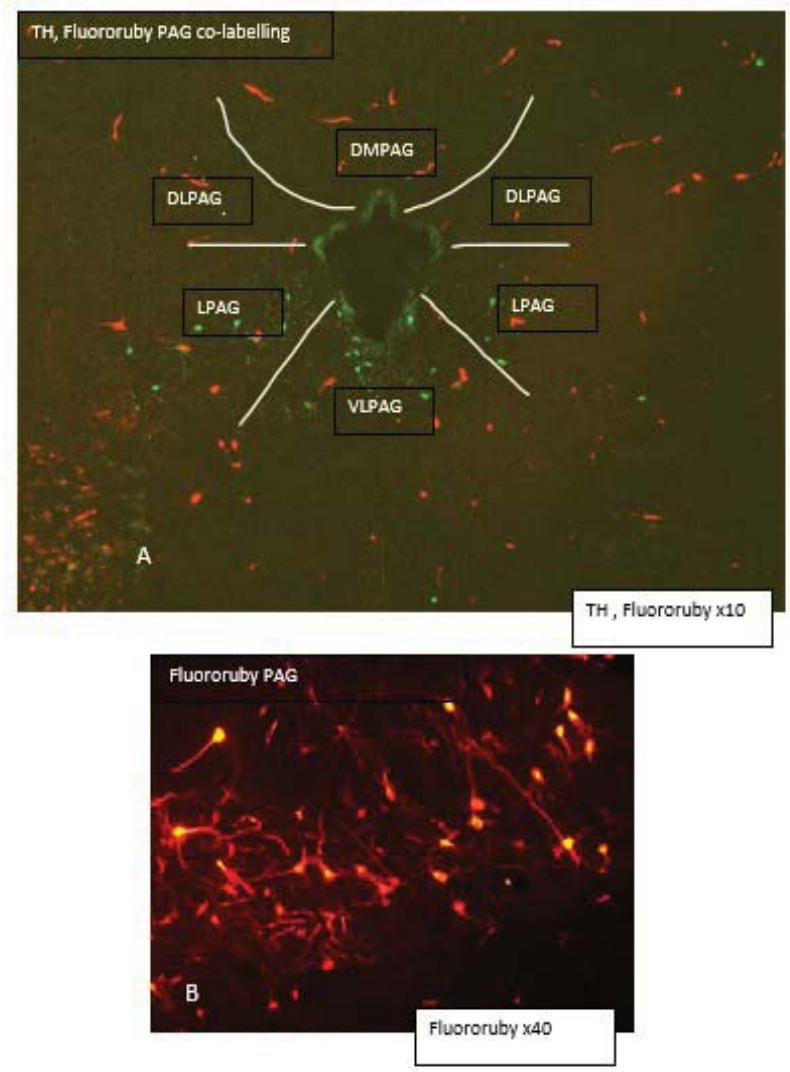

Figure (12): TH and Fluororuby. Figure (A) shows dopaminergic fibers and neurons (TH) co-labelled with Fluororuby tracer (yellow color). Figure (B) shows Fluororuby tracer staining neurons and fibers in PAG.
{PAG: periaqueductal gray, DMPAG: dorsomedial periaqueductal gray, DLPAG: dorsolateral periaqueductal gray, LPAG: lateral periaqueductal gray, VLPAG: ventrolateral periaqueductal gray}

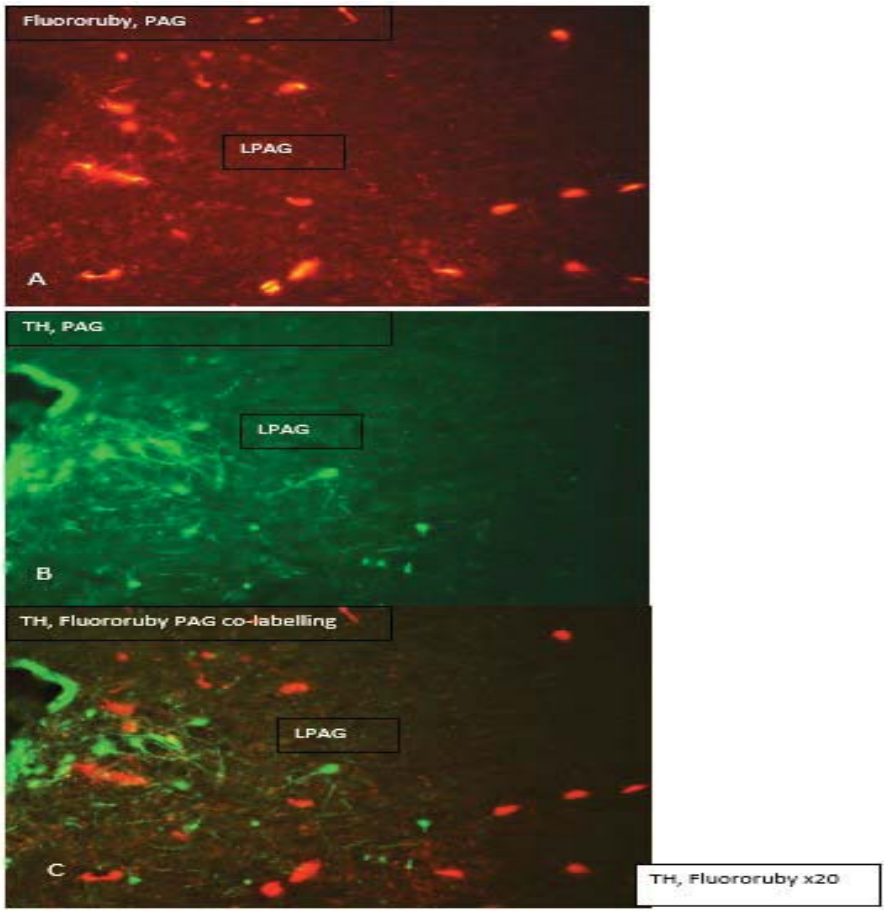

Figure (13): TH and Fluororuby. Figure (A) shows Fluororuby tracer staining neurons and fibers in LPAG. Figure (B) shows dopaminergic fibers and neurons (TH) in LPAG. Figure (C) shows dopaminergic fibers and neurons (TH) co-labelled with Fluororuby tracer (yellow color) in LPAG.

Third part - Fluororuby

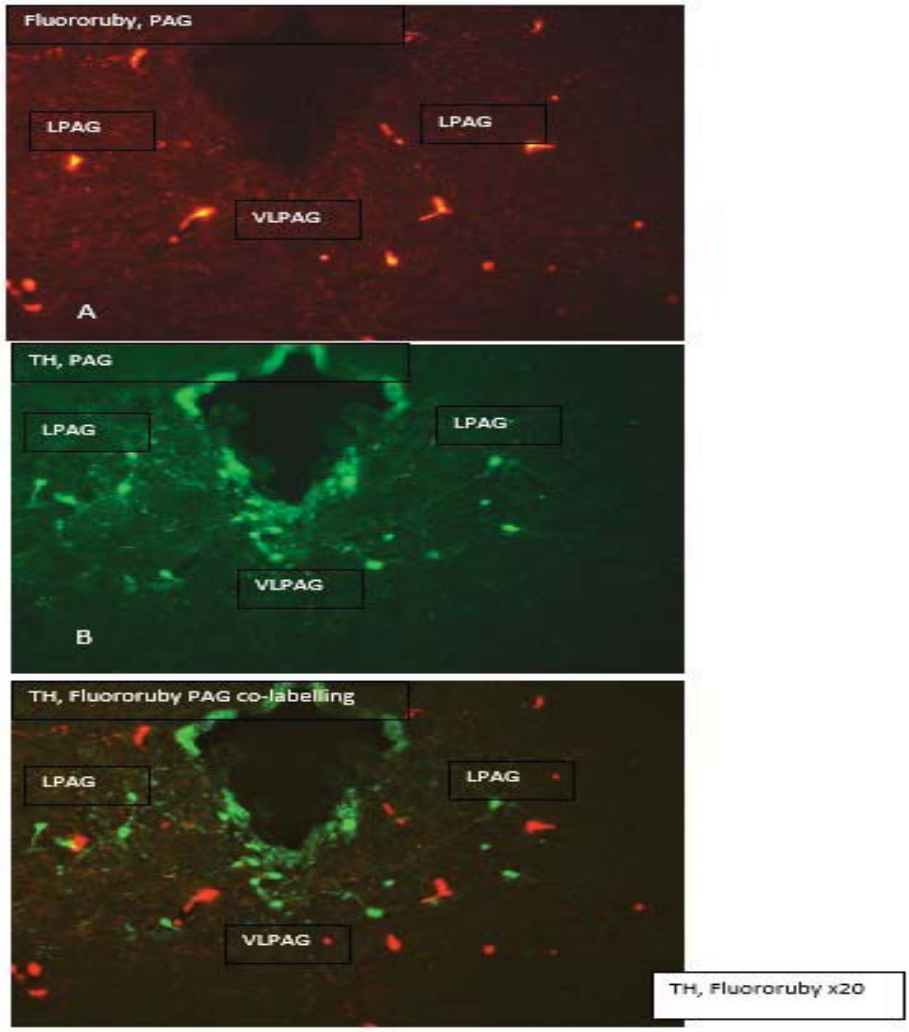

Figure (14): TH and Fluororuby. Figure (A) shows Fluororuby tracer staining neurons and fibers in LPAG and VLPAG. Figure (B) shows dopaminergic fibers and neurons (TH) in LPAG and VLPAG. Figure (C) shows dopaminergic fibers and neurons (TH) co-labelled with Fluororuby tracer (yellow color) in LPAG and VLPAG.

Third part - Fluororuby

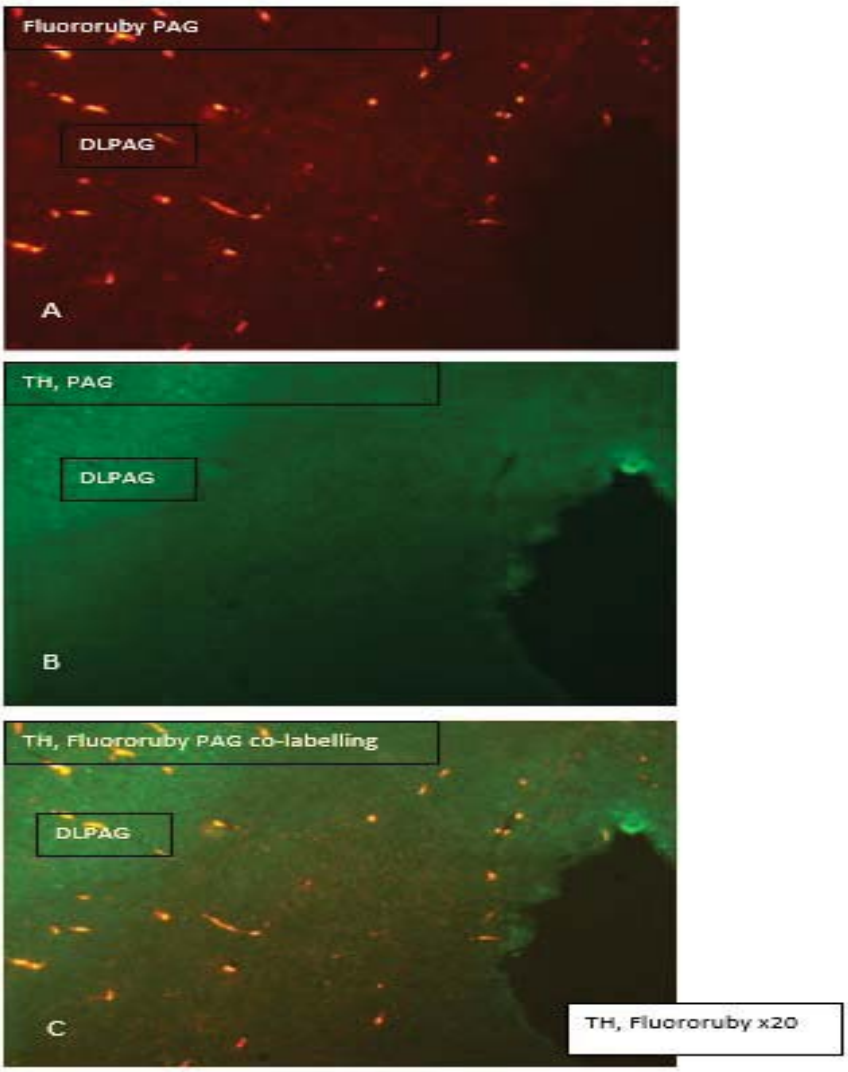

Figure (15): TH and Fluororuby. Figure (A) shows Fluororuby tracer staining neurons and fibers in DLPAG. Figure (B) shows dopaminergic fibers and neurons (TH) in DLPAG. Figure (C) shows dopaminergic fibers and neurons (TH) co-labelled with Fluororuby tracer (yellow color) in DLPAG.

Third part - Fluororuby

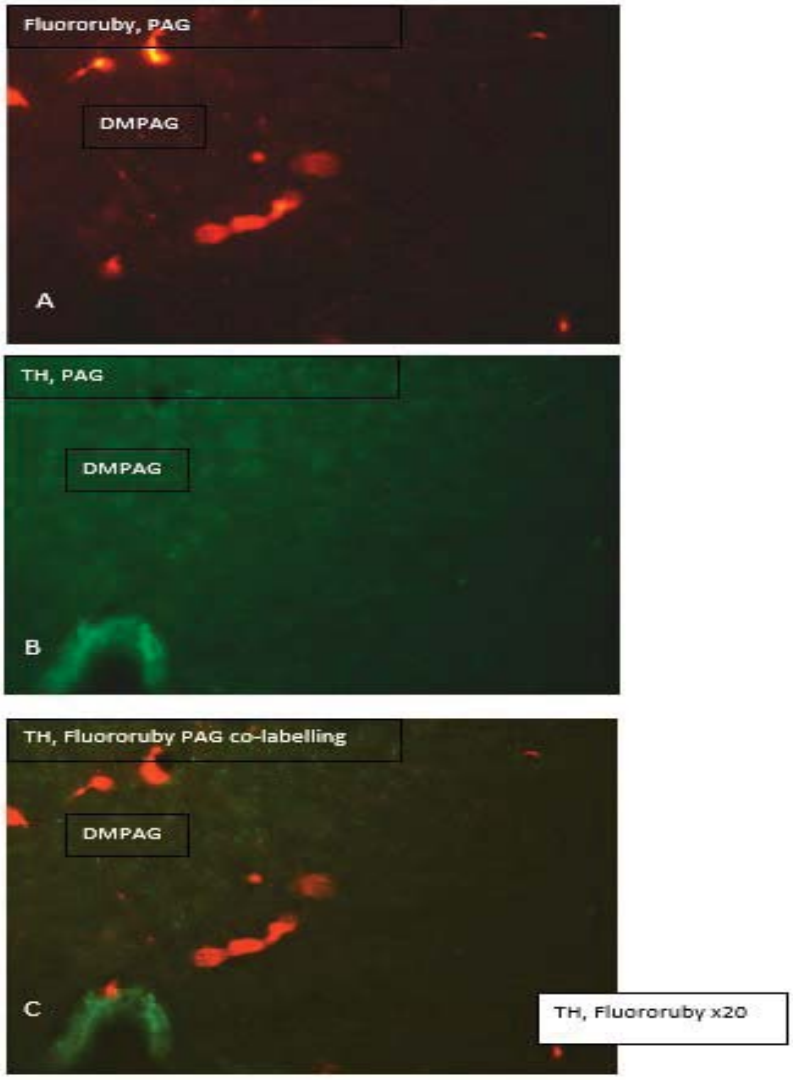

Figure (16): TH and Fluororuby. Figure (A) shows Fluororuby tracer staining neurons and fibers in DMPAG. Figure (B) shows dopaminergic fibers and neurons (TH) in DMPAG. Figure (C) shows dopaminergic fibers and neurons (TH) co-labelled with Fluororuby tracer (yellow color) in DMPAG.

4. Discussion

Our studies showed the effect of degeneration of the SNpc dopaminergic cells on the behavior of our PD rat model, in which painful behavior was demonstrated by different behavioral experiments, in addition to the expression of pain molecular markers. Besides, the immunohistochemical and western blot experiments which have proven the increase in excitatory neurotransmitters and the decrease in inhibitory ones. Our studies extended further to question the relationship between the SNpc dopaminergic loss and the spinal pain process occurring in our PD model. Thus, we injected anterograde fluorescent tracer (Fluororuby) in the SNpc, and studied the labelled structures in the brainstem and the cervical segments of the spinal cord. Tyrosine hydroxylase was used to co-label the Fluororuby stained cells to examine if they have dopaminergic origin or not.

In the past, experiments have shown that there were a lot of dopaminergic neurons in extranigral structures in the brain stem but they couldn't be connected to any certain fiber pathways (Beckstead et al., 1979). Besides, after injection in the spinal cord, substantia nigra wasn't labelled (Hopkins & Niessen, 1976).

So, our experiment in this study was done to check the SNpc projections. FR was injected in SNpc at different levels and was traced in different structures. These structures were also co-labelled with TH immunostaining which labels dopaminergic neurons and fibers. The injection site was validated by taking sections in the substantia nigra where pars compacta cells were stained with FR and co-labelled with TH.

Hopkins & Niessen (1976) have shown that SNpc gave projections around the medial lemniscus when injected medially, this medial pathway went through the VTA and along the middle of tegmentum to give fibers to caudal part of median raphe nucleus and dorsal raphe nucleus. On the other hand, the lateral pathway which went through central, cuneiform, and parabrachial areas of tegmentum ended ipsilaterally majorly and to lower extent contralaterally to central grey substance. While SNpr (not as SNpc) only gave sparse and diffuse projections in the central grey substance.

Thus, sections in the PAG were studied showing FR and TH staining in DMPAG, DLPAG, LPAG and VLPAG. According to Beitz (1982); substantia nigra projected to ventral and ventrocaudal regions of central grey. PAG coordinates motor and limbic inputs and relay them to spinal cord directly and indirectly. In addition, Liang et al. (2011) stated that PAG had a lot of spinal projections.

In our study, we found co-labelling of FR and TH in the four divisions of the PAG.

Finally, cervical spinal cord sections were taken. It was evident that FR tracer and TH

immunolabelling have stained LSp (lateral spinal nucleus) and LatC (lateral cervical nucleus of the spinal cord), but the dorsal spinal horn was lacking the labelling.

The nociceptive processes taking place in the spinal cord of PD rat model might be explained by the work of Sandkühler (2009) and Domenici et al. (2019) as they stated that PAG (ventrolateral region) is involved in pain where dopaminergic and GABAergic neurons are interconnected. Dopamine, Noradrenaline and Serotonin are all involved in pain modulation by decreasing their amount, while the increase of GABA in vlPAG may be due to a compensatory mechanism. Chronic pain in Parkinson's disease is due to disequilibrium between descending inhibitory and excitatory (facilitatory) pathways. GABA dysregulation in vlPAG leads to excitation of the descending facilitatory system, decreasing spinal opioids causing painful sensation.

General Discussion & Conclusion

General Discussion and Conclusion

1- General Discussion

Parkinson's disease is the second neurodegenerative disease worldwide. It has both motor and non-motor symptoms, in which pain is the main non-motor symptom (Skogar and Lokk, 2016; Buhmann et al., 2020). In this study, we made a PD animal model and tested behavioral, molecular and cellular mechanisms involved in PD pain. We made bilateral 6-OHDA animal lesion in the Medial Forebrain Bundle.

1.1. PD model verification:

6-OHDA is a neurotoxin which exerts its action through oxidative stress producing reactive oxygen species, mitochondrial dysfunction and decreasing concentration of antioxidant enzymes leading to oxidative stress and degeneration of neurons (Konnova and Swanberg, 2018). 6-OHDA affects dopaminergic and noradrenergic neurons, thus, desipramine was given 30 minutes before surgery to increase 6-OHDA specificity for dopaminergic neurons (Dieb et al., 2016).

We verified our PD model validity using body weight, immunohistochemistry and behavioral tests. Since bilateral 6-OHDA MFB lesion causes aphagia and adipsia, animals were weighed after surgery and monitored all through the experiment. They were syringe-fed with water, pellets and milk for survival. There was a significant decrease in weight of 6-OHDA lesioned group which was less than sham one. In addition, Tyrosine hydroxylase immunohistochemistry has shown significant dopaminergic cells neurodegeneration in 6-OHDA lesioned group. Cell death percentage in both SNpc and VTA was 67.8%, in VTA only was 56.7 % and in SNpc only was 89.9 % after 6-OHDA lesion. While motor function of rats was tested using Rotarod test, through which 6-OHDA lesioned rats were significantly incapable of holding their limbs to the rotating rods due to motor dysfunction, as has also been shown in the study by Campos et al. (2013). As was mentioned in Ma et al. (2014), our 6-OHDA rat models had limb rigidity in contrast to sham ones showing motor deficits. All these tests' results have been confirmatory of the success of our PD rat model.

1.2. Behavioral pain tests:

PD non-motor symptoms are not connected to motor symptoms, pain and motor symptoms may not occur on the same body side, pain may occur before motor symptoms by years and the severity of pain is irrelevant to motor severity (Skogar and Lökk, 2016). Accordingly, after verifying our PD model, we performed multiple behavioral experiments to test for thermal and mechanical allodynia and hyperalgesia.

1.2.1. Thermal pain behavioral tests:

For thermal tests, cold allodynia and hyperalgesia were performed using acetone drop test and thermal place preference test, respectively.

In acetone drop test, there was an increase in number of flinches, reaction time and latency in 6-OHDA lesioned group than sham one indicating cold allodynia, which was decreased after intraperitoneal administration of D2R agonist ropinirole shown by the decrease of the reaction time and latency (systemic effect). For the place preference test, 6-OHDA lesioned rats spent less time on the test plates with temperatures 10 °C and 15 °C than sham ones, indicating increased cold hypersensitivity. Skogar and Lökk (2016) has mentioned that in humans, lesions in dopaminergic systems aggravate pain while the increase in dopamine is used to treat chronic pain, also, SNpc 6-OHDA injection led to time decrease on hot-plate test. Besides, Domenici et al. (2019) showed that there was an increased sensitivity to thermal stimulus that was treated with dopamine.

1.2.2. Mechanical pain behavioral test:

In von Frey test (10g), 6-OHDA lesioned rats showed mechanical static allodynia where the pain score (paw withdrawals) was higher than sham rats. While on intrathecal administration of dopamine agonist, pain score evidently decreased showing its segmental effect in the spinal cord. This effect was confirmed by Puopolo (2019) who showed the influence of Quinipirole (D2 agonist) given intrathecally, which led to the decrease of mechanical pain sensitivity with Von Frey anesthesiometer.

At last, Randall- test was used to examine mechanical hyperalgesia, 6-OHDA lesioned rats had greater mechanical hyperalgesia than sham group signified by the increase of vocalization at 50 %. This is concomitant with the result stated by Wood (2008); which showed the shortening of paw pressure response time on being subjected to painful stimuli when dopaminergic fibers were degenerated using 6-OHDA.

- Mechanisms implicated in neuropathic pain are going to be discussed on segmental (spinal cord) and suprasegmental (cingulate and insular cortices) bases.

1.3. Mechanism of spinal pain process:

1.3.1. Molecular pain markers:

In this study, pERK and CFOS were increased upon acetone stimulation to the hind paw in the 6-OHDA lesioned rats' group more than sham ones, while D2R agonist intraperitoneal administration decreased these markers' expression in SDH.

These findings were supported by Zhuang et al. (2005) and Gao & Ji (2009) who have mentioned that pERK and CFOS are pain molecular markers which are expressed under painful stimuli either thermal, mechanical, chemical or electrical. pERK and CFOS are directly proportionate to stimulus intensity, besides their spreading from superficial to deep laminae of dorsal horn with increasing stimulus intensity. In addition, increasing the time of stimulus application increases their expression. pERK is involved in increased reactivity of pain neurons located in the CNS especially those of dorsal spinal horn resulting in neuropathic pain presence and maintenance. pERK and CFOS are expressed under low intensity non-painful stimuli in some pathological conditions as nerve injury in dorsal spinal horn neurons and chronic constriction Injury (CCI).

Also, Gao & Ji (2009) has mentioned that activation of ERK 1 & 2 via their phosphorylation by MAPk or ERK kinases (MEK) depends on activation of Ras, Raf + and MEk cascades. After activation, CAMP- response element binding protein (CREB) transcriptional factor is activated which is necessary for long-term synaptic plasticity processes and several neuronal genes transcription processes. pERK is localized in the dorsal horn neurons located superficially in the spinal cord which receives 1ry afferents carrying pain signals from the hind paw.

This was confirmed by Sandkühler (2009) & Géranton et al. (2010) who have stated that pERK is released when C- fibers are subjected to painful stimulus where post translational modification in the form of phosphorylation of extracellular signal – regulated kinase takes place. These changes do not occur within A β fibers. C-FOS is released in A δ /C fibers but not in Aβ fibers. The injury to ascending pathway from spinal dorsal horn lamina I and III led to the reduction of mechanical hyperalgesia. Besides, pERk may be involved in neuropathic pain pathogenesis as mechanical hyperalgesia decreased when pERK inhibitor (PD98059) is injected intrathecally. pERK and CFOS are involved in neuropathic pain and they

decrease when analgesics and anti-inflammatory medications are used (Zhuang et al., 2005; Gao & Ji, 2009; Sandkühler, 2009).

1.3.2. Pain mechanisms:

Pain may occur in PD due to neurodegeneration of spinal cord including dorsal laminae. In addition to changes in internal circuits in spinal dorsal horn and degeneration of descending pathways from the brainstem (Biagioni, 2021).

The spinal cord nociceptor neurons may have exaggerated excitability due to the release of neurotransmitters Glutamate and Calcitonin gene related peptide and Tachykinins as substance P neuropeptides and Neurokinin A. Prolonged binding of these neurotransmitters and tachykinins to receptors leads to the activation of NMDA receptors (N- methyl- D- aspartate) which results in the augmentation of intracellular level of calcium through N-type calcium channels. Thus, the dorsal horn neurons become sensitized and respond with lower threshold and longer duration to painful stimuli, in addition to the increase in the area of neurons ready to receive these painful stimuli i.e. wind – up phenomenon. Another proposed mechanism of neuropathic pain is central disinhibition where the activity of inhibitory pathways is decreased or ceased. These changes lead to allodynia which is the occurrence of pain when subjected to non-painful stimulus (e.g. touch that is conveyed through Aß fibers becomes painful through the same fibers) (Pasero, 2004).

Tactile Allodynia occurs as a result of the decrease in the descending inhibitory inputs to the excitatory polysynaptic interneurons linking low threshold mechanoreceptors [LTMRs] Aß fibers to projecting neurons in lamina I of the dorsal spinal horn (Todd, 2015).

There are excitatory interneurons mainly in lamina III and express VGLUT3 [Vesicular glutamate transporter] which have a role in mechanical allodynia pathogenesis (Peirs et al., 2015).

Lamina I and II have interneurons releasing GABA neurotransmitter which impedes painful signals from excitatory interneurons releasing somatostatin which are present in lamina II of dorsal spinal horn. They are connected with Aß touch fibers and small diameter afferents. These inhibitory interneurons may be target for modulations of PKC - γ interneurons which might decrease mechanical allodynia (Petitjean et al., 2015).

Lamina I spinothalamic neurons have more cold responsive neurons than warm ones. This pain pathway goes to the insular cortex (Viana, 2018).

TRPM8 (Transient receptor potential melastatin 8) might be involved in the process of cold allodynia. But there are contradictory data as in different conditions, TRPM8 agonists and

antagonists decrease pain (Li et al., 2013).

TRP (transient potential channels) respond to thermal stimuli (which are non-selective cation channels) when activated leading to influx of Na+ and Ca++ into nerve endings where depolarization occurs (Viana, 2018).

1.3.2.1. Excitatory markers in the spinal cord:

In the current study, PKCγ expression was increased in SDH mostly in cells of lamina IIi and in scattered cells within lamina III in 6 - OHDA lesioned more than sham ones. Ropinirole intraperitoneal administration led to a significant decrease of PKCγ expression in 6-OHDA +D2R agonist rats when compared to 6-OHDA lesioned animals.

According to Alba-Delgado (2018), there is an assumption that due to fast interactions in mechanical allodynia, it takes place in spinal and medullary dorsal horns. Remodeling occurs in PKCγ interneurons. 5-HT 2A receptor in PKC, ERK ½ pathway may be involved in mechanical allodynia through descending fibers releasing 5-HT.

Moreover, in tactile allodynia, stimulation of fibers which in normal conditions convey touch sensation, provokes pain. Normally, when local inactive circuit having PKCγ cells becomes activated, it leads to allodynia (Miraucourt et al., 2007).

Dieb et al. (2015) and Peirs et al. (2016) have explained that in medullary dorsal horn, pERK has a crucial role in developing thermal and mechanical hypersensitivity. Dynamic mechanical allodynia involves induction of PKCγ in lamina IIi and III, besides pERK½ induction in superficial dorsal medullary horn either spontaneously or after using a stimulus as a part of neuropathic pain. pERK ½ and PKCγ could have synaptic connections linking them. When PKCγ was inhibited, medullary dorsal horn pERK1/2 and dynamic mechanical allodynia decreased. Axons of PKCγ are connected majorly to cell bodies of pERK1/2. Thus, ERK½ is stimulated by PKCγ which receive projections from A β fibers. Normally, physiological connection between A β fibers mechanoreceptors and pain conveying pathway is inactive under physiological conditions due to the expression of large amount of GABA and Glycine inhibitory neurotransmitters. If a pathological event happens, these inhibitory neurotransmitters decrease leading to excitation of pERK ½ and PKCγ causing painful sensation under non-painful light mechanical stimulus. This is most probably due to the stimulation of cells in lamina I via PKCγ– pERK1/2 communication pathways. Martin et al. (2001) mentioned that on activation, PKCγ is increased, and translocation happens from cytosol to neuronal cell membrane in superficial laminae of dorsal horn contributing to allodynia.

Also, Sluka & Audette (2006) and P eirs et al. (2016) confirmed that non-harmful stimuli are conveyed by LTMRs (low threshold mechanoreceptors) ending in or below lamina IIi connected to lamina I neurons via PKCγ interneurons in static mechanical allodynia. This is explained by the facts stated by Wang et al. (2020) showing that there were feedforward inhibitory inputs to PKCγ interneurons preventing LTMR signals to be conveyed to circuits processing pain in the SDH. Inhibiting this feedforward circuits resulted in mechanical allodynia. These feedforward inhibitory circuits were modulated through Aβ fibers by affecting PKCγ expressing neurons (via GABAergic and mainly Glycinergic inhibitory interneurons), while PKCγ cells themselves mainly received A δ fibers.

Another mechanism clarified by Sluka & Audette (2006); PKCγ increases the expression of glutamate. PKCγ activates NMDA and AMPA receptors releasing glutamate leading to neuronal excitation. In the dorsal horn, PKC sensitizes neurons augmenting spontaneous firing, making neurons more reactive to mechanical stimuli. Inhibitory effects on spinothalamic tract are interfered by PKC enhancing excitation. Thus, PKC cells are involved in hyperalgesia on the long term.

Eventually, Blocking PKCγ decreased painful sensations. Blocking agents of NMDA receptors in medullary dorsal horn (MDH) or SDH decreased allodynia. PKC knockout affected chronic but not acute neuropathic pain for both mechanical and thermal stimuli. PKCγ was responsible for the chronic phase of pain one week after injury (Martin et al., 2001; Sluka & Audette, 2006; Miraucourt et al., 2007; Velazquez et al., 2007).

1.3.2.2. Inhibitory markers in the spinal cord:

Our study revealed that GAD67 expression was significantly increased in SDH in 6 - OHDA lesioned rats than sham and 6-OHDA +D2R agonist rats. Ropinirole intraperitoneal administration led to a significant decrease of GAD67 expression in 6-OHDA +D2R agonist rats when compared to 6 - OHDA lesioned animals.

GAD67 is a rate limiting enzyme for GABA synthesis. GAD expression decreased neuropathic pain (Ogawa et al., 2018). Reducing GAD65/67 led to hyperalgesia (Li et al., 2019). There is an inverse correlation between GABA and GAD67. When GABA increased more than 2.5 fold, GAD67 KDA decreased due to the alterations of GAD, stability of protein or translation of GAD mRNA (Rimvall & Martin, 1994).

Also Castro-Lopes et al. (1994) study has shown that on complete Freund's adjuvant injection, there was an increase in GAD after 4 days, while it took up to 3-4 weeks for the

GABA to increase in the spinal cord. This difference in elevation timing may be due to time requested for GAD accumulation to synthesize GABA.

Another studies by Périer et al. (2003), Wang et al. (2007) and Tseng (2009) revealed that in 6-OHDA model, GAD67 increased in basal ganglion striatum and striatopallidal neurons which was reversed by L-Dopa. GAD67 remained elevated for 6-8 months. Also, in MPTP non primate models, mRNA GAD67 was increased in SNpr and Globus Pallidus which was reversed by using L-Dopa treatment.

GABA dysfunction caused neuropathic pain and when GABA antagonist was used, it caused an increase in pain hypersensitivity (Ouachikh et al., 2018). Inhibitory GABA and Glycine cells form 1/3 of neurons in lamina I and lamina II and 40% of lamina III. Spinal cord dorsal horn projection neurons are glutamatergic in origin thus theoretically Gabaergic and Glycinergic ones are interneurons (Todd, 2015; Domenici et al., 2019).

Also, Sandkühler (2009) and Gwak & Hulsebosch (2011) added that after spinal cord injury, inhibitory GABA marker was decreased leading to an increased neuronal excitability in dorsal horn of spinal cord causing central neuropathic pain.

Besides, GABA decrease also played a role in MDH in the processing of static mechanical allodynia (Peirs et al., 2016).

Other studies demonstrated that GABAergic inhibitory interneurons decreased nociception in spinal cord and trigeminal nucleus against both acute and chronic stimuli (Millan, 2002; Domenici et al., 2019).

Meanwhile, when GABA degrading enzyme was blocked using vigabatrin, this led to a decrease of PKCγ and an increase of GABA in medullary dorsal horn. PKCγ cells have GABA receptors located on their surfaces and they receive GABAergic projections. Neuronal excitatory circuits formed by PKCγ subtypes receive parvalbumin interneurons as well. The decreased GABA led also to spontaneous pain. Polysynaptic circuits connect afferent tactile fibers with nociceptive projections in the spinal cord (Ouachikh et al., 2018).

We demonstrated that VGAT expression is significantly increased in the SDH in 6 - OHDA lesioned rats more than sham. Ropinirole intraperitoneal administration led to a very significant increase of VGAT expression in 6-OHDA +D2R agonist rats when compared to 6 - OHDA lesioned animals and sham ones.

Our result correlates with Faynveitz et al. (2019); in which VGAT labelled puncta were increased in animal models in which dopamine was depleted in 6-OHDA rat models. Dopamine depletion increased GABAergic transmission in the SNr (due to synaptic proliferation).

Also, Changes in GABA amount led to PD. GAD inhibition resulted in the reduction of

VGAT activity (Lin et al., 2010).

Parvalbumin expression was increased in the 6-OHDA lesioned rats' group more than sham ones, while D2R agonist intraperitoneal administration decreased this marker's expression in the SDH.

This may be explained by the study of Soós et al. (2004) in which parvalbumin increased in PD as a protective mechanism against increasing Ca++ inside SN cells due to increasing oxidative damage and excitotoxicity to protect it from neuronal death.

Parvalbumin cells expressed both GABAergic and Glycinergic subtypes (Todd and Sullivan, 1990; Laing et al., 1994). Most probably, parvalbumin cells disinhibited PKCγ cells. As, in the 6-OHDA conditions, there was diminution in descending pain control, leading to an increase in excitation of parvalbumin cells causing disinhibition of PKCγ cells. Thus, Parva lbumin and PKCγ were highly expressed in this case.

As was stated, PKCγ cells receive parvalbumin projections in SDH and MDH. Parvalbumin cells are crucial in tactile allodynia. Polysynaptic circuits connect 1ry afferent tactile fibers with nociceptive projections in the spinal cord (Ouachikh et al., 2018).

On the other hand, Petitjean et al. (2015) discussed PV role. When PV neurons were abolished, mechanical allodynia occurred due to stopping inhibition of PKCγ cells and the activation of PV cells enhanced the pain mechanically but not thermally.

1.3.3. Dopaminergic effect:

There are many studies explaining the effect of dopamine loss on painful sensation as follows:

Domenici et al. (2019) and Buhidma et al. (2020) have shown that the decreased threshold of mechanical nociception in 6-OHDA model was reversed through D2 receptors by giving L-Dopa as in PD patients treatment.

Similarly, when dopamine was injected in the spinal cord, it decreased thermal and mechanical pain sensitivity in ipsilateral and contralateral sides, while antagonizing dopamine has the opposite effect. Descending dopaminergic pathways stimulate substantia gelatinosa neurons post-synaptically via D2R, resulting in hyperpolarization through the activation of K+ channels (Wood, 2008). Chudler & Dong (1995) and Konnova & Swanberg (2018) also, as in our model, have studied the effect of dopamine depletion solely on pain in PD rats.

A11 dopaminergic neurons stimulation has an inhibitory effect on painful processes produced at spinal dorsal horn neurons and trigeminocervical complex neurons. After A11 area lesion using 6-OHDA, dopamine amount decreased in Lumbar spinal cord segments. Fibers transmitting pain are inhibited by D2R like agonists and

stimulated by D2R like antagonists (Orazzo et al., 1993; Lu et al., 2018; Puopolo, 2019).

All subtypes of dopamine receptors are present in the spinal cord and mesencephalic trigeminal nucleus. Dopamine inhibits post synaptic pain signals carried by A and C fibers. Also, it inhibits the synaptic transmission of pain signals from PAFs to projection neurons in Lamina I. In addition, dopamine modifies pain signals pre-synaptically by acting on D3 and D4 receptors (Puopolo, 2019).

D2 receptors are found in the spinal cord in superficial laminae and lamina X mainly by immunohistochemical studies, while using mRNA studies, mRNA encoding D2 receptors sites were present in lamina I and laminae (II - VI) showing synthesis of D2Rs by dorsal horn neurons to be manipulated in the processing of painful stimuli. Also, mRNA encoding D2R was found in dorsal root ganglion, i.e. primary afferent fibers probably have D2Rs (Millan, 2002; Wood, 2008).

In our current work, D2R expression was increased significantly in SDH in 6 - OHDA lesioned rats more than sham and 6-OHDA +D2R agonist ones. Ropinirole intraperitoneal administration led to the decrease of D2R expression in 6-OHDA +D2R agonist rats when compared to 6 - OHDA lesioned animals.

As mentioned in these studies Matsukawa et al. (2007) and Tang et al. (2021); in 6-OHDA lesioned models, D2R and D3R were changed. D2R binding elevated significantly in 6-OHDA rat models, in MPTP non – human primates and in human patients. D2Rs were concentrated in superficial dorsal horn of spinal cord. In PD, pre and post synaptic D2R were potentiated after dopaminergic lesion. Pain started one week after 6-OHDA lesion and remained for minimum 4 weeks (different time course than motor symptoms).

D2R activation can treat nociception in SDH in PD. D2R activation reduced the hyperexcitability in 6-OHDA lesioned model in the SDH having anti-nociceptive effect. D2R binding was down regulated on D2R agonist treatment. D2R agonists decreased painful sensation and increased threshold of mechanical stimuli in 6-OHDA mice model. When D2R antagonist was used, the antinociceptive effect of L-Dopa was demolished. D2R agonist inhibits C and A delta fibers glutamatergic inputs, glutamatergic interneurons in spinal cord and reticular formation in the brainstem (Matsukawa et al., 2007; Tang et al., 2021).

Moreover, when ropinirole – which is a D2R agonist- was given in a 6-OHDA mice model for 7 days, it led to an increase in GSH, catalase and SOD in the striatum which is neuroprotective (Iida et al., 1999).

Ropinirole is used either in monotherapy in early PD or concomitant with Levodopa in progressive PD. Dyskinesia was low with Ropinirole. Ropinirole has a neuroprotective

effect (Matheson & Spencer, 2000; Matsukawa et al., 2007).

1.4. The linkage between the substantia nigra and spinal pain processes (Fluororuby):

Basal ganglia play role in pain sensation. When the substantia nigra, which is a component of the basal ganglia gets stimulated electrically, this leads to modulation of pain sensation in the dorsal spinal cord horn via dopamine released from descending inhibitory pathway from midbrain (Skogar and Lökk, 2016). In addition, VTA influences pain, its degeneration leads to increasing responsiveness to pain while its stimulation decreases pain sensitivity (Young Blood et al., 2016).

The basal nuclei play crucial roles in limbic, motor, and associative pathways, while striatal neurons are involved in sensory pathways. Most of the brain dopamine is produced from nigrostriatal and mesolimbic pathways which are involved in PD and pain modulation, respectively. Mesolimbic pathway connects VTA to Nucleus Accumbens, Thalamus and Amyygdala. The mesocortical pathway connects VTA to prefrontal cortex and ACC controlling affective and motivational aspects of pain (Young Blood et al., 2016).

Descending facilitatory pathways responsible for painful stimuli originate from multiple areas as rostroventral medulla, dorsal reticular nulei and PAG; but the terminal facilitatory pathway comes from rostroventral medulla. Changes in these pathways may lead to chronic pain (Sandkühler, 2009).

In the past, experiments have shown that there are a lot of dopaminergic neurons in extranigral structures in the brain stem but they couldn't be connected to any certain fiber pathways (Beckstead et al., 1979). Besides, after injection in the spinal cord, substantia nigra wasn't labelled (Hopkins & Niessen, 1976).

Another experiment in this study was done to check the SNpc projections. FR was injected in SNpc at different levels and was traced in different structures. These structures were also co-labelled with TH immunostaining which labels dopaminergic neurons and fibers. The injection site was validated by taking sections in the substantia nigra where pars compacta cells were stained with FR and co-labelled with TH.

Hopkins & Niessen (1976) have shown that SNpc gives projections around the medial lemniscus when injected medially, this medial pathway goes through the VTA and along the middle of tegmentum to give fibers to caudal part of median raphe nucleus and dorsal raphe nucleus. On the other hand, the lateral pathway which goes through central, cuneiform, and parabrachial areas of tegmentum ends ipsilaterally majorly and to lower extent contralaterally to central grey substance. While SNpr (not as Snpc) only gives sparce and diffuse projections to the central grey substance.

Thus, sections in the PAG were studied showing FR and TH co-labelling in DMPAG, DLPAG, LPAG and VLPAG. According to Beitz (1982); substantia nigra projects to ventral and ventrocaudal regions of central grey. PAG coordinates motor and limbic inputs and relays them to spinal cord directly and indirectly. In addition, Liang et al. (2011) stated that PAG has a lot of spinal projections.

Finally, cervical spinal cord sections were taken. It was evident that FR tracer and TH immunolabelling have stained LSp (lateral spinal nucleus) and LatC (lateral cervical nucleus) of the spinal cord.

The nociceptive processes taking place in the spinal cord of PD rat model might be explained by the work of Sandkühler (2009) and Domenici et al. (2019) who stated that PAG (ventrolateral region) is involved in pain in which dopaminergic and GABAergic neurons are interconnected. The Increase of GABA in vlPAG might be due to a compensatory mechanism. Chronic pain in Parkinson's disease is due to disequilibrium between descending inhibitory and excitatory (facilitatory) pathways. GABA dysregulation in vlPAG leads to excitation of descending facilitatory system, decreasing spinal opioids causing painful sensation.

1.5. Pain matrix:

There are many data in the literature regarding the involvement of pain matrix structures (Insular and anterior cingulate cortices) in the processing of pain.

Insular and anterior cingulate cortices modulate pain. They were activated by experimental allodynia. During wearing off state, there was an increased activity in Insula and ACC which were involved in the affective motivational aspect of pain. They were involved during the off-phase treatment with L-Dopa (Wood, 2008; Garcia – Larrea & Peyron, 2013; Young Blood et al., 2016).

Substantia Nigra cells degeneration leads to augmentation of neuronal activity in multiple structures: substantia nigra pars reticulata, internal globus pallidus and subthalamic nucleus leading to inhibitory effect on the lateral thalamic region causing an increase in pain sensitivity affecting the lateral spinothalamocortical pathway connecting parietal and insular cortices which leads to disinhibition of medial spinothalamocortical pathways connecting the anterior cingulate cortex. The action of dopamine is well known in the pathogenesis of central pain nowadays (Fil et al., 2013; Young Blood et al., 2016).

Insular cortex has been proven implicated in Insular allodynic sensation. When insular cortex was injected with dopamine reuptake inhibitor (GBR- 12935), pain threshold was augmented via descending inhibitory fibers to the spinal cord. These

dopaminergic fibers are originating from VTA/SN (Wood, 2008; Garcia – Larrea & Peyron, 2013).

Also, ACC plays a crucial role in the perception of pain. It increases descending facilitatory inputs. It was involved in electrical, mechanical and thermal stimuli (Chudler & Dong, 1995; Millan, 2002; Zhuo et al., 2011).

In addition, the activation of ACC - Spinal cord projections led to increased mechanical sensitivity and the silencing of these projections led to decreased painful sensation (Thompson and Neurgebauer, 2019).

While the injection of dopamine in the ACC decreased pain correlated behaviors, but lower doses were more effective than higher ones (Wood, 2008).

1.5.1. Pain molecular markers in the ACC and the IC:

Thus, in the current work, we tested pERK pain marker in the Insular and Cingulate cortices. pERK expression was increased significantly in the Insular Cortex upon acetone stimulation to the hind paw in the 6-OHDA lesioned rats' group more than sham ones, while D2R agonist intraperitoneal administration decreased significantly this marker's expression than in 6-OHDA lesioned group.

This was confirmed by Wang et al. (2020). In neuropathic pain models (CCI and sciatic nerve injury); pERK expression was significantly increased in the insular cortex. Nociception was reversed on treatment with an ERK inhibitor in the insular cortex of rat model. Thus, ERK phosphorylation in the insular cortex was implicated in the central sensitization of neuropathic pain.

Besides, in our study, pERK expression was increased significantly in the Cingulate Cortex upon acetone stimulation to the hind paw in the 6-OHDA lesioned rats' group more than sham ones, while D2R agonist intraperitoneal administration decreased significantly this marker's expression than in 6-OHDA lesioned group.

Cao et al. (2009) explained that NMDA receptors and ERK-CREB (cAMP response element binding protein) pathway are crucial for pain processing in rat ACC.

This was confirmed by Wei & Zhou (2008) and Cao et al. (2009) who stated that mechanical allodynia led to a significant increase in pERK in ACC in neuropathic pain models which was involved in the induction and expression of chronic pain. pERK plays a crucial role in cortical plasticity and synaptic potentiation in the ACC.

2- Conclusion

The present study demonstrated a change in the balance between excitation and inhibition within structures included in the pain process pathway. These structures included dorsal spinal cord, insular and cingulate cortices. This excitation inhibition imbalance constituted the basis of mechanical and thermal pain hypersensitivities observed in 6-OHDA lesioned rats. At the molecular level, these changes are highlighted by an increase in expression of different markers (GAD67, parvalbumin, VGAT, PKCγ, pERK1/2 and cFOS). The spinal dorsal horn constitutes the first structure that processes ascending pain and the last one receiving descending inhibitory pain regulating efferents. The increase in inhibitory markers within this structure may reflect disinhibition, since there is also an increase in excitation as demonstrated by the increase of PKCγ in PKCγ cell subtype. The latter is known under pathological conditions to be responsible for pain chronicity and to transmit non-nociceptive stimuli to the nociceptive specific neurons within superficial lamina I in the spinal dorsal horn. In addition, our study demonstrated a direct projection from the SNpc to the PAG, a key structure of the pain inhibitory descending pathway. Additional studies are needed to demonstrate if SNpc dopaminergic projection target PAG interneurons or projecting neurons. At last, our study demonstrated the implication of insular and cingulate cortices which are part of both medial and lateral pain processing systems.

References

References

- Alba-Delgado, C., Mountadem, S., Mermet-Joret, N., Monconduit, L., Dallel, R., Artola, A., & Antri, M. (2018). 5-HT2A Receptor-Induced Morphological Reorganization of PKCγ-Expressing Interneurons Gates Inflammatory Mechanical Allodynia in Rat. The Journal of neuroscience : the official journal of the Society for Neuroscience, 38(49), 10489–10504. https://doi.org/10.1523/JNEUROSCI.1294-18.2018

- Alles, S., & Smith, P. A. (2018). Etiology and Pharmacology of Neuropathic Pain. Pharmacological reviews, 70(2), 315–347. https://doi.org/10.1124/pr.117.014399

- Ameyaw, E. O., Woode, E., Boakye-Gyasi, E., Abotsi, W. K., Kyekyeku, J. O., & Adosraku, R. K. (2014). Anti-allodynic and Anti-hyperalgesic effects of an ethanolic extract and xylopic acid from the fruits of Xylopia aethiopica in murine models of neuropathic pain. Pharmacognosy research, 6(2), 172–179. https://doi.org/10.4103/0974-8490.129041

- Andersen, J. V., Christensen, S. K., Westi, E. W., Diaz-delCastillo, M., Tanila, H., Schousboe, A., Aldana, B. I., & Waagepetersen, H. S. (2021). Deficient astrocyte metabolism impairs glutamine synthesis and neurotransmitter homeostasis in a mouse model of Alzheimer's disease. Neurobiology of disease, 148, 105198. https://doi.org/10.1016/j.nbd.2020.105198

- Balayssac, D., Ling, B., Ferrier, J., Pereira, B., Eschalier, A., & Authier, N. (2014). Assessment of thermal sensitivity in rats using the thermal place preference test: description and application in the study of oxaliplatin-induced acute thermal hypersensitivity and inflammatory pain models. Behavioural pharmacology, 25(2), 99–111. https://doi.org/10.1097/FBP.0000000000000026

- Balestrino, R., & Schapira, A. H. V. (2020). Parkinson disease. European Journal of Neurology, 27(1), 27–42. https://doi.org/10.1111/ene.14108

- Barrot M. (2012). Tests and models of nociception and pain in rodents. Neuroscience, 211, 39–50. https://doi.org/10.1016/j.neuroscience.2011.12.041

- Beckstead, R. M., Domesick, V. B., & Nauta, W. J. H. (1979). Efferent connections of the substantia nigra and ventral tegmental area in the rat. Brain research, 175(2), 191–217. https://doi.org/10.1016/0006-8993(79)91001-1

- Beitz A. J.(1982). The organization of afferent projections to the midbrain periaqueductal gray of the rat. Neuroscience, 7(1), 133–159. https://doi.org/10.1016/0306-4522(82)90157-9

- Berrocal, Y. A., Almeida, V. W., Puentes, R., Knott, E. P., Hechtman, J. F., Garland, M., & Pearse, D. D. (2014). Loss of Central Inhibition: Implications for Behavioral Hypersensitivity after Contusive Spinal Cord Injury in Rats. Pain Research and Treatment, 2014, 178278. https://doi.org/10.1155/2014/178278

- Biagioni, F., Vivacqua, G., Lazzeri, G., Ferese, R., Iannacone, S., Onori, P., Morini, S., D'Este, L., & Fornai, F. (2021). Chronic MPTP in Mice Damage-specific Neuronal Phenotypes within Dorsal Laminae of the Spinal Cord. Neurotoxicity research, 39(2), 156–169. https://doi.org/10.1007/s12640-020-00313-x

- Blesa, J., Phani, S., Jackson-Lewis, V., & Przedborski, S. (2012). Classic and new animal models of Parkinson's disease. Journal of biomedicine & biotechnology, 2012, 845618. https://doi.org/10.1155/2012/845618

References

- Bowyer, J. F., & Schmued, L. C. (2006). Fluoro-Ruby labeling prior to an amphetamine neurotoxic insult shows a definitive massive loss of dopaminergic terminals and axons in the caudate-putamen. Brain Research, 1075(1), 236–239. https://doi.org/10.1016/j.brainres.2005.12.062

- Buhidma, Y., Rukavina, K., Chaudhuri, K. R., & Duty, S. (2020). Potential of animal models for advancing the understanding and treatment of pain in Parkinson's disease. Npj Parkinson's Disease, 6(1), 1. https://doi.org/10.1038/s41531-019-0104-6

- Buhmann, C., Kassubek, J., & Jost, W. H. (2020). Management of Pain in Parkinson's Disease. Journal of Parkinson's disease, 10(s1), S37–S48. https://doi.org/10.3233/JPD-202069

- Campos, F., Carvalho, M., Cristovão, A., Je, G., Baltazar, G., Salgado, A., Kim, Y.-S., & Sousa, N. (2013). Rodent models of Parkinson's disease: Beyond the motor symptomatology. Frontiers in Behavioral Neuroscience, 7, 175. https://doi.org/10.3389/fnbeh.2013.00175

- Cao, H., Gao, Y. J., Ren, W. H., Li, T. T., Duan, K. Z., Cui, Y. H., Cao, X. H., Zhao, Z. Q., Ji, R. R., & Zhang, Y. Q. (2009). Activation of extracellular signal-regulated kinase in the anterior cingulate cortex contributes to the induction and expression of affective pain. The Journal of neuroscience : the official journal of the Society for Neuroscience, 29(10), 3307–3321. https://doi.org/10.1523/JNEUROSCI.4300-08.2009

- Castro-Lopes, J. M., Tölle, T. R., Pan, B., & Zieglgänsberger, W. (1994). Expression of GAD mRNA in spinal cord neurons of normal and monoarthritic rats. Molecular Brain Research, 26(1–2), 169–176. https://doi.org/10.1016/0169-328X(94)90088-4

- Charron, G., Doudnikoff, E., Canron, M.-H., Li, Q., Véga, C., Marais, S., Baufreton, J., Vital, A., Oliet, S. H. R., & Bezard, E. (2014). Astrocytosis in parkinsonism: Considering tripartite striatal synapses in physiopathology? Frontiers in Aging Neuroscience, 6, 258. https://doi.org/10.3389/fnagi.2014.00258

- Chudler, E. H., & Dong, W. K. (1995). The role of the basal ganglia in nociception and pain: Pain, 60(1), 3–38. https://doi.org/10.1016/0304-3959(94)00172-B

- Cordero-Erausquin, M., Inquimbert, P., Schlichter, R., & Hugel, S. (2016). Neuronal networks and nociceptive processing in the dorsal horn of the spinal cord. Neuroscience, 338, 230–247. https://doi.org/10.1016/j.neuroscience.2016.08.048

- Dawson, T. M., Ko, H. S., & Dawson, V. L. (2010). Genetic animal models of Parkinson's disease. Neuron, 66(5), 646–661. https://doi.org/10.1016/j.neuron.2010.04.034

- De Miranda, B. R., & Greenamyre, J. T. (2017). Etiology and Pathogenesis of Parkinson's Disease. In R. Franco, J. A. Doorn, J. C. Rochet (Eds.), Oxidative Stress and Redox Signalling in Parkinson's Disease, pp. 1-26. Royal Society of Chemistry. DOI: 10.1039/9781782622888-00001

- Delgado-Morales, R. (Ed.). (2017). Neuroepigenomics in Aging and Disease (Vol. 978). Springer International Publishing. https://doi.org/10.1007/978-3-319-53889-1

References

- Deuis, J. R., Dvorakova, L. S., & Vetter, I. (2017). Methods Used to Evaluate Pain Behaviors in Rodents. Frontiers in Molecular Neuroscience, 10, 284. https://doi.org/10.3389/fnmol.2017.00284

- Dieb, W., Ouachikh, O., Durif, F., & Hafidi, A. (2014). Lesion of the dopaminergic nigrostriatal pathway induces trigeminal dynamic mechanical allodynia. Brain and Behavior, 4(3),368–380. https://doi.org/10.1002/brb3.214

- Dieb, W., & Hafidi, A. (2015). Mechanism of GABA involvement in post-traumatic trigeminal neuropathic pain: activation of neuronal circuitry composed of PKCγ interneurons and pERK1/2 expressing neurons. European journal of pain (London, England), 19(1), 85–96. https://doi.org/10.1002/ejp.525

- Dieb, W., Alvarez, P., & Hafidi, A. (2015). PKCγ-Positive Neurons Gate Light Tactile Inputs to Pain Pathway Through pERK1/2 Neuronal Network in Trigeminal Neuropathic Pain Model. Journal of Oral & Facial Pain and Headache, 29(1), 70–82. https://doi.org/10.11607/ofph.1353

- Dieb, W., Ouachikh, O., Alves, S., Boucher, Y., Durif, F., & Hafidi, A. (2016). Nigrostriatal dopaminergic depletion increases static orofacial allodynia. The journal of headache and pain, 17, 11. https://doi.org/10.1186/s10194-016-0607-z

- D'Mello, R., & Dickenson, A. H. (2008). Spinal cord mechanisms of pain. British journal of anaesthesia, 101(1), 8–16. https://doi.org/10.1093/bja/aen088

- Domenici, R. A., Campos, A. C. P., Maciel, S. T., Berzuino, M. B., Hernandes, M. S., Fonoff, E. T., & Pagano, R. L. (2019). Parkinson's disease and pain: Modulation of nociceptive circuitry in a rat model of nigrostriatal lesion. Experimental Neurology, 315, 72–81. https://doi.org/10.1016/j.expneurol.2019.02.007

- Duty, S., & Jenner, P. (2011). Animal models of Parkinson's disease: A source of novel treatments and clues to the cause of the disease: Animal models of Parkinson's disease. British Journal of Pharmacology, 164(4), 1357–1391. https://doi.org/10.1111/j.1476-5381.2011.01426.x

- Faynveitz, A., Lavian, H., Jacob, A., & Korngreen, A. (2019). Proliferation of Inhibitory Input to the Substantia Nigra in Experimental Parkinsonism. Frontiers in Cellular Neuroscience, 13, 417. https://doi.org/10.3389/fncel.2019.00417

- Fil, A., Cano-de-la-Cuerda, R., Muñoz-Hellín, E., Vela, L., Ramiro-González, M., & Fernández-de-las-Peñas, C. (2013). Pain in Parkinson disease: A review of the literature. Parkinsonism & Related Disorders, 19(3), 285–294. https://doi.org/10.1016/j.parkreldis.2012.11.009

- Ford B. (2010). Pain in Parkinson's disease. Movement disorders: official journal of the Movement Disorder Society, 25 Suppl 1, S98–S103. https://doi.org/10.1002/mds.22716

- Fukuzaki, K., Kamenosono, T., & Nagata, R. (2000). Effects of ropinirole on various parkinsonian models in mice, rats, and cynomolgus monkeys. Pharmacology, biochemistry, and behavior, 65(3), 503–508. https://doi.org/10.1016/s0091-3057(99)00240-3

- Gao, Y.-J., & Ji, R.-R. (2009). C-Fos or pERK, Which is a Better Marker for Neuronal Activation and Central Sensitization After Noxious Stimulation and Tissue Injury? The Open Pain Journal, 2(1), 11–17. https://doi.org/10.2174/1876386300902010011

References

- Garcia, J., Barbosa Neto, J., Amâncio, E., & Fonoff, E. (2016). Central neuropathic pain. Revista Dor., 17(1). https://doi.org/ 10.5935/1806-0013.20160052.

- Garcia-Larrea, L., & Magnin, M. (2008). Physiopathologie de la douleur neuropathique: revue des modèles expérimentaux et des mécanismes proposés [Pathophysiology of neuropathic pain: review of experimental models and proposed mechanisms]. Presse medicale (Paris, France : 1983), 37(2 Pt 2), 315–340. https://doi.org/10.1016/j.lpm.2007.07.025

- Garcia-Larrea, L., & Peyron, R. (2013). Pain matrices and neuropathic pain matrices: a review. Pain, 154 Suppl 1, S29–S43. https://doi.org/10.1016/j.pain.2013.09.001

- Géranton, S. M., Tochiki, K. K., Chiu, W. W., Stuart, S. A., & Hunt, S. P. (2010). Injury Induced Activation of Extracellular Signal-Regulated Kinase (ERK) in the Rat Rostral Ventromedial Medulla (RVM) is Age Dependant and Requires the Lamina I Projection Pathway. Molecular Pain, 6, 1744-8069-6–54. https://doi.org/10.1186/1744-8069-6-54

- Goetz, C. G., Tanner, C. M., Levy, M., Wilson, R. S., & Garron, D. C. (1986). Pain in Parkinson's disease. Movement disorders: official journal of the Movement Disorder Society, 1(1), 45–49. https://doi.org/10.1002/mds.870010106

- González, A., Ugarte, G., Restrepo, C., Herrera, G., Piña, R., Gómez-Sánchez, J. A., Pertusa, M., Orio, P., & Madrid, R. (2017). Role of the Excitability Brake Potassium Current IKD in Cold Allodynia Induced by Chronic Peripheral Nerve Injury. The Journal of neuroscience : the official journal of the Society for Neuroscience, 37(12), 3109–3126. https://doi.org/10.1523/JNEUROSCI.3553-16.2017

- Graham, D. L., Durai, H. H., Garden, J. D., Cohen, E. L., Echevarria, F. D., & Stanwood, G. D. (2015). Loss of dopamine D2 receptors increases parvalbumin-positive interneurons in the anterior cingulate cortex. ACS chemical neuroscience, 6(2), 297–305. https://doi.org/10.1021/cn500235m

- Gwak, Y. S., & Hulsebosch, C. E. (2011). GABA and central neuropathic pain following spinal cord injury. Neuropharmacology, 60(5), 799–808. https://doi.org/10.1016/j.neuropharm.2010.12.030

- Hölscher C. (2020). Brain insulin resistance: Role in neurodegenerative disease and potential for targeting. Expert Opinion on Investigational Drugs, 29(4), 333–348. https://doi.org/10.1080/13543784.2020.1738383

- Hopkins, D. A., & Niessen, L. W. (1976). Substantia nigra projections to the reticular formation, superior colliculus and central gray in the rat, cat and monkey. Neuroscience Letters, 2(5), 253–259. https://doi.org/10.1016/0304-3940(76)90156-7

- Iida, M., Miyazaki, I., Tanaka, K., Kabuto, H., Iwata-Ichikawa, E., & Ogawa, N. (1999). Dopamine D2 receptor-mediated antioxidant and neuroprotective effects of ropinirole, a dopamine agonist. Brain research, 838(1-2), 51–59. https://doi.org/10.1016/s0006-8993(99)01688-1

- Inquimbert, P. & Scholz, J. (2012). Chapter 54 - Pain, Editor(s): Scott T. Brady, George J. Siegel, R. Wayne Albers, Donald L. Price, Basic Neurochemistry (Eighth Edition), Academic Press, Pages 928-941, https://doi.org/10.1016/B978-0-12-374947-5.00054-7.

References

- Jankovic, J., & Tan, E. K. (2020). Parkinson's disease: Etiopathogenesis and treatment. Journal of Neurology, Neurosurgery & Psychiatry, 91(8), 795–808. https://doi.org/10.1136/jnnp-2019-322338

- Ji, R. R., Baba, H., Brenner, G. J., & Woolf, C. J. (1999). Nociceptive-specific activation of ERK in spinal neurons contributes to pain hypersensitivity. Nature neuroscience, 2(12), 1114–1119. https://doi.org/10.1038/16040

- Kim, K. J., Lee, S. H., Hwang, S. J., & Oh, S. J. (2005). Expression of pERK in the Neurons and Microglia in the Spinal Cord of the Rat with Neuropathic Pain. Journal of Korean Neurotraumatology Society, 1(1), 19. https://doi.org/10.13004/jknts.2005.1.1.19

- Kouli, A., Torsney, K. M., & Kuan, W. L. (2018). Parkinson's Disease: Etiology, Neuropathology, and Pathogenesis. In T. B. Stoker (Eds.) et. al., Parkinson's Disease: Pathogenesis and Clinical Aspects. Codon Publications.

- Konnova, E. A., & Swanberg, M. (2018). Animal Models of Parkinson's Disease. In T. B. Stoker (Eds.) et. al., Parkinson's Disease: Pathogenesis and Clinical Aspects. Codon Publications.

- Labno C. (n.d.). Basic image quantification - unige. Université de Genève. Retrieved November 27, 2021, from https://www.unige.ch/medecine/bioimaging/files/1914/1208/6000/Quantification.pdf.

- Laing, I., Todd, A. J., Heizmann, C. W., & Schmidt, H. H. (1994). Subpopulations of GABAergic neurons in laminae I-III of rat spinal dorsal horn defined by coexistence with classical transmitters, peptides, nitric oxide synthase or parvalbumin. Neuroscience, 61(1), 123–132. https://doi.org/10.1016/0306-4522(94)90065-5

- Li, C., Lei, Y., Tian, Y., Xu, S., Shen, X., Wu, H., Bao, S., & Wang, F. (2019). The etiological contribution of GABAergic plasticity to the pathogenesis of neuropathic pain. Molecular Pain, 15, 174480691984736. https://doi.org/10.1177/1744806919847366

- Li, H., Shen, L., Ma, C., & Huang, Y. (2013). Differential expression of miRNAs in the nervous system of a rat model of bilateral sciatic nerve chronic constriction injury. International Journal of Molecular Medicine, 32(1), 219–226. https://doi.org/10.3892/ijmm.2013.1381

- Liang, H., Paxinos, G., & Watson, C. (2011). Projections from the brain to the spinal cord in the mouse. Brain Structure and Function, 215(3–4), 159–186. https://doi.org/10.1007/s00429-010-0281-x

- Lin, B., Levy, S., Raval, A. P., Perez-Pinzon, M. A., & DeFazio, R. A. (2010). Forebrain Ischemia Triggers GABAergic System Degeneration in Substantia Nigra at Chronic Stages in Rats. Cardiovascular Psychiatry and Neurology, 2010, 1–16. https://doi.org/10.1155/2010/506952

- Lippoldt, E. K., Ongun, S., Kusaka, G. K., & McKemy, D. D. (2016). Inflammatory and neuropathic cold allodynia are selectively mediated by the neurotrophic factor receptor GFRα3. Proceedings of the National Academy of Sciences of the United States of America, 113(16), 4506–4511. https://doi.org/10.1073/pnas.1603294113

References

- Liu, S., Tang, Y., Shu, H., Tatum, D., Bai, Q., Crawford, J., Xing, Y., Lobo, M. K., Bellinger, L., Kramer, P., & Tao, F. (2019). Dopamine receptor D2, but not D1, mediates descending dopaminergic pathway-produced analgesic effect in a trigeminal neuropathic pain mouse model. Pain, 160(2), 334–344. https://doi.org/10.1097/j.pain.0000000000001414

- Lu, Y., Dong, H., Gao, Y., Gong, Y., Ren, Y., Gu, N., Zhou, S., Xia, N., Sun, Y.-Y., Ji, R.-R., & Xiong, L. (2013). A feed-forward spinal cord glycinergic neural circuit gates mechanical allodynia. Journal of Clinical Investigation, 123(9), 4050–4062. https://doi.org/10.1172/JCI70026

- Lu, D. S., Chen, C., Zheng, Y. X., Li, D. D., Wang, G. Q., Liu, J., Shi, J., & Zhang, F. (2018). Combination Treatment of Icariin and L-DOPA Against 6-OHDA-Lesioned Dopamine Neurotoxicity. Frontiers in molecular neuroscience, 11, 155. https://doi.org/10.3389/fnmol.2018.00155

- Ma, Y., Zhan, M., OuYang, L., Li, Y., Chen, S., Wu, J., Chen, J., Luo, C., & Lei, W. (2014). The effects of unilateral 6-OHDA lesion in medial forebrain bundle on the motor, cognitive dysfunctions and vulnerability of different striatal interneuron types in rats. Behavioural Brain Research, 266, 37–45. https://doi.org/10.1016/j.bbr.2014.02.039

- Martin, W. J., Malmberg, A. B., & Basbaum, A. I. (2001). PKCγ Contributes to a Subset of the NMDA-Dependent Spinal Circuits That Underlie Injury-Induced Persistent Pain. The Journal of Neuroscience, 21(14), 5321–5327. https://doi.org/10.1523/JNEUROSCI.21-14-05321.2001

- Matheson, A. J., & Spencer, C. M. (2000). Ropinirole: a review of its use in the management of Parkinson's disease. Drugs, 60(1), 115–137. https://doi.org/10.2165/00003495-200060010-00007

- Matsukawa, N., Maki, M., Yasuhara, T., Hara, K., Yu, G., Xu, L., Kim, K. M., Morgan, J. C., Sethi, K. D., & Borlongan, C. V. (2007). Overexpression of D2/D3 receptors increases efficacy of ropinirole in chronically 6-OHDA-lesioned Parkinsonian rats. Brain Research, 1160, 113–123. https://doi.org/10.1016/j.brainres.2007.05.030

- May A. (2006). A review of diagnostic and functional imaging in headache. The Journal of Headache and Pain, 7(4), 174–184. https://doi.org/10.1007/s10194-006-0307-1

- McCain J. (2013). The MAPK (ERK) Pathway: Investigational Combinations for the Treatment Of BRAF-Mutated Metastatic Melanoma. P & T : a peer-reviewed journal for formulary management, 38(2), 96–108.

- Melzack, R., & Wall, P. D. (1965). Pain mechanisms: a new theory. Science (New York, N.Y.), 150(3699), 971–979. https://doi.org/10.1126/science.150.3699.971

- Mestre, C., Pélissier, T., Fialip, J., Wilcox, G., & Eschalier, A. (1994). A method to perform direct transcutaneous intrathecal injection in rats. Journal of pharmacological and toxicological methods, 32(4), 197–200. https://doi.org/10.1016/1056-8719(94)90087-6

- Millan M. J. (2002). Descending control of pain. Progress in neurobiology, 66(6), 355–474. https://doi.org/10.1016/s0301-0082(02)00009-6

- Miraucourt, L. S., Dallel, R., & Voisin, D. L. (2007). Glycine Inhibitory Dysfunction Turns Touch into Pain through PKCgamma Interneurons. PLoS ONE, 2(11), e1116. https://doi.org/10.1371/journal.pone.0001116

References

- Nance, D. M., & Burns, J. (1990). Fluorescent dextrans as sensitive anterograde neuroanatomical tracers: Applications and pitfalls. Brain Research Bulletin, 25(1), 139–145. https://doi.org/10.1016/0361-9230(90)90264-Z

- Nass, R., & Chen L. (2008). Caenorhabditis elegans Models of Human Neurodegenerative Diseases. In: Conn P.M. (eds) Sourcebook of Models for Biomedical Research. Humana Press. https://doi.org/10.1007/978-1-59745-285-4_12

- Ogawa, N., Terashima, T., Oka, K., Chan, L., & Kojima, H. (2018). Gene therapy for neuropathic pain using dorsal root ganglion–targeted helper-dependent adenoviral vectors with GAD67 expression: PAIN Reports, 3(6), e695. https://doi.org/10.1097/PR9.0000000000000695

- Orazzo, C., Pieribone, V. A., Ceccatelli, S., Terenius, L., & Hökfelt, T. (1993). CGRP-like immunoreactivity in A11 dopamine neurons projecting to the spinal cord and a note on CGRP-CCK cross-reactivity. Brain research, 600(1), 39–48. https://doi.org/10.1016/0006-8993(93)90399-8

- Ouachikh, O., Hafidi, A., Boucher, Y., & Dieb, W. (2018). Electrical Synapses are Involved in Orofacial Neuropathic Pain. Neuroscience, 382, 69–79. https://doi.org/10.1016/j.neuroscience.2018.04.041

- Pasero C. (2004). Pathophysiology of neuropathic pain. Pain management nursing : official journal of the American Society of Pain Management Nurses, 5(4 Suppl 1), 3–8. https://doi.org/10.1016/j.pmn.2004.10.002

- Peirs, C., Bourgois, N., Artola, A., & Dallel, R. (2016). Protein Kinase C γ Interneurons Mediate C-fiber-induced Orofacial Secondary Static Mechanical Allodynia, but Not C-fiber-induced Nociceptive Behavior. Anesthesiology, 124(5), 1136–1152. https://doi.org/10.1097/ALN.0000000000001000

- Peirs, C., Patil, S., Bouali-Benazzouz, R., Artola, A., Landry, M., & Dallel, R. (2014). Protein kinase C gamma interneurons in the rat medullary dorsal horn: distribution and synaptic inputs to these neurons, and subcellular localization of the enzyme. The Journal of comparative neurology, 522(2), 393–413. https://doi.org/10.1002/cne.23407

- Peirs, C., Williams, S. P., Zhao, X., Walsh, C. E., Gedeon, J. Y., Cagle, N. E., Goldring, A. C., Hioki, H., Liu, Z., Marell, P. S., & Seal, R. P. (2015). Dorsal Horn Circuits for Persistent Mechanical Pain. Neuron, 87(4), 797–812. https://doi.org/10.1016/j.neuron.2015.07.029

- Périer, C., Marin, C., Jimenez, A., Bonastre, M., Tolosa, E., & Hirsch, E. C. (2003). Effect of subthalamic nucleus or entopeduncular nucleus lesion on levodopa-induced neurochemical changes within the basal ganglia and on levodopa-induced motor alterations in 6-hydroxydopamine-lesioned rats: STN or EP lesion on levodopa-induced changes. Journal of Neurochemistry, 86(6), 1328–1337. https://doi.org/10.1046/j.1471-4159.2003.01960.x

- Petitjean, H., Pawlowski, S. A., Fraine, S. L., Sharif, B., Hamad, D., Fatima, T., Berg, J., Brown, C. M., Jan, L.-Y., Ribeiro-da-Silva, A., Braz, J. M., Basbaum, A. I., & Sharif-Naeini, R. (2015). Dorsal Horn Parvalbumin Neurons Are Gate-Keepers of Touch-Evoked Pain after Nerve Injury. Cell Reports, 13(6), 1246–1257. https://doi.org/10.1016/j.celrep.2015.09.080

References

- Puopolo M. (2019). The hypothalamic-spinal dopaminergic system: a target forpain modulation. Neural regeneration research, 14(6), 925–930. https://doi.org/10.4103/1673-5374.250567

- Qamar, M., Sauerbier, A., Politis, M., Carr, H., Loehrer, P., & Chaudhuri, K. R. (2017). Presynaptic dopaminergic terminal imaging and non-motor symptoms assessment of Parkinson's disease: Evidence for dopaminergic basis? Npj Parkinson's Disease, 3(1), 5. https://doi.org/10.1038/s41531-016-0006-9

- Qu, S., Ondo, W. G., Zhang, X., Xie, W. J., Pan, T. H., & Le, W. D. (2006). Projections of diencephalic dopamine neurons into the spinal cord in mice. Experimental brain research, 168(1-2), 152–156. https://doi.org/10.1007/s00221-005-0075-1

- Raina, G., Taliyan, R., & Sharma, P. (2012). Pathophysiology of neuropathic pain: a systemic review. International Journal Of Pharmaceutical Sciences And Research, 1, 3530-3542. http://dx.doi.org/10.13040/IJPSR.0975-8232.3(10).3530-42

- Randall, L.O. & Selitto, J. J. (1957). A method for measurement of analgesic activity on inflamed tissue. Archives internationales de pharmacodynamie et de therapie, 111(4): 409- 419.

- REXED B. (1952). The cytoarchitectonic organization of the spinal cord in the cat. The Journal of comparative neurology, 96(3), 414–495. https://doi.org/10.1002/cne.900960303

- Rimvall, K., & Martin, D. L. (1994). The Level of GAD67 Protein Is Highly Sensitive to Small Increases in Intraneuronal γ-Aminobutyric Acid Levels. Journal of Neurochemistry, 62(4), 1375–1381. https://doi.org/10.1046/j.1471-4159.1994.62041375.x

- Roy, T., & Ghosh, S. (2013). Screening and Measurement Tools for Neuropathic Pain: Their Role in Clinical Research and Practice. International Journal of Pharmaceutical Sciences Review and Research, 21(2), 97-107.

- Sandkühler J. (2009). Models and Mechanisms of Hyperalgesia and Allodynia. Physiological Reviews, 89(2), 707–758. https://doi.org/10.1152/physrev.00025.2008

- Sandkühler J. (2017). Neuroinflammation and Neuroplasticity in Pain (Vol. 1). Oxford University Press. https://doi.org/10.1093/acrefore/9780190264086.013.56

- Schmued, L., Kyriakidis, K., & Heimer, L. (1990). In vivo anterograde and retrograde axonal transport of the fluorescent rhodamine-dextran-amine, Fluoro-Ruby, within the CNS. Brain research, 526(1), 127–134. https://doi.org/10.1016/0006-8993(90)90258-d

- Schmued, L. C., & Heimer, L. (1989). Circuitry of the extended amygdala: tracing method that shows the detailed morphology of neurons, their Introducing the use of fluorescent dextrans for rapid, anterograde and axons and terminals: Immunohistochemical localization of an axonally retrograde tract tracing. Sot. Neurosci. Abstr., 15:306.

- Shill, H. A., & Stacy, M. (2009). Update on ropinirole in the treatment of Parkinson's disease. Neuropsychiatric disease and treatment, 5, 33–36.

References

- Skagerberg, G., Björklund, A., Lindvall, O., & Schmidt, R. H. (1982). Origin and termination of the diencephalo-spinal dopamine system in the rat. Brain research bulletin, 9(1-6), 237–244. https://doi.org/10.1016/0361-9230(82)90136-8

- Skogar, O., & Lokk, J. (2016). Pain management in patients with Parkinson's disease: challenges and solutions. Journal of multidisciplinary healthcare, 9, 469–479. https://doi.org/10.2147/JMDH.S105857

- Sluka, K. A., & Audette, K. M. (2006). Activation of protein kinase C in the spinal cord produces mechanical hyperalgesia by activating glutamate receptors, but does not mediate chronic muscle-induced hyperalgesia. Molecular pain, 2, 13. https://doi.org/10.1186/1744-8069-2-13

- Smith, B. H., Lee, J., Price, C., & Baranowski, A. P. (2013). Neuropathic pain: a pathway for care developed by the British Pain Society. British journal of anaesthesia, 111(1), 73–79. https://doi.org/10.1093/bja/aet206

- Sommer, C., Leinders, M., & Üçeyler, N. (2018). Inflammation in the pathophysiology of neuropathic pain. Pain, 159(3), 595–602. https://doi.org/10.1097/j.pain.0000000000001122

- Soós, J., Engelhardt, J. I., Siklós, L., Havas, L., & Majtényi, K. (2004). The expression of PARP, NF-kappa B and parvalbumin is increased in Parkinson disease. Neuroreport, 15(11), 1715–1718. https://doi.org/10.1097/01.wnr.0000136175.51954.ce

- Suzuki, I., Tsuboi, Y., Shinoda, M., Shibuta, K., Honda, K., Katagiri, A., Kiyomoto, M., Sessle, B. J., Matsuura, S., Ohara, K., Urata, K., & Iwata, K. (2013). Involvement of ERK phosphorylation of trigeminal spinal subnucleus caudalis neurons in thermal hypersensitivity in rats with infraorbital nerve injury. *PloS one*, *8*(2), e57278. https://doi.org/10.1371/journal.pone.0057278

- Takahashi, Y., Nakajima, Y., Sakamoto, T. (1994). Dermatome mapping in the rat hindlimb by electrical stimulation of the spinal nerves. Neurosci Lett, 168(1-2):85-88.

- Tang, D. L., Luan, Y. W., Zhou, C. Y., & Xiao, C. (2021). D2 receptor activation relieves pain hypersensitivity by inhibiting superficial dorsal horn neurons in parkinsonian mice. Acta pharmacologica Sinica, 42(2), 189–198. https://doi.org/10.1038/s41401-020-0433-3

- Thompson, J. M., & Neugebauer, V. (2019). Cortico-limbic pain mechanisms. Neuroscience letters, 702, 15–23. https://doi.org/10.1016/j.neulet.2018.11.037

- Tieu K. (2011). A guide to neurotoxic animal models of Parkinson's disease. Cold Spring Harbor perspectives in medicine, 1(1), a009316. https://doi.org/10.1101/cshperspect.a009316

- Todd A. J. (2015). Plasticity of inhibition in the spinal cord. Handbook of experimental pharmacology, 227, 171–190. https://doi.org/10.1007/978-3-662-46450-2_9

- Todd A. J. (2017). Identifying functional populations among the interneurons in laminae I-III of the spinal dorsal horn. Mol Pain 13:1744806917693003.

References

- Todd, A. J., & Sullivan, A. C. (1990). Light microscope study of the coexistence of GABA-like and glycine-like immunoreactivities in the spinal cord of the rat. The Journal of comparative neurology, 296(3), 496–505. https://doi.org/10.1002/cne.902960312

- Tremblay, M., Silveira, M. M., Kaur, S., Hosking, J. G., Adams, W. K., Baunez, C., & Winstanley, C. A. (2017). Chronic D2/3 agonist ropinirole treatment increases preference for uncertainty in rats regardless of baseline choice patterns. The European journal of neuroscience, 45(1), 159–166. https://doi.org/10.1111/ejn.13332

- Tseng K. Y. (Ed.) (2009). Cortico-Subcortical Dynamics in Parkinson's Disease. Humana Press. https://doi.org/10.1007/978-1-60327-252-0

- van der Wal, S., Cornelissen, L., Behet, M., Vaneker, M., Steegers, M., & Vissers, K. (2015). Behavior of neuropathic pain in mice following chronic constriction injury comparing silk and catgut ligatures. SpringerPlus, 4(1), 225. https://doi.org/10.1186/s40064-015-1009-4

- Velazquez, K., Mohammad, H., & Sweitzer, S. (2007). Protein kinase C in pain: Involvement of multiple isoforms. Pharmacological Research, 55(6), 578–589. https://doi.org/10.1016/j.phrs.2007.04.006

- Viana F. (2018). Nociceptors: thermal allodynia and thermal pain. Handbook of clinical neurology, 156, 103–119. https://doi.org/10.1016/B978-0-444-63912-7.00006-0

- Wang, H., Katz, J., Dagostino, P., & Soghomonian, J. J. (2007). Unilateral 6-hydroxydopamine lesion of dopamine neurons and subchronic l-DOPA administration in the adult rat alters the expression of the vesicular GABA transporter in different subsets of striatal neurons and in the substantia nigra, pars reticulata. Neuroscience, 145(2), 727–737. https://doi.org/10.1016/j.neuroscience.2006.12.001

- Wang, Q., Zhang, X., He, X., Du, S., Jiang, Z., Liu, P., Qi, L., Liang, C., Gu, N., & Lu, Y. (2020). Synaptic Dynamics of the Feed-forward Inhibitory Circuitry Gating Mechanical Allodynia in Mice. Anesthesiology, 132(5), 1212–1228. https://doi.org/10.1097/ALN.0000000000003194

- Wei, F., & Zhuo, M. (2008). Activation of Erk in the anterior cingulate cortex during the induction and expression of chronic pain. Molecular pain, 4, 28. https://doi.org/10.1186/1744-8069-4-28

- Welchko, R. M., Lévêque, X. T., & Dunbar, G. L. (2012). Genetic Rat Models of Parkinson's Disease. Parkinson's Disease, 2012, 1–6. https://doi.org/10.1155/2012/128356

- Wood P. B. (2008). Role of central dopamine in pain and analgesia. Expert review of neurotherapeutics, 8(5), 781–797. https://doi.org/10.1586/14737175.8.5.781

- Yoon, C., Wook, Y. Y., Sik, N. H., Ho, K. S., & Mo, C. J. (1994). Behavioral signs of ongoing pain and cold allodynia in a rat model of neuropathic pain. Pain, 59(3), 369–376. https://doi.org/10.1016/0304-3959(94)90023-X

- Young Blood, M. R., Ferro, M. M., Munhoz, R. P., Teive, H. A. G., & Camargo, C. H. F. (2016). Classification and Characteristics of Pain Associated with Parkinson's Disease. Parkinson's Disease, 2016, 1–8. https://doi.org/10.1155/2016/6067132

References

- Yoshizumi, M., Parker, R. A., Eisenach, J. C., & Hayashida, K. (2012). Gabapentin inhibits γ-amino butyric acid release in the locus coeruleus but not in the spinal dorsal horn after peripheral nerve injury in rats. Anesthesiology, 116(6), 1347–1353. https://doi.org/10.1097/ALN.0b013e318254e6fd

- Zhuang, Z. Y., Gerner, P., Woolf, C. J., & Ji, R. R. (2005). ERK is sequentially activated in neurons, microglia, and astrocytes by spinal nerve ligation and contributes to mechanical allodynia in this neuropathic pain model: Pain, 114(1), 149–159. https://doi.org/10.1016/j.pain.2004.12.022

- Zhuo, M., Wu, G., & Wu, L.-J. (2011). Neuronal and microglial mechanisms of neuropathic pain. Molecular Brain, 4(1), 31. https://doi.org/10.1186/1756-6606-4-31